

A MINIATURISED RAMAN SPECTROMETER FOR LIFE DETECTION IN ICE

by

CHIARA RUSSANO
4503414

MASTER OF SCIENCE THESIS

in MSc Aerospace Engineering
Track Spaceflight
Profile Space Engineering

at **Delft University of Technology**
in collaboration with **FH Aachen University of Applied Sciences**

to be defended publicly on August 30th, 2017

Supervisors: **Ir. Prem Sundaramoorthy** TU Delft/Space Systems Engineering
Prof. Dr. Ing. Bernd Dachwald FH Aachen/Aerospace Engineering



An electronic version of this thesis is available at <http://repository.tudelft.nl/>



Copyright © Spaceflight/Space Systems Engineering
All rights reserved.

"As for the future, your task is not to foresee, but to enable it."
Antoine-Marie-Roger de Saint-Exupéry

ABSTRACT

The objective of this MSc thesis was to design a miniaturised Raman spectrometer that can be used in terrestrial deep ice applications of the IceMole probe. This probe is a manoeuvrable subsurface system for clean in situ analysis and sampling, developed at FH Aachen University of Applied Sciences since 2008, that is now part of a bigger DLR collaborative initiative, called Enceladus Explorer (EnEx). It combines melting with a hollow rotating ice screw and it now presents a cross sectional area of 80 mm × 80 mm.

Raman spectroscopy is a promising non-destructive technique that allows to identify both mineral and biological compounds with a minimum amount of sample, by measuring the inelastic scattering of light. In order to achieve an appropriate design for the instrument, the project followed a systems engineering approach. The first step was the derivation of the requirements related to the technical constraints dictated by the miniaturised design of the probe and to the performances that allow the spectrometer to detect potential biosignatures.

The design process was carried out by successive choices so as to propose a final configuration, developed as a CAD model in the software CATIA™. The instrument performs its measurements through a sapphire window in the IceMole probe, looking directly into the ice. It excites the sample with a laser wavelength of 532 nm transmitted via a dichroic beamsplitter. The scattered light is collected by a long-pass edge filter and a 30° off-axis parabolic mirror that focuses the light into a collimator. The light is then delivered to a CCD spectrometer via an optical fibre. The spectrometer is able to measure a spectral range of 546.9 – 700 nm with an accuracy of at least 0.4 nm, combination of the characteristics of the optical components. The final result is a Raman spectrometer design modelled by the use of off-the-shelf components, selected through systems engineering trade-offs. The final dimensions of the instrument are 65 mm × 65 mm × 150 mm, with a mass of ~ 1.1 kg.

The outcome of this thesis will have to be verified and validated in order to ensure the correct working of the system, the compliance with the derived requirements and the validity of the use of this instrument to satisfy the customers' needs and expectations. Therefore, a preliminary verification plan was proposed in accordance to systems engineering.

Eventually, the future of such a Raman spectrometer will be space exploration and life detection missions as payload of the subsurface probe. The space targets for those missions are the ones identified as most promising for harbouring potential living micro-organisms: the polar caps of Mars, Jupiter's moon Europa and Saturn's moon Enceladus.

ACKNOWLEDGEMENTS

The realisation of this project has been possible not only because of my efforts, but also thanks to the people that have supported me during these months. First, I would like to thank my supervisor in Aachen Prof.Dr.Ing. Bernd Dachwald, for giving me the chance of being part of the IceMole project, for introducing me in the topic of this thesis and for his continuous support during these months. In the same way, I want to thank my supervisor in Delft Ir. Prem Sundaramoorthy, for the support even at distance, with our Skype calls and the suggestions for improving the work.

I would like also to thank the EnEx-nExT team, Clemens Espe, Marco Feldmann, Gero Francke and Fabian Baader, for allowing me to work with them, for sharing with me the office, for their help and for the experience in the project. Moreover, I want to thank the DLR experts that I met in Berlin, who lost their time for allowing me to discuss with them about my project: Dr. Ute Böttger, Dr. Mickael Baqué, Christian Williges, Christian Schultz, Dr. Sergey Pavlov, Franziska Hanke and Dr. Jean-Pierre de Vera, that even if he was not there, he made the meeting possible.

This is the final chapter of my university adventure. These last five years have been one hell of a ride, always in a hurry and without the time to think or look back, but I never felt alone, even if I was far away from home, and it was worthy. I met some amazing people with whom I shared all of this and much more that I would like to thank to be part of it.

My friends in Delft, the *Bombers*, Alex, Chiara, Giovanni G, Giovanni P, Livio and Mattia, who try to help me to fight against the sadness of the Dutch weather and the distance from our loved-hated Italy. Thanks guys for the laughs even in the darkest moments during our not-so-short study-breaks at the library.

Among them, Livio deserves a special thank, for sharing with me the adventure in Aachen, for being supportive in my crazy stressed moments, for helping me e per le nostre figuracce. And above all, thanks to Chiara, my dearest companion in these last two years. We have shared these years in the Master since the first day, by creating an amazing friendship. Thank you for the countless hours of study together and the even more countless hours spent for our chats and our calls while we were away. Thanks for your support and for sharing with me all those stressful moments for the thesis.

Then, my friends, my amazing family in Turin, *Geriatrics*, Agostino, Alessandra, Alida, Ciccio, Davide, Emilia, Flavia, Gianluca, Gianni, Giuglia, Giusy, Leandro, Marco, Mauro, Pepe, Puti, Silvia, Stefania and Valentina. Grazie per essere stati la mia famiglia per tre anni e per aver continuato ad esserlo anche negli ultimi due: dove siete voi, c'è casa, e non importa se per stare insieme dobbiamo finire dall'altra parte del pianeta.

Many thanks to Leandro and Flavia, my first friends in Turin and my support group during this thesis period. Mi avete insegnato per primi quanto poco può significare la distanza e nonostante le innumerevoli sfighe e paturnie siete sempre riusciti a sopportarmi. Grazie

anche per gli imbruttimenti (soprattutto di Leandro) che nei momenti giusti mi sono serviti. Thanks to my amazing girlfriends Alida, Alessandra and Valentina, for having been my home in my most difficult moments, per essere accorse ogni volta che ne avevo bisogno senza pensarci due volte, per i gelati consolatori e per quelli celebrativi, ma anche semplicemente per la nostre chiacchiere che possono andare avanti per ore. I need to thank Silvia, my genius friend, per gli innumerevoli abbracci, Giuglia, per le mille risate insieme, Emilia and Stefania, the little ones, per l'affetto infinito che ci unisce e per essere sempre state delle amiche meravigliose. Davide deserves a special thank, as he has been my main support during the time in the Netherlands e per aver sopportato tutte le mie lamentele su Delft.

The girls that showed me how strong I am, Flavia and Maria. Grazie per essere state le *mie sorelle* torinesi, per le chiamate su Skype agli orari più improbabili, per aver condiviso con me un posto che siamo riuscite a chiamare casa, alla fine, e per avermi insegnato a credere in me stessa e nelle mie capacità più di quanto io sia mai stata in grado di fare.

Then, my (almost) childhood girlfriends, that have been with me for countless years now and that know me simply with a look. Thanks to Giulia and Erika, per essermi state vicino negli ultimi dieci anni ed essere cresciute con me, nonostante la distanza e le vite così diverse. And thanks to Sara and Raffaella, per le mille avventure, le mille risate e i mille viaggi (ancora da fare). Grazie a tutte voi per aver sopportato tutti i miei malumori e per essere da sempre le mie ancora.

And last but not least, for sure, thanks to my family, who support me no matter what and always believe in me, and that has given me the chance of studying further and further from home, hiding the nostalgia. Thanks to my sister-in-law Anna, che è diventata una parte molto importante della mia famiglia, and to my big brother Mauro, che tifa per me sempre, silenziosamente, e che è sempre stato il mio punto di riferimento più importante. Thanks to my dad Maurizio, che mi ha permesso di vivermi al meglio la lontananza da casa e che mi vede sempre come la sua bambina, così che io possa fingere, ogni tanto, che niente sia cambiato. And finally, thanks to my mum Lorenza, la donna più forte che conosco, per avermi insegnato il valore di me stessa.

It is a long list of people, and probably I forgot someone, but all of them help me in finishing my university studies in so many different ways and they deserved to be named. I am really grateful to have all these amazing people in my life and thanks to them this work has been possible, for their support, motivation and all the other reasons.

Chiara Russano
Delft, August 21, 2017

TABLE OF CONTENTS

Abstract	ii
Acknowledgements	iii
List of Figures	vii
List of Tables	ix
List of Abbreviations	x
List of Symbols	xii
1 Introduction	1
1.1 Research Questions	2
1.2 Report Structure	2
I Background Information	4
2 Enceladus Explorer	5
2.1 IceMole probe	7
2.1.1 Heritage.	8
2.1.2 Current Development	9
3 Derivation of Requirements	12
3.1 Need Analysis	13
3.2 Technical Constraints.	15
3.3 Technical System Requirements	17
4 Raman Spectroscopy	19
4.1 Theory.	20
4.2 Performance	24
4.3 Instrumentation	26
4.3.1 Laser.	28
4.3.2 Filter.	28
4.3.3 Dispersion System	29
4.3.4 Detector	30
4.4 Enhancements	32
II Design	34
5 Payload Parameters	35
5.1 Optical Key Parameters.	35
5.2 Payload Requirements	38

6	Preliminary Design	41
6.1	IceMole Design Considerations	42
6.2	Components	45
6.2.1	Window	45
6.2.2	Laser	46
6.2.3	Filter	47
6.2.4	Focusing and Collection Optics	48
6.2.5	Spectrometer & Detector	50
6.3	Preliminary System Configuration	51
7	Selection of Components	53
7.1	Iteration of System Configuration	53
7.2	Trade-offs	55
7.2.1	Window	56
7.2.2	Laser	57
7.2.3	Optical Components	58
7.2.4	Spectrometer & Detector	63
7.3	Preliminary CAD Options	64
8	Definitive Design	69
8.1	Final CAD Modelling	69
8.2	Integration into IceMole	76
8.3	Mass, Power & Data Budgets	76
8.4	Cost Analysis	78
III	Verification	80
9	Verification, Validation & Calibration	81
9.1	Verification & Validation Plan	82
9.2	Verification of the Proposed Design	85
9.3	Calibration & Data Reduction	87
10	Technology Roadmap to Space Missions	89
10.1	Icy Moons and Mars' Polar Caps	90
10.2	Evaluation of the Requirements	91
10.3	Evaluation of the Proposed Design	94
IV	Final Conclusions and Future Steps	95
11	Conclusions & Next Steps	96
11.1	Conclusions	96
11.2	Recommendations and Next Steps	97
	References	100
	Appendices	108
A	Components' Technical Data Sheets	109
B	CAD Drawings	131

LIST OF FIGURES

2.1	EnEx logo	5
2.2	Reference EnEx mission scenario [Konstantinidis et al., 2015a]	6
2.3	Technical drawings of the EnEx-IceMole design and its head [Konstantinidis et al., 2015b]	10
2.4	Rendering of the current version of IceMole (Credits: EnEx-nExT)	11
3.1	NASA project life cycle	13
3.2	Derivation of requirements (adapted from Larson et al. [2009])	17
4.1	Energy transitions for Rayleigh and Raman scattering	21
4.2	Polarisation induced in a molecule electron cloud by an incident optical electric field \vec{E} [McCreery, 2000]	22
4.3	Schematic of collection variables [McCreery, 2000]	25
4.4	General diagram of a Raman spectrometer [Vandenabeele, 2013]	27
4.5	Schematics of dispersive systems [Wolffenbuttel, 2005]	30
5.1	Electromagnetic spectrum	36
6.1	90 and 180° sampling geometries for Raman spectroscopy [Gauglitz and Vo-Dinh, 2006]	42
6.2	FFBDs of high-level operation options	44
6.3	Filters options [Omega Optical, 2017]	47
6.4	Single fibre cable structure [Newport, 2017]	49
6.5	Crossed and uncrossed Czerny-Turner set-up [Rasmussen et al., 2015]	50
6.6	Preliminary system configuration	51
7.1	Iterated system configuration	54
7.2	<i>N-around-1</i> optical fibre (adapted from Slater et al. [2001])	54
7.3	Fiber optic connector options [Industrial Fiber Optics, 2017; Thorlabs, 2017b]	61
7.4	Design Option Tree (DOT) for CAD physical configurations	65
7.5	CAD physical configuration concepts	66
8.1	Rendering of modelled case	70
8.2	Working principle of an off-axis parabolic mirror [Edmund Optics, 2017e]	71
8.3	Rendering of modelled optics support	72
8.4	Rendering of modelled window support and window	72
8.5	Rendering of modelled beamsplitter support and beamsplitter	73
8.6	Rendering of modelled filter support and filter	73
8.7	Rendering of modelled collimator support, collimator and FC/APC connector	73
8.8	Rendering of the assembly of the optical components	74
8.9	Rendering of the final assembly	75
9.1	V-Model [Gill, 2015]	81

10.1 Icy environments in space	90
--	----

LIST OF TABLES

2.1	Technical data for the different IceMole probes [Dachwald et al., 2014]	9
3.1	Pugh matrix for the selection of the life detection instrument [Russano, 2017]	14
3.2	Top-level mission requirements	16
3.3	Technical requirements	18
4.1	Comparison of spectrometer types [McCreery, 2000, p.79]	27
5.1	Assumptions on laser wavelength [McCreery, 2000, p.76]	37
5.2	Payload requirements	39
7.1	Graphical trade-off for the window material [IPS Optics, 2017; Newport, 2017]	56
7.2	Graphical trade-off for laser [Cobolt, 2016; CrystaLaser, 2017; Laserglow Technologies, 2017; RGBLase, 2017]	57
7.3	Characteristics of beamsplitters [Edmund Optics, 2017a; Semrock, 2017a]	59
7.4	Characteristics of long-pass edge filters [Edmund Optics, 2017d; Semrock, 2017b]	59
7.5	Characteristics of Thorlabs single mode fiber [Thorlabs, 2017c]	62
7.6	Graphical trade-off for spectrometers [Hamamatsu, 2017; Ibsen Photonics, 2017; StellarNet, 2017; Thorlabs, 2017d]	64
8.1	Mass budget	77
8.2	Cost budget	78
9.1	V&V of requirements	84
9.2	Verification Compliance Matrix (VCM)	86
10.1	Orbital and physical characteristics of icy environments in space [Lissauer and De Pater, 2013; Procket and Pappalardo, 2007]	91

LIST OF ABBREVIATIONS

2D	2-Dimensional		
3D	3-Dimensional	ID	Identifier
AHP	Analytical Hierarchical Process	IMU	Inertial Measurement Unit
AIT	Assembly, Integration and Testing	IM	IceMole
AIV	Assembly, Integration and Verification	IR	InfraRed
APS	Acoustic Positioning System	ISTA	Institute for Space Technology & Space Applications
ARS	Acoustic Reconnaissance System	I	Inspection
AR	Anti-Reflective	JPL	Jet Propulsion Laboratory
A	Analysis	KDP	Key Decision Points
BIPM	Bureau International des Poids et Mésures - International Bureau of Weights and Measures	LASER	Light Amplification through Stimulated Emission of Radiation
BT-CCD	Back-Thinned Charged-Coupled Device	MIDGE	Minimally Invasive Direct Glacial Exploration
C*	Compliant, but need further investigation	MIE	Magnetic Improvement and Evaluation
CAD	Computer-Aided Design	MSc	Master of Science
CATIA	Computer-Aided Three-dimensional Interactive Application	NASA	National Aeronautics and Space Administration
CAUSE	Cognitive Autonomous Subsurface Exploration	NavEn	Navigation System on Enceladus
CCD	Charged-Coupled Device	NA	Numerical Aperture
CoC	Code of Conduct	NC	Non-compliant
COTS	Components-Off-The-Shelf	NEP	Nuclear Electric Power
CW	Continuous Wavelength	nExT	Environmental Experimental Testing
C	Compliant	NIST	National Institute of Standards and Technologies
DiMIce	Directional Melting in Ice	NPR	NASA Procedural Requirements
DLR	Deutschen zentrum für Luft-und Raumfahrt - German Space Administration	NRC	National Resource Council
DOT	Design Option Tree	NSF	National Science Foundation
DPSS	Diode-Pumped Solid State	OD	Optical Density
DR	Dead Reckoning	OTS	Off-The-Shelf
D	Demonstration	PDA	Photodiode Array
EnEx	Enceladus Explorer	PMT	PhotoMultiplier Tube
FFBD	Functional Flow Block Diagram	RANGE	Robust Autonomous Acoustic Navigation in Glacier Ice
FT	Fourier-transform	RF	Radio Frequency
GCMS	Gas Chromatograph-Mass Spectrometer	RMS	Root Mean Square
		RRS	Resonance Raman Spectroscopy
		RS	Raman Spectrometer

RTG	Radioisotope Thermoelectric Generator	SRR	System Requirements Review
SERRS	Surface-Enhanced Resonance Raman Spectroscopy	SYS	System
SERS	Surface-Enhanced Raman Spectroscopy	T	Testing
SF	Sensor Fusion	UV	UltraViolet
SNR	Signal-to-Noise Ratio	V&V	Verification & Validation
		VCM	Verification Compliance Matrix
		VM	Verification Method

LIST OF SYMBOLS

PHYSICAL CONSTANTS

1AU	Astronomical unit, equal to $1.496 \cdot 10^8$ km, the mean distance between Earth and the Sun [Lissauer and De Pater, 2013]
c	Speed of light in vacuum, equal to 299792458 m/s [NIST, 2017]
h	Planck's constant, equal to $6.62607004 \times 10^{-34}$ J s [NIST, 2017]

GREEK SYMBOLS

α	Polarisability
$\bar{\nu}$	Wavenumber
β	Differential cross section
$\Delta\bar{\nu}$	Raman shift
$\Delta\lambda$	Spectral resolution
η	Quantum efficiency
λ	Wavelength
λ_0	Excitation wavelength
λ_x	Corresponding wavelength
μ	Constant
ν	Frequency
ν_0	Incident frequency
ν_j	Excited frequency
Ω	Solid angle of collection
Ω_D	Solid angle collected by the spectrometer
ϕ_D	Dark signal
σ_B	Standard deviation of the background
σ_D	Standard deviation of the dark signal
σ_F	Flicker noise
σ_j	Scattering cross section
σ_R	Readout noise
σ_S	Standard deviation of the signal
σ_y	Standard deviation of peak height

θ Angle of incidence

LATIN SYMBOLS

\bar{S}	Mean value of Raman signal
\mathcal{E}	Energy
\vec{E}	Electric field
\vec{P}	Polarisation
A_D	Sample area monitored by the spectrometer
B	Background
C	Collection function (in $\text{cm}^2\text{sre}^{-1}\text{photons}^{-1}$)
D	Number density of scatters
dz	Path length or depth of field
E_0	Electrical field magnitude
f	Focal length
$f\#$	Aperture ratio
i	Current
I_0	Excitation source intensity (in W)
I_R	Raman intensity (in W)
K	Geometrical factor
L	Specific intensity
L_a	Specific intensity of analyte
N_C	Number of channels
P	Power
P_D	Power density
P_O	Incident laser intensity (in photons/s)
P_R	Scattered Raman intensity (in photons/s)
Q_j	j -th vibrational normal mode
R	Reflectance
S_a	Raman signal due to a single analyte
T	Transmittance
t	Time
t_s	Single-channel sampling time
V	Voltage

1

INTRODUCTION

The Enceladus Explorer ([EnEx](#)) initiative is a collaborative project funded by the Deutsches Zentrum für Luft-und Raumfahrt - German Space Administration ([DLR](#)), on which six German universities are working in order to develop a manoeuvrable subsurface probe able to navigate autonomously in deep ice. This project is particularly important in the context of a roadmap towards space missions, but currently its main focus is on the terrestrial applications and testing of such a probe.

The probe has been built up by FH Aachen University of Applied Sciences since 2008, as an innovative melting probe, called IceMole. IceMole merges the techniques of ice melting and drilling by combining a rotating ice hollow screw on its melting head. Moreover, it is a steerable probe because of differential heating of the plates on its head, supported by side-wall plates as well. It is a successful innovation in ice penetration, that can open the path towards the exploration of the icy environments in space, such as the polar caps of Mars and the icy moons Europa and Enceladus. In fact, these targets have gain more and more attention from astrobiology as potential habitats for living organisms [Dachwald et al., 2014; Konstantinidis et al., 2015b].

The latest version of the IceMole probe underlines the importance of miniaturisation: in fact, the new design presents a cross sectional area of $80\text{ mm} \times 80\text{ mm}$ and a length of $\sim 450\text{ mm}$. Miniaturisation is extremely advantageous for space exploration as well as for the terrestrial applications, since it allows the reduction of costs, risks and power requirements. In the context of this new IceMole design, the objective of the thesis was to analyse and design a payload that could detect life and its biosignatures in the terrestrial applications of the probe. In fact, life, intended as something that could originate, evolve and develop in its Darwinian meaning, is believed to have been preserved since its origin by icy environments such the ones in which IceMole operates [Domagal-Goldman et al., 2016; Horneck et al., 2016] . Price [2007] demonstrated indeed that ice presents the characteristics that allow life to be preserved and to exist.

During an intensive literature study presented in Russano [2017], a Raman spectrometer was identified as the most promising life detection instrument for IceMole in terms of size, technology assessment, power requirement and performance, to detect potential living micro-organisms. Raman spectroscopy is indeed a powerful non-destructive technique that

allows to identify both organic and inorganic molecules, by measuring the inelastic scattering of light [Blacksberg et al., 2016; Brewer et al., 2004; Tarcea et al., 2008].

In order to satisfy the need of a payload that could detect potential life in ice, the aim of this thesis was to design such an instrument that could comply with the miniaturised generation of the IceMole probe and that can be operational in its terrestrial applications.

1.1. RESEARCH QUESTIONS

The thesis developed around a central point and the main research question which represented the focus of the whole work was derived so as to dictate some guidelines for the development of the project. This mentioned research question is the following:

Is it be possible to design a miniaturised Raman spectrometer, considering the volumetric, technical and environmental constraints dictated by the new design of the IceMole probe and its operations?

This inquiry is the main target of this thesis and it particularly underlines the main critical aspect of the research: the compliance with the probe itself in its dimensions and operations. In order to answer to this research question, a path was followed that derives from some sub-questions which helped in identifying the steps to be taken.

First of all, *which are the critical constraints dictated by the IceMole probe?* and *which is the required performance of the Raman spectrometer?* were the two questions that permitted to derive the requirements that the instrument has to meet and that described the working of the technology. Successively, the design had to be obtained and for this process this sub-question needed to be answered: *can off-the-shelf components be used for the design of such an instrument?* The answer to this question implied some choices in the design and determined whether some modelling was necessary to achieve a satisfying final outcome. Then, an evaluation of the achieved design was needed, so as to be sure to have accomplished the goal and for this task the sub-question is the following: *does the design allow to satisfy the customers' needs by working properly?* This last sub-question is related both to the verification and validation of the Raman instrument, which are processes that had to be considered during the entire work.

One last investigation concerned the use of such an instrument in the future space applications of the ice penetration probe. To this end, the question to be answered is the following: *what has to be changed in order to have a system that can operate in the icy environments identified in the Solar system?* This inquiry is more related to the future development of the presented work than to the main research question itself, by presenting how the project will evolve.

1.2. REPORT STRUCTURE

The sub-questions were derived in order to represent a path to be followed during the work and that is remarked by the structure of the report as well. The thesis is divided into four principal parts.

Part I presents the background information, studied in order to gain as much knowledge as possible on the aspects that have to be dealt with. The EnEx initiative is explained in detail in Chapter 2. The origin of the project and the different generations of IceMole are described, so as to represent the innovation that they have brought to ice penetration. Then, by following a systems engineering approach, the derivation of requirements is performed in Chapter 3. A first need analysis is considered and the top-level mission requirements and the technical system requirements are derived from the constraints imposed by the IceMole design and operations. Then an insight on the technique of Raman spectroscopy is discussed in Chapter 4, so as to highlight the components of the instrument that have to be selected in the next phases of the project.

The main focus of the thesis is presented in Part II, where the design of the Raman spectrometer is formulated. Firstly, the main parameters of the payload are discussed and its requirements are derived in Chapter 5, after a meeting with DLR experts. Then, the design is divided in turn into three main phases. At first, a preliminary design is elaborated in Chapter 6, in order to define a preliminary system configuration that drives the design. Then, all the components are selected through extensive trade-offs in Chapter 7 and the preliminary assembly options are elaborated via Computer-Aided Design (CAD) modelling with the software CATIA™. Eventually, the definitive design is presented in Chapter 8, with its modelling through the software. Moreover, the principal budgets are defined and a preliminary cost estimation is computed.

Part III deals with the verification and the validation of the proposed design of the Raman spectrometer, always referring to the systems engineering approach and tools. Therefore, Chapter 9 presents a verification and validation plan for the requirements and the proposed design, along with the proposal for the calibration of the instrument. Then, Chapter 10 explains how and where such a Raman spectrometer can be employed in future space missions towards those targets identified as potential habitats for living micro-organisms: the polar caps of Mars and the icy moons Europa and Enceladus. For this task, the requirements and the design itself are evaluated to decide what needs to be changed for space applications.

The last Part IV presents the results of this work, what they mean and the future steps to be taken in the development of the project.

PART I:
BACKGROUND INFORMATION

2

ENCELADUS EXPLORER

The Enceladus Explorer (**EnEx**) initiative is a collaborative research and development project funded by **DLR** since 2012, on which six German universities collaborate. The motivation of this project lies on the *Cassini* spacecraft confirmation of the existence of active fissures in the South polar region of the surface of Saturn's moon Enceladus, the so-called *tiger stripes*, from which giant jets of water ice are shot into space. Measurements and analyses of these ejected plumes by the spacecraft showed that this cryovolcanic activity is powered by liquid water located below the icy surface, which could have preserved the existence of living micro-organisms, evolved in this speculative salt water ocean [DLR, 2012; Kowalski et al., 2016].



FIGURE 2.1: EnEx logo

The current aim of **EnEx** project is *to develop an autonomous steerable subsurface ice probe to demonstrate autonomous navigation in deep ice* [Konstantinidis et al., 2015b], while the final objective will be to develop a mission concept that can be used in future exploration of Enceladus to access subsurface liquid material for clean sampling and in situ analysis. Meanwhile, the attention is paid on Earth applications since the technologies needed for Enceladus and other space icy environments are still under development, because of major technological challenges due to the harsh conditions of the celestial bodies, as it is described later in Chapter 10. Moreover, because **EnEx** is developed in university research groups, the focus on terrestrial applications allows to keep the costs low.

Anyway, these applications present some major challenges as well, that were presented by Konstantinidis et al. [2015b]: liquid water must be detected in ice and the distance to a set target point has to be estimated; attitude and position with respect to the surface ground station and the target point need continuous determination; obstacles in ice must be detected; and the optimal path to get to the target has to be autonomously determined.

Figure 2.2 shows the current high-level mission architecture and scenario. The mission will comprise three main elements: an orbiter, a lander and the IceMole (described in detail in next Section). The orbiter and the lander will be reunited in a combined spacecraft and the orbiter will be used as a propulsion module. The transfer to Enceladus will be accomplished with the use of a nuclear reactor on the lander module. After orbital capture around the moon, the orbiter will select a potential landing site, through remote sensing. Landing site reconnaissance requires a high level of accuracy and autonomous hazard avoidance. In fact, the landing distance from the plumes is very important, because it cannot be too short but either too long, as the length of the communication and power tether between the lander and the probe has to be minimised. Once the landing site reconnaissance phase will be completed, the orbiter and the lander will separate and the latter will land safely close to one of the stripes. At this point the orbiter will work as communication link between the lander and Earth. Once landed, the IceMole and the elements of its navigation system will be deployed and the probe operations will start, powered by the nuclear reactor of the lander [Konstantinidis et al., 2015a,b].

At last, one of the most important considerations for the mission towards Enceladus is the planetary protection requirement. The South polar terrain of the moon, where the cryovolcanism is detected, is subjected to planetary protection restriction because it potentially hosts living micro-organisms. Therefore each element of the mission needs to be analysed in terms of risk of contamination and the necessary ways to diminish that risk within the acceptable probability of 10^{-4} have to be identified. The same rationale applies to terrestrial analogous subglacial environments to preserve both sample integrity and the pristine nature of the explored systems [Dachwald et al., 2013, 2014; Konstantinidis et al., 2015b].

Hence, neglecting the lander and orbiter under study, the EnEx initiative currently comprises the subsurface probe IceMole, the in-ice autonomous navigation payload and a surface control module. The navigation solution consists of four modules, which were deeply described by Kowalski et al. [2016]:

- a Dead Reckoning (DR), based on inertial and magnetic attitude determination. The position of the probe is determined with respect to a provided point of departure according to the attitude evolution and information on the travelled distance, acquired by means of an Inertial Measurement Unit (IMU) and differential magnetometry.
- an Acoustic Positioning System (APS), that provides the absolute positioning via trilateration of acoustic signals. It consists of: six ultrasonic emitters at a depth of ~ 1 m; four receivers in IceMole head; a signal generation system at surface; and a data acquisition system, into the IceMole payload bay.
- an Acoustic Reconnaissance System (ARS), based on sonography, that could detect possible obstacles or potential targets.
- a high-level Sensor Fusion (SF) unit, to integrate the acquired DR, APS and ARS data in order to enable their use.

2.1. ICEMOLE PROBE

The described navigation solution is therefore integrated into a research melting probe, the IceMole, a novel manoeuvrable subsurface system for clean in situ analysis and sampling,

which has been developed at FH Aachen University of Applied Sciences since 2008.

IceMole originated as a solution to overcome the major drawbacks of both conventional ice penetration methods, drilling and melting. Drills present high mass and power requirement; they are not steerable, allowing to penetrate only downwards; they cannot avoid inclusions; and their operational effort excludes their use on robotic mission to reach great depths. On the other hand, although they are considered a much better technique for in situ exploration of icy environments, conventional ice melting probes come with disadvantages, too: they penetrate only vertically downwards too and they are not steerable; they cannot overcome dust/dirt layers; and they cannot be recovered from greater depths [Dachwald et al., 2013].

IceMole presents several advantages over these ice penetration methods, which were discussed also in the preceding literature studies to this work [Russano, 2016, 2017]. This novel concept is based on the combination of the two methods, melting and drilling with a hollow ice screw, in order to allow the probe to penetrate reasonable thick layers of ice inclusions. Moreover, the screw allows close-contact between the melting head and the ice, optimising the conductive heat transfer to ice and aiding the system to steer. The probe has a quadratic cross section, so as to counteract the torque generated by the ice screw, and a melting head that allows differential heating to change direction. Optional side-wall heaters may be used to support this curve-driving capability. The required electric power is generated by a surface generator and delivered via an uncoiled tether, which is used for communication and data transmission, as well. Moreover, the probe is able to melt upwards, against gravity, in order to be recovered from the ice. Another advantage of the IceMole probe is that no drilling fluid is used and the probe can be sterilised before deployment, according to planetary protection standards and the Antarctic Code of Conduct (CoC) for the Exploration and Research of Subglacial Aquatic Environments [Dachwald et al., 2013, 2014; Konstantinidis et al., 2015b].

2.1.1. HERITAGE

Ice melting probes have a huge heritage that dates back to the beginning of the 1960s. The major example of these concepts was the *Philberth* probe, a non-recoverable, instrumented melting probe designed in 1962 to measure temperature in ice. However, the most advanced melting probe design was that of Jet Propulsion Laboratory (JPL) *Cryobot* in 1998. It was part of the Earth-Europe Program and it was designed as an implementation of the previous example: it was considerably smaller, lighter and required less power. The probe was 1 m in length and 10 cm in diameter. It relied on a Radioisotope Thermoelectric Generator (RTG) which provided 1 kW for the operations. The head and shell were provided with 4 heaters for passive melting and differential heating to permit steerability. Data were transmitted through a tether to a primary upper half of the probe containing the electronics and then transmitted to a surface lander via mini-RF ice transceivers, dropped off during the descent of the probe [Dachwald et al., 2013; Zimmerman et al., 2001]. However, *Cryobot* still presented the drawbacks of a pure melting probe.

The first generation of IceMole probe, IceMole 1, was tested in September 2010 with three successful penetration tests on the Swiss Morteratsch glacier. It presented a melting head with a required power of 3.2 kW, distributed over four heating zones. It had a length of 0.87 m, originally designed to collect ice samples. The hollow ice screw was thermally isolated from

the melting head to allow collection of unmelted ice through the interior of the screw. A simple Off-The-Shelf (OTS) camera was installed in the payload bay for testing purposes. The conducted tests demonstrated the following capabilities, reported by Dachwald et al. [2013, 2014]:

- Melting 45° upwards for ~ 1.5 m, against gravity
- Melting horizontally for ~ 5 m
- Melting 45° downwards for ~ 3 m, penetrating three obstructing non-ice layers and driving a curve of ~ 10 m
- Achieving a penetration velocity of ~ 0.3 m/h

A new advanced lighter prototype, IceMole 2, was then developed between 2010 and 2012. It presented a more sophisticated heater control system, with 12 separately controllable heating cartridges in the new parabolically shaped melting head and 8 side-wall heaters. Moreover, it was equipped with an attitude determination system. It succeeded in increasing its melting velocity up to 1 m/h. Tests were conducted on Morteratsch glacier and on Hofsjökull (Iceland) in 2012. They demonstrated the recoverability of the probe by melting a standing U-channel but, however, they revealed that the parabolic shape of the head diminished the curve-melting capability, due to the inability to generate a torque perpendicular to the longitudinal axis. However, although this drawback on the curve-driving capability, IceMole 2 testing demonstrated the capability and stability of the electronic subsystems and the software, as well as the reliability of the operations [Dachwald et al., 2014].

2.1.2. CURRENT DEVELOPMENT

Within EnEx, a new design of the probe, referred to as EnEx-IceMole, has been proposed. Table 2.1 underlines the main differences for the three generations. EnEx-IceMole presents

TABLE 2.1: Technical data for the different IceMole probes [Dachwald et al., 2014]

	IceMole 1	IceMole 2	EnEx-IceMole
Cross section	15 cm × 15 cm	15 cm × 15 cm	15 cm × 15 cm
Shape of melting head	complanate	parabolic	complanate
Max. heating power for melting head	4 × 800 W	12 × 200 W	(8 × 200 W) + (8 × 160 W)
Max. heating power for side-wall heaters	N/A	8 × 300 W	8 × 1000 W
		(partial coverage with const. heat distr.)	(full coverage with linear heat distr.)
Max. power for forward melting	3.2 kW	2.4 kW	2.9 kW
Max. power for curve driving	1.6 kW	1.8 kW	5.0 kW
Max. penetration velocity	~0.3 m h ⁻¹	~1.0 m h ⁻¹	~1.1 m h ⁻¹
Length (without ice screw)	0.9 m	1.2 m	2.0 m
Length of ice screw	7 cm	8.5 cm	6 cm
Ice-screw driving power	25 W	25 W	25 W
Mass	~30 kg	~25 kg	~60 kg
Max. pressure	1 bar	5 bar	5 bar
Bus system	SPI	CAN	CAN, Ethernet
Communications to surface	power-line modem	power-line modem	Ethernet and power-line modem
Max. data rate to surface	19.2 kbit s ⁻¹	19.2 kbit s ⁻¹	1000 Mbit s ⁻¹
Attitude and position determination system	no	simple	advanced
Decontamination and sampling system	no	no	yes
Obstacle and target detection system	no	no	yes
Field tests	Morteratschgletscher 2010	Morteratschgletscher 2012, Hofsjökull 2012	Morteratschgletscher 2013, Canada Glacier 2013
Longest channel made	~5 m	~8 m	~25 m
Min. curve radius	~10 m	N/A	~10 m

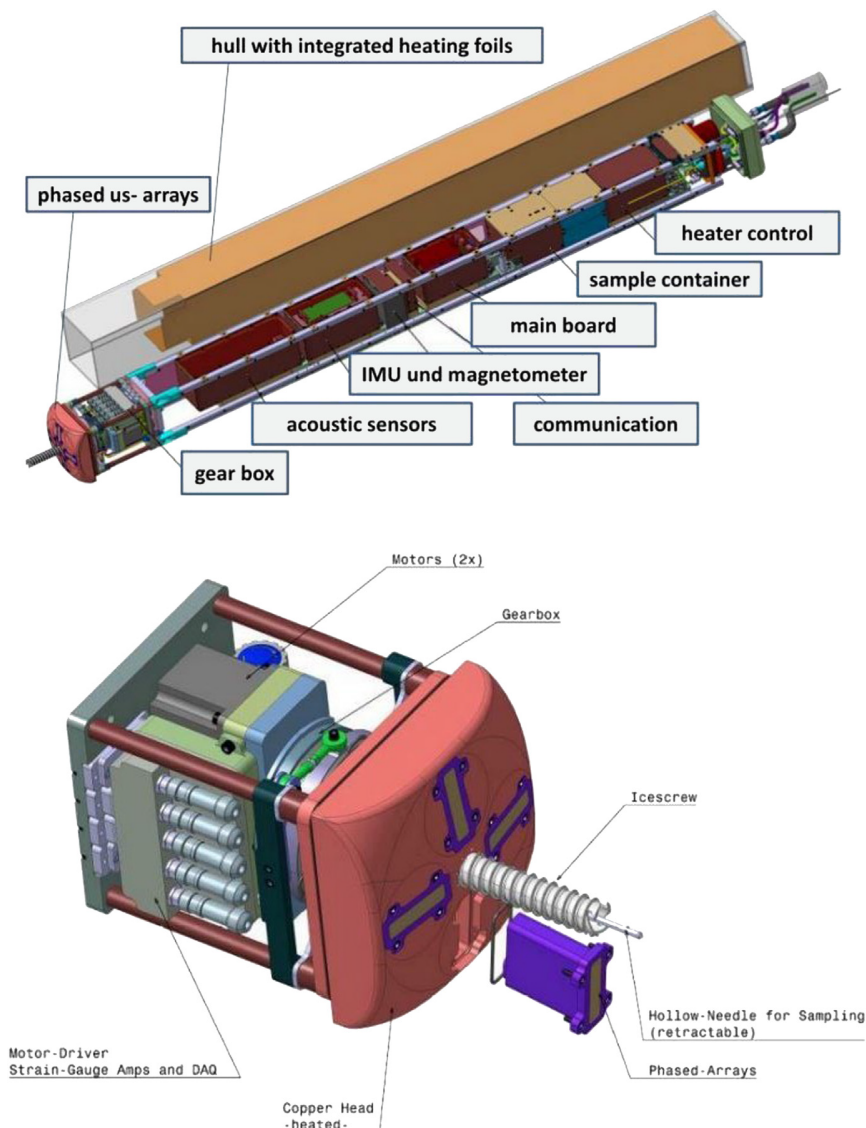


FIGURE 2.3: Technical drawings of the EnEx-IceMole design and its head [Konstantinidis et al., 2015b]

a rectangular shape with a cross sectional area of $15\text{ cm} \times 15\text{ cm}$, a length of 2 m and a mass of $\sim 60\text{ kg}$. Its technical drawings are presented in Figure 2.3. The screw is driven by a 25 W servo-controlled electric motor and gear system. The required electric power 230 V/50 Hz is provided by a surface RTG and transmitted via the three-conductor power cable [Dachwald et al., 2014; Konstantinidis et al., 2015b]. In order to avoid obstacles, detect potential targets and navigate in ice, the EnEx-IceMole owns an IMU and a magnetometer to determine its attitude. A second reference magnetometer can be found at the surface station. In the melting head, 4 ultrasonic phased arrays are integrated to detect the targeted crevasse and potential obstacles. Extra acoustic pingers on the surface emit signals, received by 4 separate on-board detectors, which use the triangulation principle to independently determine the position of the probe [Dachwald et al., 2014; Konstantinidis et al., 2015b].

The first field test of the EnEx-IceMole was conducted in June 2013 on Morteratsch glacier. The main objective was to test the stability and interoperability of the newly developed nav-

igation subsystems and the design changes in the probe, above all concerning the curve-driving capability according to the increased length. However, the main test campaign for [EnEx-IceMole](#) was conducted in Antarctica, at Blood Falls in 2015, in a collaborative exploration mission with [MIDGE](#) project. The Minimally Invasive Direct Glacial Exploration ([MIDGE](#)) project is funded by the US National Science Foundation ([NSF](#)) and it aims at clean sample return of subglacial water from a crevasse for life detection and analysis. Therefore, the main objectives of these tests were to reach the crevasse and collect clean sampling. In order to meet the clean-access requirements, IceMole arrived at the field site sterilised, then it was subjected to a field-based cleaning step for decontamination at a pressure of 10 bar and to an in situ decontamination of the sampling mechanisms immediately before sample collection, with a 3% hydrogen peroxide (H_2O_2) solution [Dachwald et al., 2014; Konstantinidis et al., 2015b; Leimena et al., 2010]. During testing at Blood Falls, the [EnEx-IceMole](#) probe was able to return to surface clean in situ samples, thanks to these decontamination methods and to its working principle that allows it to be recovered from ice.

However, the designing and development of the probe for a future astrobiological mission to Enceladus has still a long technological roadmap to face. It will be a multi-stage process, so each phase will focus on optimising the several capabilities of the probe. Currently, [EnEx-nExT](#) research team is working on the miniaturisation of the probe and on the development of a scientific payload, able to provide sample measurements in situ in order to detect potential biosignatures. The new design of the probe is presented in [Figure 2.4](#). The rectangular shape is maintained but the dimensions are reduced to a cross sectional area of 80 mm × 80 mm and a length of ~ 450 mm. In this way, the mass is reduced to ~ 6 kg but the power required for operations is still quite high, equal to ~ 5 kW.

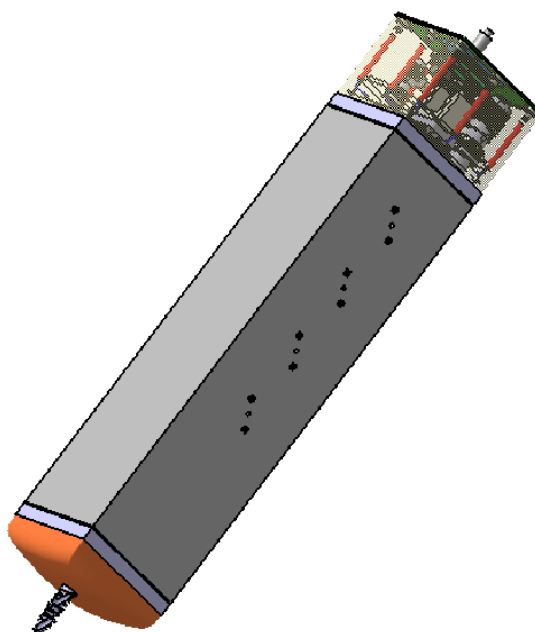


FIGURE 2.4: Rendering of the current version of IceMole (Credits: EnEx-nExT)

3

DERIVATION OF REQUIREMENTS

In the context of the [EnEx-nExT](#) research, a scientific payload for in ice detection of potential life was investigated. The payload is considered to be operational for the latest generation of IceMole, which means that the strict constraints on the size of the payload have to be considered. The instrument to be designed was selected to be a Raman spectrometer, the most promising instrument in terms of performance, size, technological assessment and power requirement in order to be able to detect potential living micro-organisms in ice. Therefore, with a view to designing a system that is targeted to be used in practical applications, the following work was carried out considering a systems engineering approach.

Systems engineering allows to develop an operable system that meets requirements within imposed constraints, considering and balancing the contributions of structural, mechanical, electrical, software, systems safety, and power engineers, plus many others, to produce a coherent whole [Larson et al., 2009, p.3]. It is a methodical, disciplined approach for the design, realisation, technical management, operations and retirement of a system, i.e. a set of interrelated components working together to accomplish a common purpose [NASA, 2007, p.3]. Another detailed definition for systems engineering is provided by the US Air Force Military Standard 449A (1974), in which it is identified as the efforts to: *(1) transform an operational need into a description of system performance parameters and a system configuration through the use of an iterative process of definition, synthesis, analysis, design, test and evaluation; (2) integrate related technical parameters and ensure compatibility of all related, functional, and program interfaces in a manner that optimises the total system definition and design; (3) integrate reliability, maintainability, safety, survivability, human and other such factors into the total technical engineering effort to meet cost, schedule and technical performance objectives* [US Air Force, 1974]. Therefore, following a systems engineering approach means to focus on the interdisciplinarity of the project in order to succeed in the realisation of a successful, robust and trustworthy system.

According to this field, the National Aeronautics and Space Administration ([NASA](#)) has defined a precise way of developing a system, and it has set a precise project life cycle, shown in [Figure 3.1](#), which indicates the categorisation of what has to be done to accomplish a project. As can be noticed, every project is divided into two major phases, formulation and implementation, in turn subdivided into project-level phases, separated by Key Decision Points ([KDP](#)), which determine the readiness of the project [Larson et al., 2009, p.18][NASA,

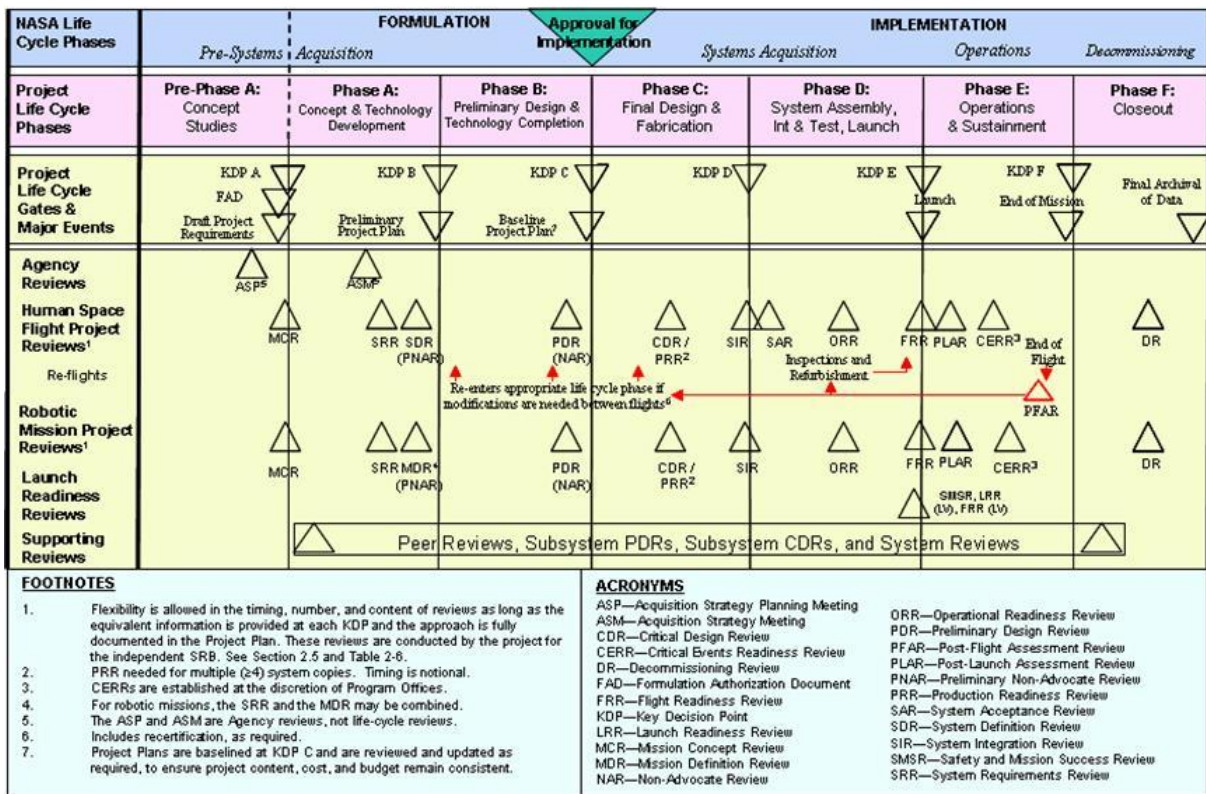


FIGURE 3.1: NASA project life cycle (Credits: NASA NPR 7123.1)

2007, p.19]. In this project, the entire formulation phase was fully elaborated: ideas and alternatives for the concept were elaborated, the feasibility determined, the system-level requirements derived, and a preliminary design for each product generated [NASA, 2007, p.7].

In particular, this Chapter deals with the preliminary tasks of the life cycle. Hence, it focuses on the definition of the need and the context of the project and the system to design. It summarises the preliminary concept studies that brought to the choice of the selected system and it presents the preliminary considerations on the concept and its top-level requirements. These topics are discussed in Section 3.1. Then, the technical constraints and the boundaries for the system to comply are presented in Section 3.2, so as to better identify the guidelines that need to be followed and the operational context in which the designed system will operate. From this analysis, the high-level technical system requirements are derived in Section 3.3, considering the main aspects that characterise the project: miniaturisation and biosignatures detection, which drive the design of the Raman spectrometer.

3.1. NEED ANALYSIS

Recently, the exploration in icy environments has gained particular attention from the scientific community as well as the space community. In fact, some features of ice were identified as particularly interesting for biology research: ionic impurities result to be insoluble in ice crystal structure and, when in contact with mineral surfaces, ice develops a nanometre-thick film of unfrozen water. These reasons, along with the fact that water is an essential element for life to arise, allow the scientists to believe that ice may have preserved habitats for life, both on Earth and on those celestial bodies well-renowned by now to have surface or sub-

surface water, such as Mars and the icy moons of Jupiter and Saturn [Price, 2007]. This interest in the habitability of icy environments complies with the research topics of astrobiology, whose aim is to study the present, past and/or future life in the whole Universe [Horneck et al., 2016].

The astrobiology research has now gained so much attention that even in the context of the [EnEx](#) initiative and IceMole development is now a priority task. Therefore, one of the current objectives of the research project focuses on the chance of using a payload capable of perform biological measurements, accomplishing the aim of detecting potential living organisms by their biosignatures. In the following statement, the drive of this whole project is summarised considering both the current terrestrial and the future extraterrestrial applications of [EnEx](#):

MISSION NEED *There is a need to provide for biological measurements in terrestrial applications, so as to detect potential living forms and it is necessary to miniaturise the systems, with a view towards space applications.*

This need underlines the major features of this project and its main goals, by using a precise set of words. *Biological measurements* reflect exactly the aspiration of the scientists of detecting elements in the samples that can be linked to life. This aspect complies both with a terrestrial application and with a space one. For the latter, the main experimental aspect of the project is considered: *miniaturisation* complies with the current trend of reducing size and, therefore, cost of the systems, so as to increase the availability of designing and launching space missions.

To fulfil these main goals, a preliminary study of concepts was carried out during a three-months internship, in order to select the best solution to perform the required measurements and to promise a miniaturised solution, applicable in space. Because of the constraints dictated by the [EnEx](#) initiative, the preliminary choice of concepts was made among technologies that are suitable in performing biological measurements in situ. The choice of performing measurements in situ is due to the fact that return to surface (or to Earth) is not always, often never, possible. To select the best payload, a trade-off in terms of performance, size, power and technology assessment was performed considering as options: a Gas Chromatograph-Mass Spectrometer ([GCMS](#)), a Raman spectrometer, a fluorescence spectrometer, and an antibody microarray. Among these concepts, the Pugh matrix in [Table 3.1](#)

TABLE 3.1: Pugh matrix for the selection of the life detection instrument [Russano, 2017]

Criteria	Weighting Factor	GCMS	Raman Spectrometer	Fluorescence Spectrometer	Antibody Microarray
Performance	5	1	1	0	-1
Size	5	-1	1	1	1
Power	3	0	1	0	0
Technology Assessment	2	1	0	0	0
Total		2	13	5	0

shows that one option stands out as the best: a Raman spectrometer. A deep explanation about this trade-off and the reasoning behind the filling of the matrix can be found in Russano [2017].

A Raman spectrometer is indeed able to recognise samples by measuring the inelastic scattering of light, related to molecular vibrations. It allows to obtain both biological and mineral measurements, requiring a minimum amount of sample for which little or no preparation is needed. It is a non-destructive technique and gives no problems in water measurements [Tarcea et al., 2008]. A better insight on how Raman spectroscopy works is given later in Chapter 4.

The amazing promises of this technology drove the aim of this project, that was indeed the design of such an instrument, taking care of the IceMole probe uses and developments. The following mission statement summarises this objective:

MISSION STATEMENT *Designing a Raman spectrometer that is able to perform in situ biological measurements and that fits on the miniaturised version of the IceMole subsurface probe.*

From this sentence, the main drivers of the project are set: from one side, the scientific aspect is highlighted with *in situ biological measurements*; from the other, the expression *the miniaturised version of IceMole* makes clear that the instrument has to comply with the technical constraints dictated by the new design of the probe. As a consequence, the top-level mission requirements were derived and they are shown in Table 3.2. Notice that for each statement a rationale is presented, so as not to create capabilities, i.e. functional requirements, that are not needed. Each requirement presents an Identifier (ID), so as to keep traceability for later derivations, and it is associated to a standard Verification Method (VM), that can be Demonstration (D), Testing (T), Inspection (I), Analysis (A) or the combination of two or more. The aspects related to the VM are then elaborated in a preliminary verification plan in Part III.

The requirements concern the main aspects of the system to design: first of all, they underline the importance of performing in situ measurements that can provide significant results in detecting potential biosignatures; then, they consider the integration into the new generation of IceMole, which means that the instrument has to comply with the probe, its operations and with the same requirements on autonomy and sterilisation. Notice that these top-level requirements support the mission need presented above, emphasising what is particular relevant for the system to design and which are the main tasks to accomplish. However, they are not specific requirements, they only present the operational terms of the systems and are solution independent [Larson et al., 2009, pp.47-48].

3.2. TECHNICAL CONSTRAINTS

The design and the development of the system strongly depend on its operational context: the EnEx initiative dictates the basis, so as the working principle and the new development of the IceMole probe. Both EnEx and IceMole were deeply described during two different literature studies (Russano [2016, 2017]) and presented in Chapter 2, therefore only the main critical points necessary for the derivation of requirements are summarised hereafter.

TABLE 3.2: Top-level mission requirements

Req. ID	Requirement	Rationale	Reference	VM
SYS-01	<i>The system shall perform measurements of the sample in situ</i>	The operational context requires the measurements to be performed in situ because the return of the sample to surface (or Earth, in space applications) is not possible	Mission statement; Chapter 2	D
SYS-02	<i>The system shall be able to identify potential biosignatures in the sample</i>	Biosignatures are related to potential living forms by definition	Mission statement; Horneck et al. [2016]; Price [2007]	A,T
SYS-03	<i>The system shall comply with the miniaturised design of IceMole</i>	The miniaturisation aspect is important in order for the system to be carried by the probe	Section 2.1	A,I
SYS-04	<i>The system shall work in terrestrial applications of IceMole</i>	EnEx initiative is still in the terrestrial application phase, so there is no need to design the system for space	Chapter 2	T
SYS-05	<i>The system shall operate autonomously</i>	Autonomy is an essential aspect of exploration missions because of long time delays in command transmissions	Chapter 2	D
SYS-06	<i>The system shall comply with NRC Antarctica CoC recommendation 7</i>	EnEx operates in sites with strict contamination regulations	Chapter 2	T

The aim of the current [EnEx](#) project is *to develop an autonomous steerable subsurface ice probe to demonstrate autonomous navigation in deep ice* [Konstantinidis et al., 2015b]. This statement dictates the first constraints that the outcome of this project will face, the environmental constraints. The operational context is deep ice, hence the system has to be able to withstand particular conditions of pressure and temperature. Notice that in this case these are terrestrial conditions, while they can change once the mission aim will be moved towards space applications, in particular to Enceladus' conditions. This is discussed later in Chapter 10.

Another aspect concerning the environmental constraints is contamination: the sites in which [EnEx](#) performs its testing are subjected to strict regulations of contamination, e.g. the Blood Falls, in Antarctica, at the borders of Taylor Glacier, is preserved by the National Resource Council (NRC) [CoC](#) recommendation 7. This means for the system to comply with a very high level of sterilisation, the same to which the whole probe is subjected to.

Then, the need of interfacing with the probe into which the system will be integrated implies other constraints. The new current design of IceMole shown in Figure 2.4 is based on

reducing its size in order to verify the applicability of the probe for space missions. It now presents a cross sectional area of 80 mm × 80 mm. This aspect results in the most challenging constraint for the system to be designed: it is fundamental to consider the volumetric constraints deriving by the new design of the probe which in turn influence the performance of the optical system. Few relatively new miniaturised concepts have been proposed for a similar use, but the miniaturisation level required by the design of IceMole has not been achieved before. However, these concepts can be used as guidelines to design the system, since they already underlined the critical points to be faced, such as in Blacksberg et al. [2016]; Courreges-Lacoste et al. [2007]; Edwards et al. [2012]; Rull et al. [2010, 2011]; Wang et al. [2003].

The last important constraint that has to be taken into account is the power requirement: currently, IceMole is powered by surface RTGs which transmit electrical power via a three-conductor power cable. Therefore there is not a strict requirement linked to power. However, the miniaturisation of the concept requires that also power is reduced and this will be achieved in the next steps of the development of the probe. Hence, also the payload must comply with this decreasing of power demands and has to limit the amount of power required to operate.

3.3. TECHNICAL SYSTEM REQUIREMENTS

According to the operational scenario of the IceMole probe and its current design, the requirements of the system to design can be derived. Considering the integration into the probe, more specific system requirements can be derived. Figure 3.2 shows the path to arrive at system requirements, starting from the mission need. Notice that the whole project derives from a capability-driven approach, that is fitting on the new miniaturised generation of IceMole probe, and not from a science-driven one.

Therefore, the fact that the Raman spectrometer has to be integrated into the probe implies that the described constraints in Section 3.2 are to be taken into account. In this way, the final system can be operational on the probe and during its applications. Table 3.3 shows the technical requirements directly dependent on the constraints and they practically represent how the system to be designed will interface with the already existing IceMole. The

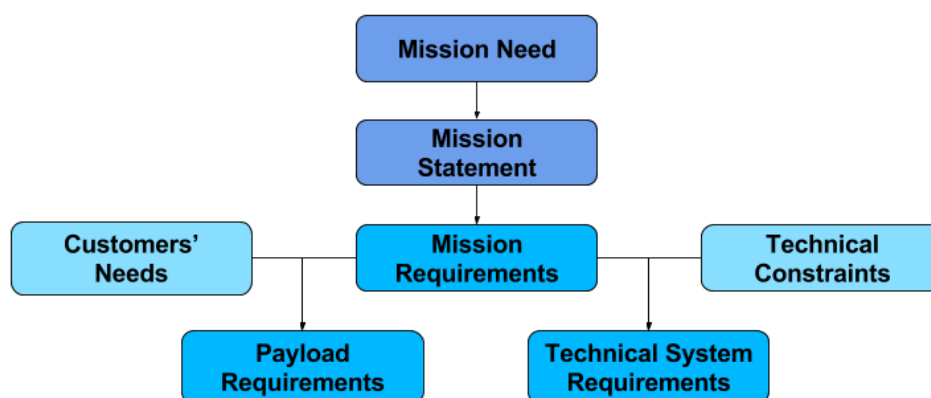


FIGURE 3.2: Derivation of requirements (adapted from Larson et al. [2009])

TABLE 3.3: Technical requirements

Req.ID	Requirement	Rationale	Reference	VM
SYS-03- IM-01	<i>The system shall have a size of less than 65mm × 65mm × 150mm</i>	The new design of IceMole dictates constraints on volume	Table 3.2; Section 3.2	A
SYS-03- IM-02	<i>The system shall weigh less than 2kg</i>	The new design of IceMole dictates constraints on mass. The value is dictated by the developing concept of ExoMars Raman laser spectrometer	Table 3.2; Edwards et al. [2012]	A
SYS-03- IM-03	<i>The system shall work at 24V DC</i>	24V DC is IceMole power bus	Table 3.2	A
SYS-03- IM-04	<i>The system shall consume less than 5W, when in stand-by mode</i>	IceMole has a limited amount of power available	Table 3.2; Section 3.2	A
SYS-04- IM-01	<i>The system shall operate under atmospheric pressure</i>	IceMole terrestrial operations work at atmospheric pressure	Table 3.2; Section 3.2	T
SYS-04- IM-02	<i>The system shall work in a temperature range between -15 and 15°C</i>	IceMole operates in icy environments, but the surrounding water of the probe should be at ~ 0°C, because it has melted	Table 3.2; Section 3.2	T
SYS-04- IM-03	<i>The system shall not be space-qualified yet</i>	IceMole is still in its terrestrial development, therefore it is not necessary to design a system that is already space-qualified	Table 3.2; Chapter 2	
SYS-05- IM-01	<i>The system shall communicate through the same protocol of the probe</i>	IceMole communicates with surface through a cable and same protocol means easier ways to do that because there is no need for translation of data	Table 3.2	A,D
SYS-06- IM-01	<i>The system shall undergo the same sterilisation process as the probe</i>	IceMole sterilisation process has been already proved to be successful	Table 3.2	T

parent requirements can be identified in SYS-03 and SYS-04 which consider the miniaturisation aspect and the operational constraints of the [EnEx](#) initiative. All the requirements relates to the characteristics of IceMole: its volume, its mass, the power requirement, the environmental conditions (pressure and temperature), data communication and sterilisation process. For this reason, they are identified with the acronym **IM** and they were derived in accordance with the [EnEx-nExT](#) research group, who is working on the development of the probe.

4

RAMAN SPECTROSCOPY

Raman spectroscopy is a spectroscopic technique based on measuring the inelastic scattering of monochromatic light, that provides information about molecular vibration and rotation and that allows sample identification and quantification. Hence, Raman spectroscopy uses scattered light to gain knowledge about molecular vibration which can provide information on quantitative and qualitative analysis of the individual compounds. It is in fact a technique particularly used in chemical and biological applications because of the specificity of the relation between vibrations and chemical bonds of molecules [Kudelski, 2008; Princeton Instruments, 2017].

The Raman effect has been named after Sir Chandrasekhara Venkata Raman, an Indian Nobel-Prize-winner physicist who first reported this phenomenon in 1928. Studying the scattering of light, Sir Raman and his student Kariamanickam Srinivasa Krishnan noticed that there was energy exchange between the incident photon and the internal excitations of the scattering medium, corresponding to the partial exchange of energy into atomic vibrations of molecules. This is related to the inelastic nature of this phenomenon, for which the light is scattered with higher or lower frequency with respect to the incident beam [Adar, 2001; Das and Agrawal, 2011; Raman and Krishnan, 1928].

The development of this technique however did not followed a precise and solid path along the years, but it was tied to the availability and the innovation of the instrumentation. In fact, the progress was very slow mainly because of the weakness of the Raman signal itself: every $10^6 - 10^8$ photons scattered, only one is Raman scattered. With the introduction of more sensitive and advanced components, Raman spectroscopy has gained more and more attention from the scientific community: for instance, the introduction of the laser as excitation source particularly enhances the magnitude of the phenomenon, as well as the use of Charged-Coupled Device (CCD) improves the detection and the new Rayleigh rejection filters helps in reducing the light background effects. Moreover, most of the components have been miniaturised so that they can now be used in portable hand-held systems, which promise a potential application in space [Adar, 2001; Kudelski, 2008].

Raman spectroscopy is a complementary method to mid-InfraRed (IR) spectroscopy: both the techniques are based on vibrational spectroscopy so as to provide information on the molecular structure. Together, the spectra obtained from these techniques give a com-

plete overview of the composition of the sample. Anyway, Raman presents few advantages with respect to IR spectroscopy: little or no sample preparation is required; optical fibres can be used; water is not a weak Raman scatterer as for the IR domain; and the Raman spectra are "cleaner" as their bands are narrower [Larkin, 2011, pp.1-5] [Serdyuk et al., 2007, pp.573-599].

Hence, Raman spectroscopy results to be a very promising tool at the moment: it allows to determine complete chemical composition for any inorganic, organic and biological compounds as well as to identify the principal mineral phases; it has a good performance in water domains and it requires little or no sample preparation at all. It is a powerful non-destructive technique that allows to analyse solid, liquid or gaseous samples [Tarcea et al., 2007, 2008]. These reasons are at the basis of the selection of the Raman spectrometer as topic of this work.

Section 4.1 introduces the physical and mathematical aspects behind the phenomenon of Raman scattering, deriving the relationships that tie the main parameters of Raman spectroscopy and trying to obtain an equation for the intensity of the phenomenon. After that, Section 4.2 shows the equations for deriving the signal of the instrument according to the intensity of the spectrum and the geometrical factors concerning the optics. Moreover, a deep discussion concerning the Signal-to-Noise Ratio (SNR) is presented, so as to obtain the best performance for the instrument. Then, the major components of a Raman spectrometer are presented in Section 4.3, with a view to understanding how each of them affects the performance. Finally, the methods to enhance the weakness of the Raman effect are described in Section 4.4, among which Resonance Raman Spectroscopy (RRS) and Surface-Enhanced Raman Spectroscopy (SERS) are shown as the best.

4.1. THEORY

During the interaction of light with matter, the photons can be absorbed or scattered, or they can not interact at all with the matter and pass it through. What happens depends on energy characteristics of the incident photons, which is described by

$$\mathcal{E} = h\nu_0 \quad (4.1)$$

where h is Planck's constant, equal to $6.62607004 \times 10^{-34}$ J s [NIST, 2017] and ν_0 is the incident frequency. If this energy equals the energy gap between the ground state of a molecule and one of its excited states, the photon may be absorbed and the molecule promoted to the higher energy state. On the other hand, if that does not happen, the photon can be scattered without the need for its energy to match with the energy gap [Smith and Dent, 2013, pp.1-7].

Figure 4.1 shows how the scattering can happen: the dominant process is what is called Rayleigh scattering, when the photons are scattered with small changes or no changes at all from the monochromatic incident scattering ν_0 . This is an elastic scattering. If instead the process is inelastic, the energy of the scattered photons is different from the incident one, higher or lower, and the effect is called Raman scattering, which has a much weaker intensity with respect to the first scattering [Smith and Dent, 2013, pp.1-7].

Theoretically speaking, scattering of light is based on the molecular deformations due to the polarisation induced by the oscillating electric field of the incoming light. The induced

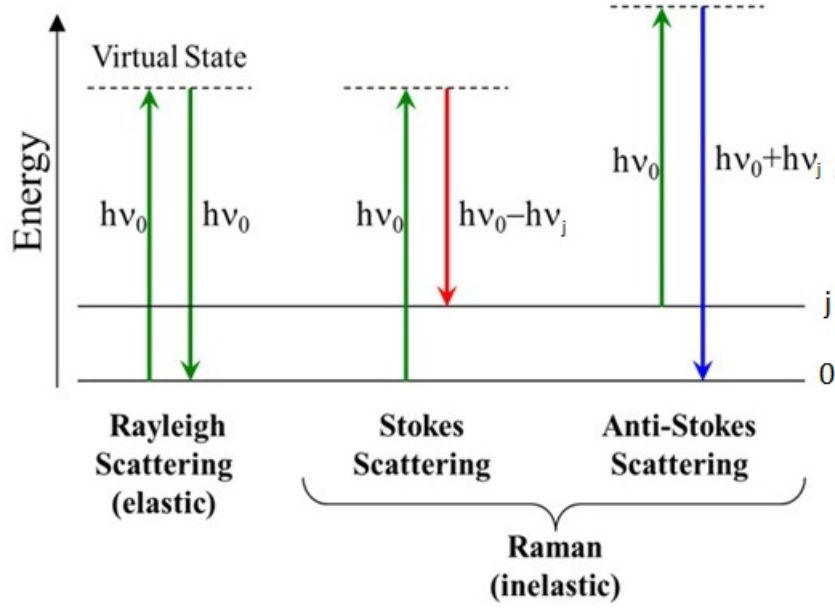


FIGURE 4.1: Energy transitions for Rayleigh and Raman scattering

dipole radiates back the scattered light, with or without exchanging energy with vibrations in the molecule [McCreery, 2000, p.15]. As stated by McCreery [2000, p.15], the induced polarisation \vec{P} scales with polarisability α and the incident electric field \vec{E} as

$$\vec{P} = \alpha \vec{E} \quad (4.2)$$

The above Equation (4.2) is well represented by Figure 4.2, in which the scattering is only shown in 90° and $\sim 180^\circ$ directions, but it can actually be in various directions. However, the oscillating nature of light is underlined, because the incident optical electric field is indeed governed by

$$E = E_0 \cos(2\pi\nu_0 t) \quad (4.3)$$

On the other hand, the polarisability α of Equation (4.2) is a tensor dependent on the molecular vibrations. The latter are considered to be composed of normal modes Q_j , of which there are $3n - 6$ in a molecule with n atoms (or $3n - 5$ for linear molecules) [McCreery, 2000, p.15].

$$Q_j = Q_j^0 \cos(2\pi\nu_j t) \quad (4.4)$$

Once the normal modes are defined as in Equation (4.4), the polarisability can be expressed as a Taylor series in [Vandenabeele, 2013, p.3]

$$\alpha = \alpha_0 + \sum_j \left(\frac{\partial \alpha}{\partial Q_j} \right) Q_j + \frac{1}{2} \sum_{j,k} \left(\frac{\partial^2 \alpha}{\partial Q_j \partial Q_k} \right) Q_j Q_k + \dots \quad (4.5)$$

In a first approximation, only the first two terms in this Equation can be considered. As result of Equations (4.3) and (4.5) and considering that $\cos a \cos b = [\cos(a+b) + \cos(a-b)]/2$, Equation (4.2) can be manipulated as [McCreery, 2000, p.16]

$$P = \alpha_0 E_0 \cos(2\pi\nu_0 t) + E_j Q_j^0 \left(\frac{\partial \alpha}{\partial Q_j} \right) \frac{\cos(2\pi(\nu_0 + \nu_j) t) + \cos(2\pi(\nu_0 - \nu_j) t)}{2} \quad (4.6)$$

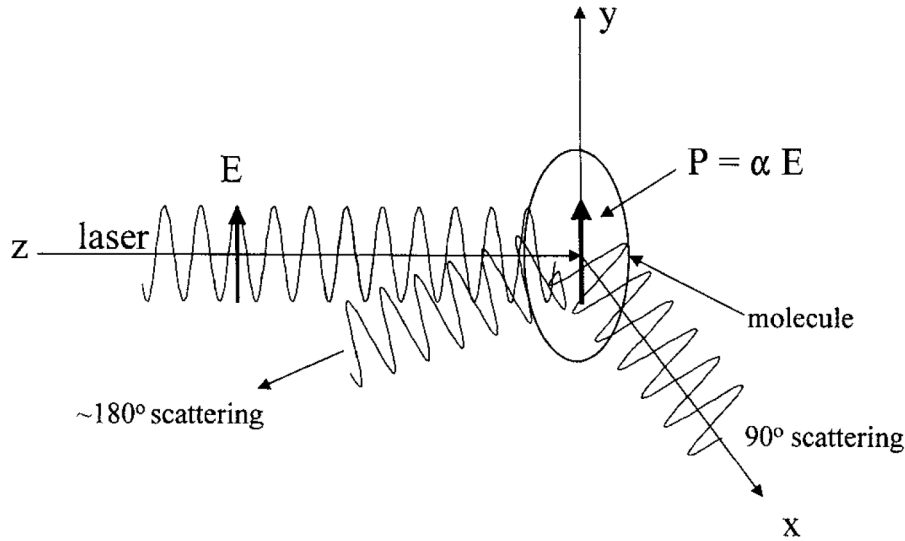


FIGURE 4.2: Polarisation induced in a molecule's electron cloud by an incident optical electric field \vec{E} . Scattering is shown in 90 and $\sim 180^\circ$ direction [McCreery, 2000, p.16]

As claimed by McCreery [2000, p.16], Equation (4.6) demonstrates that light is scattered at three different frequencies. The first term of the relation corresponds to the Rayleigh scattering, at the same frequency of the incident light and with a magnitude proportional to α_0 , the inherent polarisability of the molecule. The second term is the anti-Stokes Raman scattering, which occurs at $\nu_0 + \nu_j$, while the last term is the Stokes Raman scattering at $\nu_0 - \nu_j$. Indeed, this is what is shown in Figure 4.1.

What is important to notice is that both polarisation and scattering, no matter if elastic or not, are strongly dependent on the intensity of the excitation source, usually a laser. Moreover, Raman scattering is yielded only by vibrations that change the polarisability (i.e. the derivative in Equation (4.6) is different from 0). But most importantly, Raman shifts can be both positive and negative [McCreery, 2000, pp.16-17].

RAMAN INTENSITY

It is important to keep in mind that Raman scattering is a very weak effect, it has $\sim 10^{-6}$ times the intensity of Rayleigh scattering. In fact, the derivative $\partial\alpha/\partial Q_j$ is generally much smaller than α_0 . Therefore, the Raman intensity, expressed in W, can be computed from [McCreery, 2000, p.18]

$$I_R = \mu(\nu_0 \pm \nu_j)^4 \alpha_j^2 Q_j^2 \quad (4.7)$$

where μ is a constant. As can be noted, the intensity is strictly related to the frequency of Raman scattering to the fourth power, which in turn depends on the excitation frequency. Equation (4.7) can also be written in terms of wavenumbers, which are expressed in cm^{-1} and are equal to $\bar{\nu} = \nu/c = \lambda^{-1}$, where c is the light velocity in vacuum ($c = 299792458 \text{ m/s}$ [NIST, 2017]). As so, the relation becomes [McCreery, 2000, p.18]

$$I_R = \mu'(\bar{\nu}_0 \pm \bar{\nu}_j)^4 \alpha_j^2 Q_j^2 \quad (4.8)$$

where μ' comprises the factor c^4 .

However, usually the most important parameter in the description of Raman intensity is the scattering cross section σ_j , which is empirically determined. This parameter depends proportionally on the probability of a photon to be Raman scattered with a particular Raman shift. The definition of Raman intensity is then expressed as [McCreery, 2000, p.20]

$$I_R = I_0 \sigma_j D dz \quad (4.9)$$

in which I_0 is the laser intensity, D is the number density of scatters (molecules/cm³) and dz is the path length of the laser in the sample, or the spectrometer depth of field. Confronting this last Equation (4.9) and Equation (4.7), σ_j is comparable and related to the frequency. This parameter is usually determined by quantitatively comparing the Raman signal for an unknown to that for a standard with known cross section, which is listed [McCreery, 2000, p.20].

Anyway, σ_j is often intended as the integrated cross section whose integration is over all directions of the sample and over the wavelength range of an entire Raman band. Therefore, in practice, a differential Raman cross section β , expressed in cm²molecule⁻¹sr⁻¹, has been identified in [McCreery, 2000, p.22]

$$\beta = \frac{d\sigma_j}{d\Omega} \quad (4.10)$$

where Ω represents the solid angle of collection. This parameter is a strong function of the angle of observation and the polarisation.

Another way to interpret Raman intensity is in photons/s. In this case, Equation (4.9) can be rewritten as [McCreery, 2000, p.21]

$$P_R = P_0 \sigma'_j D dz \quad (4.11)$$

in which σ'_j is indicated differently because it has a slightly different dependency from the frequency than σ_j . Considering Equation (4.10), Raman intensity can be restated in terms of β too, as [McCreery, 2000, p.30]

$$P_R = P_0 \beta D dz \quad (4.12)$$

where P_R is now the Raman scattering in a steradian of collection solid angle, rather than the total scattering in all directions. However, the incident laser light is usually expressed in terms of power density P_D (in photons/cm²s), so that the last relation becomes [McCreery, 2000, p.30]

$$P_R = P_D \beta D dz \quad (4.13)$$

The last important parameter in the description of the intensity of Raman scattering is the specific intensity, often referred to as radiance [McCreery, 2000, p.30]:

$$L = P_D \beta D K \quad (4.14)$$

with K denoting a geometrical factor tied to the observation geometry. The specific intensity mainly depends on the sample with β and D and on the laser with P_D , but not on spectrometer parameters.

4.2. PERFORMANCE

Equation (4.13) allows to predict the overall Raman scattering intensity, considering the dependency on the sample and on the laser source. However, to be analysed, the scattering magnitude needs to be translated into a usable Raman signal, through [McCreery, 2000, p.35]

$$S_a = L_a C t_s \quad (4.15)$$

This relation reduces the discussion to a single Raman shift or a single analyte: S_a is the signal due to the analyte of interested, L_a is the radiance for a specific Raman band of a particular analyte, C is a collection optics function in $\text{cm}^2 \text{sr e}^- \text{photons}^{-1}$ and t_s is the single-channel sampling time. It is important to underline that the specific intensity is a function of the sample and laser power, while C depends on collection and detection characteristics, and it can be expressed as [McCreery, 2000, p.37]

$$C = A_D \Omega_D T \eta \quad (4.16)$$

where η is the quantum efficiency of the instrument, i.e. the fraction of photons reaching the detector; A_D is the sample area monitored by the spectrometer and collection optics, which is usually determined by a limiting aperture in the spectrometer; Ω_D is the solid angle collected by the spectrometer and transmitted into the wavelength analyser, which is defined as

$$\Omega_D = \frac{\pi}{4(f\#)_D^2} \quad (4.17)$$

in which $f\#$ is the aperture ratio or f-number of the optics. Finally, T is the transmittance, equal to the fraction of light within A_D and Ω_D monitored by the spectrometer that reaches the detector. It consists both of the transmission of the optics and the transmission within the spectrometer itself [McCreery, 2000, p.37]. Now that all parameters have been defined, Equation (4.15) can be manipulated by substituting in it Equations (4.14) and (4.16), to obtain [McCreery, 2000, p.40]

$$S = (P_D \beta D K) (A_D \Omega_D T \eta) t_s \quad (4.18)$$

Figure 4.3 summarises this discussion, presenting a schematic of the collection variables defined above.

Because Raman scattering is a very weak effect, as explained in Section 4.1, there are some interferences and side-effects that need to be watched out when designing a Raman spectrometer. They can be found deeply described in Vandenameele [2013, pp.39-45]. First of all, absorption must be avoided. The absorbed particles are released by radiationless transition to heat, that is transferred to the environment. Absorption reduces the intensity of Raman scattered radiation, because the number of incident photons decreases. Another parameter that must be carefully handled is the intensity of the laser beam. In fact, it is true that the Raman signal is proportional to it, but actually if the input energy in the system is too high, that might occur in some destructive effects, such as heating, photo-decomposition or laser ablation of the sample. However, the most severe interference with Raman signal is due to fluorescence. This effect occurs when the molecule is excited to a certain electronic state and then decays to a lower energy level and to the ground electronic state, while emitting radiation. Methods to avoid fluorescence are the selection of the excitation wavelength, using longer values, or the use of post-processing mathematical tools [Vandenameele, 2013, pp.39-45]. Last big problem encountered by Raman spectroscopy is due to the presence of

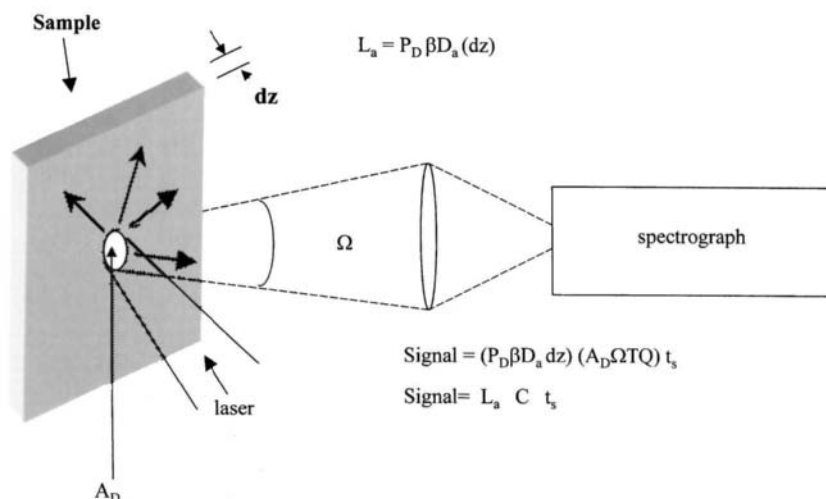


FIGURE 4.3: Schematic of collection variables [McCreery, 2000, p.36]

ambient light or background radiation. They cannot be avoided in all measurements and they negatively influence the noise signal.

SIGNAL-TO-NOISE IN RAMAN SPECTROSCOPY

Every spectroscopic technique is limited in extracting analytical information by the noise. With this term, all possible detected signals that do not contain relevant information are intended [Vandenabeele, 2013, p.95]. All those effects that are to be avoided can be considered noise, such as fluorescence, spikes or background radiation.

The parameter that characterises the noise is the Signal-to-Noise Ratio (SNR), for which the efforts to increase it are always huge. The SNR for a particular measurement is rigorously defined as the inverse of the relative standard deviation of the measured value [McCreery, 2000, p.49]

$$\text{SNR} = \frac{\bar{S}}{\sigma_y} \quad (4.19)$$

where \bar{S} is the average peak height and σ_y is its standard deviation. Because of statistical nature of Equation (4.19), the most accurate determination of the SNR is by acquiring several repetitions of the spectrum. Otherwise, another valid solution is to subtract two successive spectra so as to eliminate the inputs of the Raman band and background, and derive in this way only the noise value [McCreery, 2000, p.50].

Therefore, considering that the value for S was already derived in Equation (4.18), an estimate for σ_y is now needed. The total noise contains contributions of different factors such in [McCreery, 2000, p.52]

$$\sigma_y = \sqrt{\sigma_S^2 + \sigma_B^2 + \sigma_D^2 + \sigma_F^2 + \sigma_r^2} \quad (4.20)$$

where σ_S is the standard deviation of the signal, σ_B is the standard deviation of the background, σ_D is the standard deviation of the dark signal, σ_F is the flicker noise and σ_r is the readout noise.

If no other noise sources exist, the standard deviation of S is derived by laws of statistics and it is defined as shot noise limit, which means that the standard deviation when counting any random event equals the square root of the number of events counted [McCreery, 2000, p.53]

$$\sigma_S = \sqrt{S} \quad (4.21)$$

Background is a general term used to refer to those detected photons that arise from the laser and sample and that are different from the Raman photons at the frequency of interest. In particular, background includes luminescence of cell, sample or optics and stray light, including fluorescence, thermal emission, Rayleigh scattering, and reflection [Blacksberg et al., 2016][McCreery, 2000, p.54]. Background magnitude can be expressed in similar terms to the signal, as [McCreery, 2000, p.54]

$$B = P_D \beta_B D_B K A_D \Omega T \eta t_S \quad (4.22)$$

where the subscript B indicates sample components generating background. Because of this relation, background is governed by shot noise as well:

$$\sigma_B = \sqrt{B} \quad (4.23)$$

The dark signal ϕ_D is the rate of spontaneous generation of electrons in the detector, caused mainly by thermal effects. Therefore, the electrons generated by this process are counted as [McCreery, 2000, p.56]

$$\sigma_D = \sqrt{\phi_D t} \quad (4.24)$$

Flicker noise is usually related to absorption or emission spectroscopy but it also applies to Raman, in case the variation in laser intensity causes proportional variation in Raman scattering and in the measured signal [McCreery, 2000, p.56].

Finally, readout noise depends on the process of converting electrons from the detector to a useful form, such as a digital value stored in a computer. It is intended as a standard deviation of a large number of readouts from a constant detector signal, even if it is not proportional to the measurement time [McCreery, 2000, p.57][Vandenabeele, 2013, p.99].

By substituting Equations (4.21), (4.23) and (4.24) in Equations (4.20) and (4.19), the final definition of the SNR can be obtained [McCreery, 2000, p.52]

$$\text{SNR} = \frac{S}{\sqrt{S + B + \phi_D t + \sigma_F^2 + \sigma_R^2}} \quad (4.25)$$

Obviously, if one or more contributions to the total noise are very big compared to the others, then these can be neglected and the noise is said to be limited.

4.3. INSTRUMENTATION

Instrumentation played a fundamental role in the development of Raman spectroscopy technique. In fact, its current promising employ in organic and inorganic measurements is mainly due to the development of its components such as [Slater et al., 2001]:

- The commercialisation and acceptance of Rayleigh rejection filters as effective replacements for zero-dispersion double monochromators

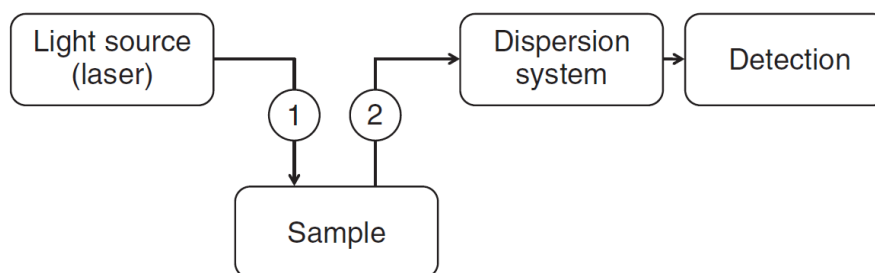


FIGURE 4.4: General diagram of a Raman spectrometer. 1 and 2 are the optics respectively to focus the laser and collect the scattered radiation [Vandenabeele, 2013, p.62]

- The availability of compact lasers
- The advent of the **CCD** detectors
- A refinement in sampling optics and devices
- The availability of powerful personal computers with associated software

Generally, a Raman spectrometer presents a configuration similar to the one in Figure 4.4, but components can change according to the tasks and options to achieve a defined requirement. A light source, usually a laser, excites a sample through a collimated beam, by means of the use of focusing optics (1 in the Figure). The excited scattered photons are collected by optics (2 in the Figure, this time) and transmitted to the spectrometer, where dispersion, i.e. separation of wavelengths, and detection happen [Vandenabeele, 2013, p.62].

According to the employed dispersive method, the market of Raman spectrometers distinguishes between two important types: dispersive/**CCD** Raman spectrometers, which rely on a dispersive grating for separation of light, and Fourier-transform (**FT**) Raman spectrometers, which instead use a Michelson interferometer. The main advantages and disadvantages of the two types of instruments are summarised in Table 4.1 [McCreery, 2000, p.79].

To fully understand the entries of this Table, all the components are analysed in the fol-

TABLE 4.1: Comparison of spectrometer types [McCreery, 2000, p.79]

	Advantages	Disadvantages
Dispersive/CCD	<ul style="list-style-type: none"> • Sensitive • Higher SNR • Laser $\lambda = 200 - 800$ nm (limited by response CCD) • Low laser power • (Usually) No moving parts 	<ul style="list-style-type: none"> • Resolution varies across spectrum • More fluorescence • Spectral coverage/resolution trade-off
FT-Raman	<ul style="list-style-type: none"> • Excellent frequency precision • Higher $A\Omega$ • Laser $\lambda \geq 1064$ nm • Better fluorescence avoidance • Good libraries 	<ul style="list-style-type: none"> • Lower SNR • Often high laser power • Full spectral coverage with constant resolution

lowing Subsections, with a view to understand how each of them influences the performance of the system and how they developed during the years. The components are presented in the same order through which the excitation light first and the scattered light then encounter them: so laser, filter, dispersive system and detector.

4.3.1. LASER

LASER originally stands for Light Amplification through Stimulated Emission of Radiation and it is an intense source of monochromatic light that has been introduced in Raman spectroscopy since the 1960s. The main characteristic of lasers is that they are very intense coherent light sources, which allow to obtain a narrow, collimated beam to direct to the sample [Vandenabeele, 2013, pp.61-100]. A laser consists of a gain medium, i.e. a material that amplifies light by stimulated emission; a mechanism to energise it, which is called optical or electrical pumping of the laser according to the way used; and something to provide optical feedback. Its performance is based on amplification of the signal through stimulated emission, which has as result that all particles emit electromagnetic radiation, whereby an intense, coherent laser beam is formed [Siegman, 1986, p.2].

Different lasers exist on the market, according to their specific optical characteristics and the desired power and wavelength. The main requirements that a laser used as excitation source for Raman spectroscopy has to satisfy are [Vandenabeele, 2013, pp.61-100]:

- Frequency stability
- Narrow bandwidth
- Low divergence

4.3.2. FILTER

As resulting from Equation (4.6), the main requirement for Raman systems is to filter out the radiation at the laser wavelength, so as to detect only the Raman shifts. The filter not only needs to reject the Rayleigh scattering, but it also has to reject the reflected laser radiation. This is fundamental because otherwise the Rayleigh scattering would be about 8 or more orders of magnitude more intense. There are two main categories of filters used in Raman spectroscopy [Slater et al., 2001]:

- Edge filters (long-pass or low-pass filters), which generally block all wavelengths above or below a certain threshold
- Notch filters (also called band-block filters), which differ from the first ones because they block a range of wavelengths and information are seen at low and high frequency. They are really small and efficient and they allow to reduce the size of the instruments [Smith and Dent, 2013, p.26].

According to their working principle, filters can be also classified as dielectric, holographic and absorption filters. The first type can be used both for edge and notch filters, they are based on the principle that the optical transmission functions can vary according to thickness, order and refractive index of dielectric coatings. They rely on interference. The holographic filters instead consist of two glass plates and a gelatine-based material in between, in which a standing wave pattern is generated. They generally have a superior performance in Optical Density (**OD**), i.e. how well the filter rejects a certain wavelength range,

but, however, they rapidly degrades. On the other hand, the absorption filters in the classical configuration of colour filters are generally too gradual, so much of the Raman spectrum can be lost [McCreery, 2000, pp.170-178][Vandenabeele, 2013, pp.61-100].

Besides these technologies, other filtering approaches were used in Raman spectroscopy before the advent of these usable filters: for instance, an early approach for creating a notch filter was implemented in the triple monochromator, which is able to attenuate the laser wavelength by a factor up to 10^{10} and allows to detect signal with very small Raman shift.

4.3.3. DISPERSION SYSTEM

The dispersion system is probably the main component of a Raman spectrometer, or at least the one that plays the major role. In fact, as spectrometer, the instrument has to be able to disperse the light, in function of the wavelength.

The classification of spectrometer types depends on the dispersion element or approach used. The dispersion can happen either as a function of space, for dispersive/[CCD](#) Raman spectrometers, or as a function of time, in [FT](#)-Raman spectrometers. Usually, the elements that are employed are prisms, gratings or interference of split components. Prisms are not suitable for miniaturisation, therefore they are be treated in this project; on the other hand, gratings characterise dispersive Raman spectrometer, while interferometers are used in [FT](#)-Raman spectroscopy [Vandenabeele, 2013, pp.61-100][Wolffenbuttel, 2005].

A diffraction grating is a linear repetition of elements, that can be reflecting or transmitting. Reflection types have a series of small steps or grooved mirror elements, whose distance is comparable to the wavelength of the light to be dispersed. The output reflection constructively interferes at different angles for each wavelength, creating the spectrum. Transmission types have a similar principle, except that they have a surface relief that produces a stepped-phase discontinuity in transmission through a medium of higher reflective index, as opposed to a reflective-phase discontinuity. Gratings have particular advantages: they have a broad wavelength range and the ability to scan. However, they are very sensitive to contamination and suffer from "dropouts", i.e. large changes in diffraction efficiency [Slater et al., 2001]. The typical configuration of a spectrograph using a grating as dispersive element is shown in [Figure 4.5a](#). The simplest configuration is called Czerny-Turner configuration. It lets light pass through a narrow entrance slit and then convert it into a parallel beam by a collimating lens or mirror. The dispersion occurs at the grating and the resulting spectrum is projected on the exit slit using a focusing lens or mirror [Wolffenbuttel, 2005]. This configuration allows simplicity and wavelength flexibility, but it also presents some disadvantages such in the imaging performance, therefore it has been implemented in new elaborated variants [Slater et al., 2001].

On the other hand, an interference-based spectrometer involves splitting of the incident light beam into two parts which interfere with each other. The two beams have a well-defined difference in length, whose variation in time allows to scan a defined part of the spectrum. According to this value, constructive or destructive interference occurs and the detector registers a signal or not, respectively [Wolffenbuttel, 2005]. A [FT](#)-Raman spectrometer usually relies on a Michelson interferometer, shown in [Figure 4.5b](#). This set-up consists of a beamsplitter and two mirrors, so as two optical paths are defined. One of the mirrors is

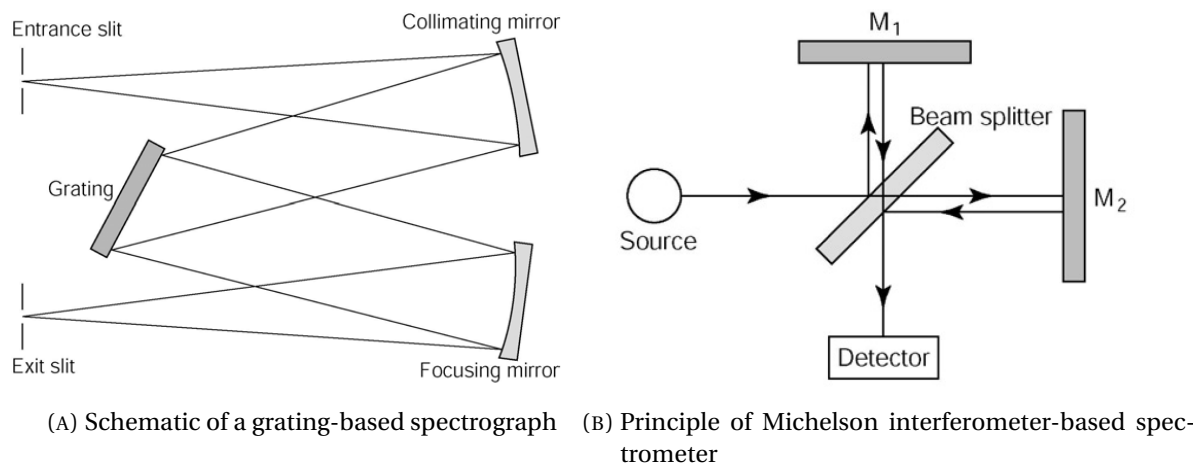


FIGURE 4.5: Schematics of dispersive systems [Wolffenbuttel, 2005]

fixed, the other can be translated during the experiment. Light beams with different wavelengths are sent to the interferometer, and each of these generates its own pattern, which are superimposed and detected by the detector. Multiple scans are usually recorded one after the other and added together, so as to increase the quality of the detection [Vandenabeele, 2013, pp.61-100][Wolffenbuttel, 2005].

4.3.4. DETECTOR

Because of the weakness of the Raman effect, it is fundamental to select a detector that is very sensitive and low-noise. The main parameters for the choice of the best detectors in Raman applications are therefore listed [McCreery, 2000, pp.179-202][Vandenabeele, 2013, pp.61-100]:

- Quantum efficiency η , the probability that a photon that impinges onto the detector generates a measurable signal
- Response curve, the graph showing η in function of the wavelength (or the Raman shift)
- The number of channels N_C , which is usually the number of signals that can be measured independently from each other (for a CCD it is the number of pixels along the wavenumber axis)
- The dark signal ϕ_D , defined as the average generation of electrons when the detector is not exposed to light
- The dark noise σ_D and the readout noise σ_R

Ideally, a detector should operate in a shot-noise-limited regime, with long integration times that yield to a good SNR. It should have a high quantum efficiency, a large number of closely spaced elements, wide dynamic range (i.e. the difference between the maximum and minimum detectable signal levels), and wide wavelength range, which depends on the excitation laser used and on the location of the bands of interest [Slater et al., 2001].

According to the number of channels, detectors are distinguished in single-channel and multichannel detectors.

Single-Channel Detectors. Historically, they were the first ones to be used: they have a high sensitivity but they suffer from a very high background signal. However, the main disadvantage is that it is possible to measure only a single wavelength, so that the complete spectrum needs to be achieved with repetitively time-consuming measurements [Vandenabeele, 2013, pp.61-100].

The first modern electronic detector available for Raman spectrometer was the PhotoMultiplier Tube (**PMT**). In general, a **PMT** works in this way: the photon collides with a photocathode, which is a metal surface with a low work function for photoelectron generation. If the energy of the photon exceeds the work function, a photoelectron is generated with a probability equal to η , which now can be defined as the fraction of photons that create photoelectrons and results in a signal. The ejected electron is then accelerated and amplified as in a conventional **PMT**, until a pulse of several thousand electrons strikes the anode, and the pulse is detected by a pulse height discriminator [McCreery, 2000, p.181]. The major drawbacks of the **PMTs** are the long time required to measure a whole spectrum, the reduction of the wavelength response, the susceptibility to damage the photocathode, the high-voltage requirement of the device and the photon-counting electronics, the need of cooling to reduce the dark noise originating in the photocathode, and the fragile nature of the device itself [Slater et al., 2001]. For all these reasons, **PMTs** are now rarely used, leaving the place to multichannel detectors.

Multichannel Detectors. Multichannel detectors are based on linear arrays of single-channel detectors. Each part of the spectrum is projected along the linear axis of the detector and hence each channel corresponds to a particular wavelength or wavenumber, allowing to obtain the complete spectrum at once [Vandenabeele, 2013, pp.61-100].

The ultimate multichannel detector is a **CCD**, which consists of a 2-Dimensional (**2D**) array of light-sensitive elements: the spectrum projected along one of the dimensions of the **CCD** is combined with the pixels of the other direction. These devices are silicon-fabricated technologies that gained their potential in the 1990s. A **CCD** architecture has usually three functions: photon detection and charge collection, charge transfer, and conversion of charge into a measurable voltage, then digitised and transferred to the control computer. In fact, the signal is read out by sequentially changing the voltage level of the electrodes for each row of wells on the detector. This causes the electrons from one row of wells to shift into an adjacent row, and so on [Adar, 2001][McCreery, 2000, pp.179-202].

The main advantages presented by **CCDs** are [Slater et al., 2001]:

- The ability to measure many wavelengths at once
- The large wavelength range (400 – 1000 nm)
- The large dynamic range
- The high quantum efficiency
- The ability to store and move charge
- Low read noise and low dark noise, when cooled
- The long durability when exposed to intense radiation
- The robust packaging and long detector life

For all these reasons, **CCDs** are now the first choice as detectors in dispersive Raman

spectroscopy.

When instead a FT-Raman spectrometer is used, the preferred detector is a semiconductor detector, with a small band gap, often in indium gallium arsenide (InGaAs), which allows to decrease the fluorescence when IR excitation is used.

4.4. ENHANCEMENTS

As Raman effect has demonstrated to be a very weak effect, but a powerful tool for many applications, some advanced techniques have been improved to obtain a better performance. These methods assure a better use of the technique, but above all they have allowed to Raman spectroscopy to become more and more a trustworthy technology over the years and to be employed in all kinds of applications, from biology to mineralogy, from medicine to art.

Although there are several outstanding techniques that aim to enhance the basic performance of Raman spectroscopy, two among them stand out for their wide use nowadays: Resonance Raman Spectroscopy (RRS) and Surface-Enhanced Raman Spectroscopy (SERS).

Resonance Raman Spectroscopy (RRS). RRS rises up on the fact that if the frequency of the excitation radiation is tuned to one of the absorption bands of the analyte, the response of the Raman spectrum increases significantly. In fact, this allows the laser beam vibration to match with the energy of an electronic transition. The achieved enhancement reaches the order of 10^6 : in this way, even with very low concentration of the analytes, they can be detected by the RRS [Das and Agrawal, 2011; Kudelski, 2008] [Smith and Dent, 2013, pp.93-112].

It is widely exploited above all in the analysis of chromophoric biological samples. However, although it is very sensitive, RRS is a very selective technique because it is enhanced only for the particular frequency of the excitation radiation, that however it is currently available in a wide range of the light spectrum. In particular, RRS is employed in bioanalytical analysis, for example for the detection of nucleic acids, proteins and their interactions with drugs. [Efremov et al., 2008; Kudelski, 2008].

However, the fact that the laser wavelength is selected to be close to the absorption band of an analyte implies that the light is absorbed and sample damage can occur: therefore, in order to minimise this drawback, usually a sampling method in which the sample does not stand in the laser light but only passes through is employed [Smith and Dent, 2013, pp.93-112].

Surface-Enhanced Raman Spectroscopy (SERS). On the other hand, SERS aims at increasing the Raman cross-section σ_j , by achieving an enhancement up to 10^6 . To do so, roughened surface metal materials on which the sample is adsorbed (i.e. adsorption is the exchange of molecules between two materials, which is a kind of adhesive or gluing effect, according to the different nature of molecules) are used to enhance the electric field. These substrates are usually metal-coated alumina nano-particles, not expensive, that can improve the stability of the measurements [Das and Agrawal, 2011; Kudelski, 2008; Smith, 2008].

The working principle is the following: the metal surface interacts with the incident light

and some photons can even be directly adsorbed by the metal; then the Raman scattering energy is mainly located where the interaction happens; the effectiveness is achieved by the lying of the molecules on the surface where a strong field gradient is created and allows to increase the polarisability; then the energy is scattered from the nano-scale roughness features on the metallic surface [Smith, 2008][Vandenabeele, 2013, pp.47-60]. Therefore, two are the main factors that increase the intensity of the Raman scattering: first, the electromagnetic enhancement created by the roughness of the metal surface and second, the chemical enhancement due to the molecules being adsorbed by the surface [Das and Agrawal, 2011].

SERS is very sensitive above all in the recognition of molecules in aqueous environments. Unfortunately, this high performance is difficult in being realised in practice, because of the several chemical processes, such as oxidation, that can occur with metals that diminish the enhancement and of the difficulties in preparing the substrates. Moreover, the interpretation of the collected spectra is not easy. Therefore, **SERS** is also used in combination with **RRS**, in what is called Surface-Enhanced Resonance Raman Spectroscopy (**SERRS**). In such a method, the enhancement is even higher, up to 10^{14} , and not only a metallic substrate is used but also the resonance is achieved by tuning the excitation wavelength in resonance with the analyte [Efremov et al., 2008; Smith, 2008][Smith and Dent, 2013, pp.113-135].

PART II:
DESIGN

5

PAYLOAD PARAMETERS

The design of an optical system includes several steps that need to be considered, as stated by Fischer et al. [2008, pp.167-178]. This process can be summarised as:

1. Obtain and review all the optical specifications
2. Select a starting point, that is supposed to be able to meet the above specifications
3. Establish the variables and the constraints to change during the design process
4. Set the error function in order to determine the best behaviour during change of variables
5. Optimise
6. Evaluate the performance according to acceptance criteria
7. Repeat the steps from 3 to 6 until the desired performance is not met
8. Perform a tolerance analysis
9. Actually start the manufacturing process and obtain the components
10. Assembly the components

As can be seen, the whole design process is an iterative process, which aims at obtaining the required specifications and performance, changing the parameters and optimise the whole.

The aim of this Chapter is indeed to define the specifications for the Raman spectrometer. Section 5.1 identifies and discusses the main parameters in Raman spectroscopy with the objective to select the best solutions for this project. Then, Section 5.2 presents a meeting with experts at DLR in Berlin, during which a System Requirements Review (SRR) was simulated and the final specifications for the instruments were derived as payload requirements, according to the mission need.

5.1. OPTICAL KEY PARAMETERS

As optical instrument, Chapter 4 showed how the performance of a Raman spectrometer is dictated by some particular parameters. According to McCreery [2000, p.75], the principal criteria to be considered for the selection of the type of instrument are the following:

1. Laser wavelength and power, which relate to fluorescence background, the detection limit, and the electrical and cooling requirements;

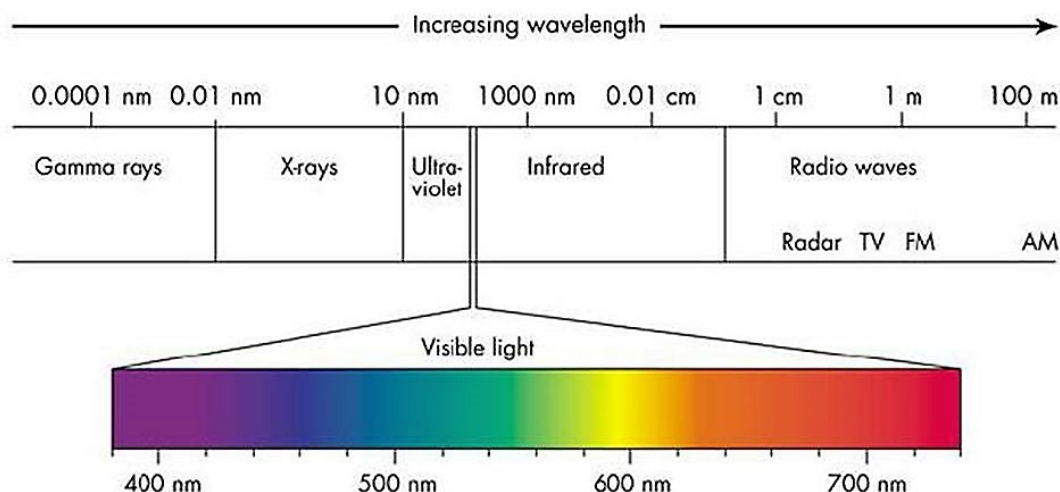


FIGURE 5.1: Electromagnetic spectrum

2. Dispersive or non-dispersive analyser, tied to spectral coverage and resolution, and sensitivity, whose advantages and disadvantages were already presented in Table 4.1;
3. Sampling mode, which depends on sample chemical phase, testing environment and required autonomy;
4. Data analysis, which relates to quantitative and qualitative analysis;
5. Capital and operational costs, which not only include costs for the components, but also for installation, maintainability and operations.

The choice of the laser wavelength usually depends on three main factors: Raman cross section, detector sensitivity and background scattering from the sample. σ_j usually decreases with increasing of laser wavelength as shown by Equation (4.9), therefore, except in the case where resonance is required, a shorter wavelength increases the cross section and the sensitivity. In fact, it is also known that Raman intensity is inversely proportional to the fourth power of the wavelength as identified in Equation (4.7). Moreover, shorter wavelengths are detected with higher quantum efficiency and less noise, but they also present a huge drawbacks on fluorescence background. In terms of SNR, it is important to maximise the ratio according to Equation (4.25) by choosing the wavelength that allows to obtain the largest signal S while minimising the factor $(\sigma_B^2 + \sigma_D^2)$ [McCreery, 2000, pp.76-77]. In general, the assumptions in Table 5.1 can be made for shorter and longer wavelengths.

Figure 5.1 shows the electromagnetic spectrum, where the classification of radiation, according to the wavelength range, is presented. Considering the characteristics of short and long wavelengths for their use in Raman spectroscopy, usually a relative shorter wavelength is chosen, but with attention of not to increase the background fluorescence [Bisson and Whitten, 2015].

The most common wavelengths used for Raman spectroscopy are in the green domain (532 nm), in the UltraViolet (UV) spectrum (< 350 nm) and in the near-IR spectrum (785 nm or 1024 nm). UV excitation is probably the best choice when the objective is to detect biosignatures, because it exhibits a large resonance effect with these molecules, but it is not suitable in the case of mineralogy studies. However, the measurements with UV excitation sources

TABLE 5.1: Assumptions on laser wavelength [McCreery, 2000, p.76]

Shorter wavelength	Longer wavelength
Larger cross section	Smaller cross section
Lower detection noise	
Dispersive spectrometer	Non-dispersive spectrometer
Higher background	Lower background
Often background shot noise limited	Generally detector noise limited
Generally higher SNR	Lower SNR requires higher laser power

are one shot measurements, because with this wavelength excitation, the biosignatures are destroyed. Moreover, it gives a higher chance of fluorescence [Blacksberg et al., 2016]. Anyway, in the deep UV region, fluorescence is excited but no interference exists, therefore this range can still be used [Tarcea et al., 2008]. Another thing important to consider is that UV is dangerous for humans, therefore its use in the project would need a safety mechanism for installation and beginning of operations, in order not to risk damages.

Green excitation sources are common in laboratory instruments. The performance in detecting biosignatures is worse than for UV, but at the same time, it allows to detect a wider range of molecules, even if it requires a higher power. It allows to cover spectral ranges both for minerals and organic substances. Besides, even if it does not eliminate completely the fluorescence effect, this is weaker than for UV excitation [Blacksberg et al., 2016; Wang et al., 2003].

One solution to the fluorescence problem is to use the near-IR excitation. Near-IR excitation wavelength is considered as an industry standard, and this type of laser has sufficient output power, compact size, long lifetime as well as a relatively low price. The disadvantage of IR excitation over green excitation is that the Raman return is significantly weaker leading to lower SNR as well as longer collection times [Blacksberg et al., 2016]. Besides, the accuracy is limited, because for some applications this longer wavelength decreases the intensity too much [Gnyba et al., 2011].

Therefore, the best solution for this project, considering its aim, is a green excitation source at 532 nm, which results to be the best compromise among the performance in detecting potential biosignatures, the availability and cost of the components, the fluorescence background and the safety for terrestrial operations.

Spectral resolution is defined as the ability to resolve spectral features and bands into their separate components. It defines how many spectral peaks the spectrometer can resolve. It means that according to this parameter, spectral information can be lost, if the resolution is too low, or the measurement time can be very long, if it is too high. Obviously, the reference parameter depends on the type of application and it is required directly by the analysts: chemical recognition usually requires low/medium resolution, but higher values can be required for identification of more precise features [BWTek, 2017; Horiba Scientific, 2017; Rasmussen et al., 2015].

When it comes to the use of dispersive gratings, the spectral resolution is always a parameter of great importance for the performance. In Raman spectrometers spectral resolution is determined by four main factors: the focal length (i.e. the distance between the dispersive grating and the detector), to which the parameter is proportional; the diffraction grating groove density; the laser wavelength; and the detector (the smaller the pixel the higher the achievable resolution) [Horiba Scientific, 2017]. Therefore, it is understandable that the spectral resolution is strongly dependent on the size and the level of miniaturisation of the instrument. It is always present in a trade-off with the spectral coverage, as the resolution increases with the increasing of the volume [Guldimann and Kraft, 2011; Wang et al., 2003]. Resolution can be increased up to the theoretical diffraction limit, by decreasing the spectral bandpass by reducing the slit width, or increasing the focal length, the number of grooves or by combining these methods. These techniques imply respectively, decrease of the optical throughput for a smaller slit width, larger instruments for the increase of the focal length and an increase of cost for increasing the number of grooves [Lewis et al., 1993]. So, all these parameters have to be considered as trade-off parameters to select the components.

The last main driving parameter in the design of a Raman spectrometer is the **SNR**, which was already deeply explained in Section 4.2.

As underlined, all the optical parameters depend on each other, therefore it is important to establish some payload requirements to start the design of the instrument.

5.2. PAYLOAD REQUIREMENTS

The parameters presented above and the requirements in Chapter 3 were presented and discussed with a team of experts at **DLR** Institute of Optical Sensor Systems (Institut für Optische Sensorsysteme) and Institute of Planetary Sciences (Institut für Planetenforschung) in Berlin on March 20th, 2017. The meeting was thought as a sort of System Requirements Review (**SRR**), in which the experts worked as stakeholders of the project and presented their needs and requirements for the Raman spectrometer to design.

A **SRR** is a formal review required by the **NASA** project life cycle (as presented in Figure 3.1) who aims at ensuring that the system and performance requirements identified by the designer are complete and consistent with the stakeholders' expectations. Moreover, during a **SRR** the preliminary project plan is discussed and elaborated [AcqNotes, 2017; Kratzke, 2015]. In the **SRR** of this project, not all criteria addressed by AcqNotes [2017] were elaborated, but the aim of the meeting was to stay as close as possible to a simulation of a real systems engineering meeting in order to discuss the acceptance of the requirements by the experts.

The meeting started with the presentation of the project and in particular with a deep explanation of **EnEx** and the working principle of IceMole. In addition, the preliminary concept decision was presented and discussed. The experts resulted very interested in such a project and, although they were not sure that terrestrial and space applications to Enceladus can be comparable at this point, they agreed that a Raman spectrometer is the most promising instrument to use. However, the discussion suggested other instruments to be added to the mission in future as well, to obtain the best possible result. After that, a debate was held to decide the preliminary allocation of the system, as well as the components to inte-

grate to obtain the most suitable configuration. Both these issues are addressed in Chapter 6.

According to the mission need of detecting potential biosignatures in situ, the DLR experts helped deriving the payload requirements, presented in Table 5.2. All of them derive from the two top-level mission requirements SYS-01 and SYS-02, they are indicated with the acronym RS (because related to the Raman spectrometer) and they describe the performance that the instrument must achieve.

For the measurements, it is important that each experiment is not conditioned from the previous one, therefore their independence from depth is essential. In fact, each measurement can give different results because the biosignatures cannot be present at all depths, which means that the scientific return has to assure to recognise the different possible results. Besides, to ensure the detectability of the interesting molecules, the integration time

TABLE 5.2: Payload requirements

Req.ID	Requirement	Rationale	Reference	VM
SYS-01- RS-01	<i>The system shall perform independent measurements at different depths</i>	The system has to be able to provide measurements at different depths during the descend of the probe, without being affected by the previous one	Table 3.2; SRR	D,T
SYS-01- RS-02	<i>The system shall ensure adjustable integration time</i>	Integration time is a fundamental parameter to obtain significant measurements	Table 3.2; SRR	A,T
SYS-01- RS-03	<i>The system shall be calibrated before and after each measurement</i>	In order to detect potential biosignatures, it is necessary to calibrate the instrument with the known detectable substances. For better understanding of the calibration, see Chapter 9	Table 3.2; SRR	T
SYS-02- RS-01	<i>The system shall detect at least the Stokes range $1000 - 4000 \text{ cm}^{-1}$</i>	This is the range in which biosignatures can be found	Table 3.2; SRR	A,T
SYS-02- RS-02	<i>The system shall provide resolution up to 10 cm^{-1}</i>	This requirement derives from experts' need for the mission	Table 3.2; SRR; Section 5.1	A,T
SYS-02- RS-03	<i>The system shall excite the sample at 532 nm</i>	The visible wavelength allows to gain knowledge on samples not only related to biosignatures, it does not need an extra safety control device and it is the best compromise in terms of fluorescence	Table 3.2; SRR; Section 4.3; Section 5.1	A,T

must be flexible, as Raman spectroscopy usually requires stability and quite long integration time. Finally, the instrument must be calibrated as to define a reference and to subtract to the spectrum the known detectable molecules. Interesting biosignatures give signals in the spectrum in the Stokes range $1000 - 4000 \text{ cm}^{-1}$, therefore this is a minimum requirement for the Raman spectrometer. The spectral resolution should be up to 10 cm^{-1} , which was required by the experts, because of the specific application. In this way, very specific features can be determined, but without increasing too much the necessary measurement time. Finally, the excitation wavelength to use should be 532 nm, for the reasons listed above.

Now that all the requirements were derived and they are listed in Table 3.2, Table 3.3 and Table 5.2, the design of the Raman spectrometer can be formulated.

6

PRELIMINARY DESIGN

The working principle of a Raman spectrometer was described in Chapter 4, in which the theory of the Raman effect was combined with the explanation of the instruments and components needed in order to achieve the best performance. Following the scheme in Figure 4.4, it is important to underline that the basic objective of a Raman spectrometer is to take light, break it into spectral components, transform the signal into a function of wavelength, read it out and display it through a computer. This is done by exciting a sample with a focused laser light, collecting the excited light through an optical fibre cable or a collimated lens into the spectrometer through the entrance slit. Then, the light is collimated by a mirror and directed towards a grating which disperses the spectral components at slightly varying angles. This dispersed light is focused by a second lens and imaged onto the detector [BWTek, 2017; Chimenti and Thomas, 2013; Kiselev et al., 2016].

In the context of this work, the principal aspect that needs attention is the miniaturisation of such an instrument. Miniaturised optical components must be chosen wisely so as to meet the performance requirements. In fact, the size of the components affects the performances in terms of spectral range, spectral resolution, SNR and sampling versatility [Cromcombe, 2013].

Therefore, this Chapter focuses on the preliminary design of the Raman spectrometer for IceMole, by trying to achieve all the requirements in Table 5.2. These drive the selection of the components for the instrument, above all the Stokes range to measure ($1000 - 4000 \text{ cm}^{-1}$), the spectral resolution to achieve (10 cm^{-1}) and the laser wavelength (532 nm). These values can be found either in terms of Raman shifts either in wavelengths, therefore it is important to be able to convert the values. Several converters can be found directly on the internet, for example in Photon etc. [2017], which are based on the following relationship [Ocean Optics, 2017]:

$$\Delta\bar{\nu} = \left(\frac{1}{\lambda_0} - \frac{1}{\lambda_x} \right) \cdot 10^7 \quad (6.1)$$

where $\Delta\bar{\nu}$ is the Raman shift in cm^{-1} , λ_0 is the laser wavelength and λ_x is the corresponding wavelength, both in nm. Notice that the factor 10^7 is due to the conversion of the units. Therefore, the wavelength 561.89 nm corresponds to the Stokes shift of 1000 cm^{-1} and the wavelength 675.81 nm to the shift of 4000 cm^{-1} : the Raman bandpass to analyse is then 561.89 – 675.81 nm. About the resolution is instead important by definition the difference

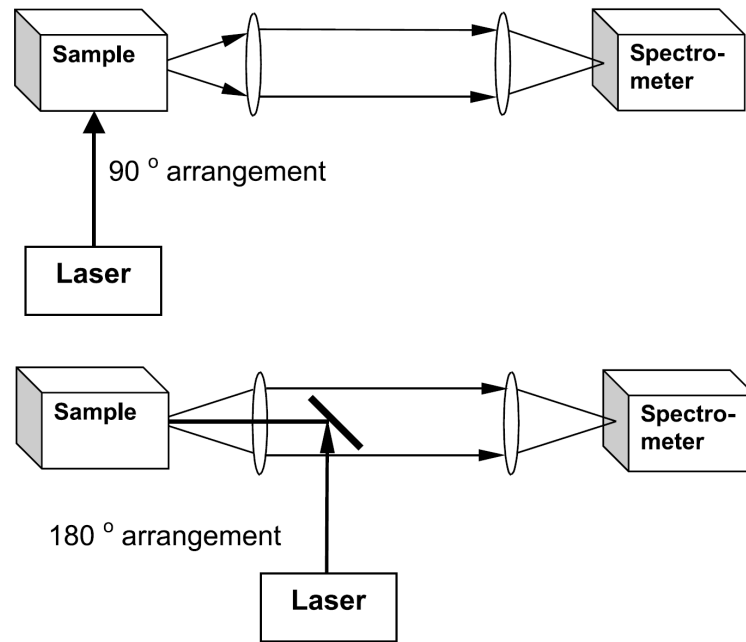


FIGURE 6.1: 90 and 180° sampling geometries for Raman spectroscopy [Gauglitz and Vo-Dinh, 2006]

$\lambda_x - \lambda_0$. In this case, the corresponding wavelength is 532.28 nm, so that the resolution is $\Delta\lambda = 0.283 \text{ nm} \approx 0.3 \text{ nm}$.

Another important consideration when it comes to the preliminary design of the instrument is the configuration geometry to be used. Two are the main options, which are shown in Figure 6.1. As can be noticed, the two configurations depend on the alignment of optics used to deliver the laser light and collect the Raman scattering. In 180° geometry, the laser beam is coaxial to the collected scattered light and a mirror or a beamsplitter is used to combine the two. It allows to perform non-invasive sampling through a window or a container. On the other hand, the 90° configuration keeps the two collection beams separate. Conventionally, for solid samples as in the case of this project, the 180° arrangement is preferred, because of simpler reproducibility [Gauglitz and Vo-Dinh, 2006; McCreery, 2000].

In the present Chapter, the first step is to consider the allocation and the operational scenario of the instrument while performing its measurements in situ. According to this, two main options are identified and discussed in Section 6.1, so as to select the best one which can comply with the next generation of the IceMole probe and its future towards the mission to Enceladus. Then, a preliminary discussion on the most promising components is carried out in Section 6.2, presenting the possible alternatives for each of them, their essential parameters and considering the chosen allocation solution and the requirements derived in the previous Chapters. Eventually, Section 6.3 presents a first system configuration, according to the most promising solutions discussed before.

6.1. ICEMOLE DESIGN CONSIDERATIONS

Section 2.1 presented the design of the different models of IceMole probe. The current miniaturised design does not include any payload, it only wants to show the feasibility of

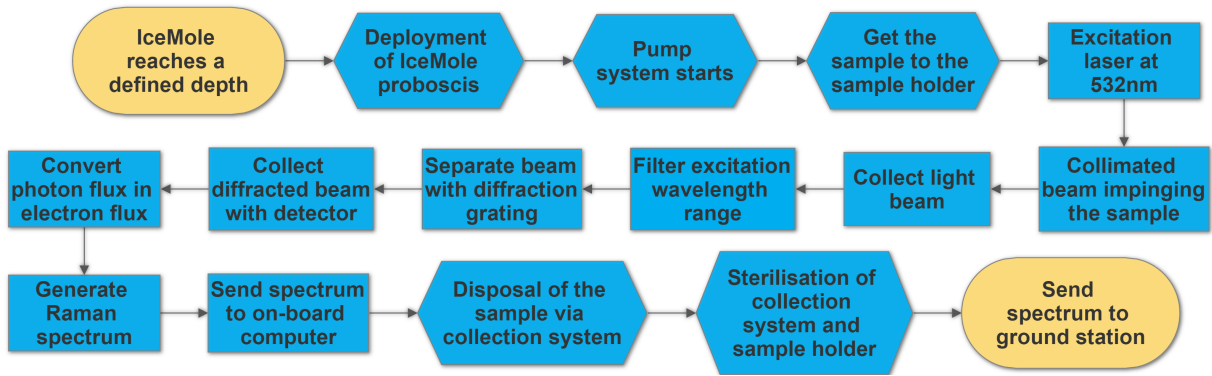
the use of the working principle of combining melting and screwing in such a small probe. However, the [EnEx](#) project is now working on the proposals for the next generation of IceMole, in which the probe should maintain the miniaturised cross sectional area, but it will also present one or more payloads for the in situ measurements of ice or water samples. The aim is to arrive at developing like a *swarm* of IceMole probes for the exploration of Enceladus, each of the probes carrying one specific or more instruments, increasing in this way the reliability and the scientific return of the mission. The Raman spectrometer will be one of the payloads among which the new generation of the probe will benefit for the measurements.

Considering the design of the miniaturised IceMole with the cross sectional area of 80 mm × 80 mm in [Figure 2.4](#), the preliminary analysis concerned the possible allocations of the instrument and its operational scenario. The selection of the allocation was driven by the similarity with [EnEx-IceMole](#), where the payload is allocated in the rear back of the probe. This solution is considered to be feasible even in the case of the miniaturised probe, so as to maintain the space needed for the elements of the navigation systems and not to put the instrument near the melting elements, that can negatively interact with the Raman spectrometer. However, the exact allocation will be decided according to the final dimensions of the instrument and the assembly with the probe by the [EnEx-nExT](#) team in accordance with the new proposal for the design of IceMole. At this stage, the project aims to standing the requirements for the future integration into the probe and it is sufficient to know that the Raman spectrometer will be allocated in the back.

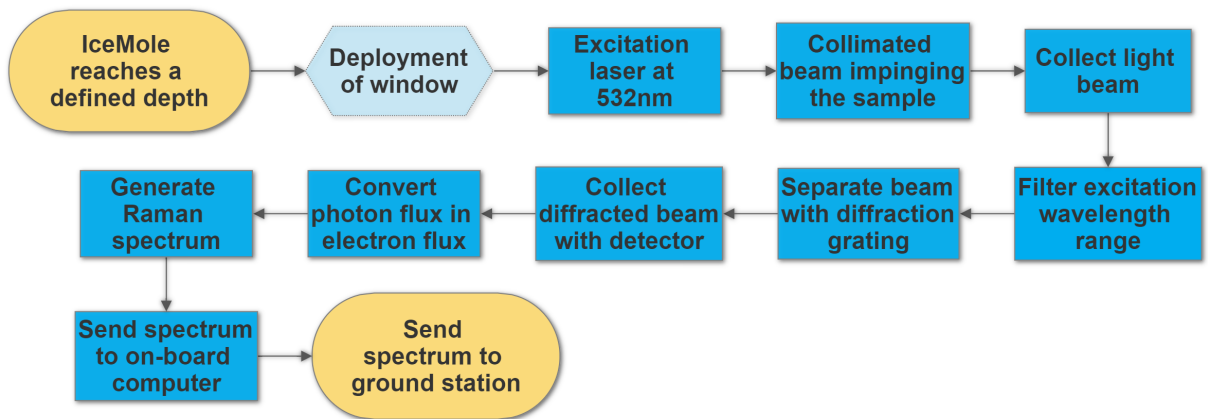
Concerning the operations of the instrument and the required changes in the design of IceMole whereby the spectrometer could perform the in situ measurements, two options were investigated at high level to decide how they will work according to the respective Functional Flow Block Diagram (FFBD), shown in [Figure 6.2](#). The main difference between the two options is that the first one employs a pump collection system, while the second one performs the measurements through a glass window. Yellow blocks indicate the start and the end of the operations respectively related to IceMole reaching a defined depth and to sending the obtained spectrum to ground station. Rectangular blocks show the steps related to the spectrometer itself and its measurements (notice that they are the same for both options), while rhomboidal blocks relate to preparation steps and final disposal steps.

Option 1. In the first case ([Figure 6.2a](#)), the spectrometer collects the ice sample from the hollow screw and performs the measurements inside the probe. In this case, the probe needs a pump in order to get the sample from the head to the rear back where a sample cuvette contains the sample. At this point, the Raman spectrometer works as described in [Chapter 4](#). Then the sample is ejected from the probe and the cuvette and the channels have to be decontaminated in order to perform the successive measurements.

The main problems concerning this option are the design of the screw for the miniaturised IceMole, the design of a pump to get the sample to the instrument, the elimination of the analysed sample and the decontamination of the instrument for each measurement. About the screw, the miniaturised IceMole does not present the hollow screw currently, as its design resulted very difficult for such a small item. However, for this option the cavity is necessary in order to deploy the proboscis to collect the sample, as it was for the previous



(A) (High-Level) FFBD of Option 1



(B) (High-Level) FFBD of Option 2

FIGURE 6.2: FFBDs of high-level operation options

generations of IceMole. At this point, the pump has to be able to transport the collected sample to the sample holder. This means that a high pressure difference has to be generated. At the same time, the pump has to be used to remove the sample from the holder as well and eject it into the ice. This step and the decontamination and sterilisation of the collection system are necessary in order to comply with the requirement on the independent measurements (see Table 5.2, SYS-01-RS-01).

Option 2. On the other hand, this option does not need the collection of the sample, as it is shown in Figure 6.2b. In fact, once IceMole arrives at the defined depth, the spectrometer performs the measurements through a window, looking at one of the sides of the channel melted by the probe. In this way, the contamination of the instrument is not a problem, because the spectrometer is not in contact directly with the sample and each measurement is independent from the other.

In this case, the main problem is the design of the window. First of all, it is important to identify the transparent material that allows to perform the measurements of the sample at best. Moreover, it has to be investigated if this window can be part of the wall of the probe, so as to stand the strains originated by the descend of IceMole, or if a mechanism of "aperture" of this window is needed. That is why in the Figure the block related to the deployment of the window is dashed and in transparency. Another problem could be the possible presence of a

thin liquid film remaining on the side wall of the hole in front of the ice. Besides the window can require safety devices if excitation wavelength ranges dangerous for humans are chosen (even if it is not the case of this project).

With the objective of not to modify extremely the design of the IceMole probe, so that the outcome of this work can be adapted to all new proposed designs, Option 2 seems to be the most feasible and the one that presents less drawbacks to overcome. From the engineering point of view, this option is preferable because its design seems to be easier and an additional collection system is not needed. Option 2 simply relies on the selection of the components which have to be assembled together to obtain a system that provides the best performance. However, attention has to be paid for what concerns the scientific aspect: in fact, the use of a window could interfere with the measurements, because they are not performed directly on the sample. Therefore, research is needed on the material to use for the window, on its transmittance according to the excitation wavelength used (532 nm), on its thickness and on how it interferes with the measurements, so as to select the best material that enhances at best the performance of the instrument.

6.2. COMPONENTS

Therefore, the design approach of the Raman spectrometer followed the scheme presented in Figure 4.4. Considering the choice that concerns the allocation of the instrument in the rear back of the probe and the use of a window, this Section presents the options available for each component, always taking care of the derived requirements and of what was said in Chapter 4 about all the system elements.

The main aspects that have to be investigated are how to design the window, how it affects the performance and which material is most suitable for IceMole applications; which laser should be used to provide for the 532 nm excitation; which type of focusing and collection optics is the best option for this work; which filter allows to obtain the required performance; and, above all, which are the main parameters for the spectrometer and the detector. After the determination of the available options and the most important criteria to perform a trade-off, the selection of the components will be elaborated in Chapter 7.

6.2.1. WINDOW

The window is the interface between the instrument and the sample. The choice of using a window allows to have an essentially non-invasive method, so as to contain the risk of contamination, at least for the one coming directly from the Raman spectrometer [Gauglitz and Vo-Dinh, 2006]. Therefore, the window has to be able to transmit both the excitation radiation and the scattered light. To achieve this aim, the material was selected according to its physical and optical properties such as light transmission, index of refraction (i.e. the ratio of the speed of light in vacuum to the speed of light through a given material at a given wavelength), reflectance, Abbe number (i.e. a measure of the material dispersion), coefficient of thermal expansion, conductivity, Knoop or Mohs hardness and Young's modulus [Edmund Optics, 2017c; Newport, 2017].

In particular, the transmittance of an optical glass is quite important in selecting the appropriate material: the transmittance is defined as the fraction of incident light of a specific

wavelength that passes through the glass and it is inversely proportional to the spectral absorption. However, not only the transmission depends on the wavelength of the incident light, but it also depends on the thickness of the material, because the higher the thickness the higher the spherical aberrations that can be encountered [AzO Optics, 2014; Schott, 2005; Slater et al., 2001]. The values of the transmittance that have to be considered are the ones for the laser wavelength 532 nm and the ones for the visible spectrum that has to be collected. For this project, the thickness of the window is supposed to be at maximum 10 mm: in fact, the wall of IceMole is currently 4 mm thick, to which some thickness has to be added in order to mount the window and so it can be considered that the window should be $\sim 7 - 8$ mm.

Other aspects that needed to be taken into account in this project are the mechanical properties of the material: considering the window as part of the wall of IceMole, the material has to guarantee not to break during the descent of the probe. For this reason, the Young's modulus and the Mohs hardness are extremely important. The first parameter refers to the ratio between stress and strain to which the material is subjected. It is linked to the elastic deformation and it is the load limit that can be applied to a solid material so that it is able to return to its original shape after the load is removed [Wikipedia, 2017a]. On the other hand, the Mohs hardness specifies how resistant a solid material is to various kinds of permanent shape changes when a compressive force is applied. In particular, the Mohs scale indicates the scratch hardness which is the hardness of a material to scratches and abrasions and it is based on relative comparison, where talc has an assigned value of 1 and diamond is assigned to 10 [IPS Optics, 2017; Wikipedia, 2017c].

A last optical property worth of consideration was birefringence: if a material is birefringent, the transmission of the light beam is subjected to a double refraction, because its refractive index depends on the polarisation of light. Since Raman measurements are sensitive to the polarisation of the beam, the material of the window should not be birefringent [Janis, 2017].

Considering the listed parameters, the most promising materials for the use in IceMole terrestrial applications were identified in [Janis, 2017; Newport, 2017]:

- **BK7**, the most common borosilicate glass used for visible and near-**IR** optics. It is also relatively hard and shows good scratch resistance.
- **UV Grade Fused Silica**, which is a non-crystalline, colourless silica glass that combines a very low thermal expansion coefficient with good optical qualities. Fused silica is ideally used with high-energy lasers due to its high energy damage threshold.
- **Crystal Quartz**, a birefringent single crystal grown using a hydrothermal process, with good transmission from the vacuum **UV** to the near-**IR**.
- **Sapphire**, which is a hard crystalline material, with good transmittance from the **UV** to the mid-**IR**, excellent transparency and resistance to chemical attack.

6.2.2. LASER

As already discussed in Chapter 5, the laser wavelength strongly influences the performance and the effectiveness of the Raman measurements and that is why the 532 nm excitation

wavelength was chosen. Laser can be divided in three main categories: Continuous Wavelength (CW), pulsed and ultra-fast, according to how the light is delivered. Among these, in the typical Raman measurements, the CW is preferred to a pulsed laser so as to assure a stable output power than could vary between 10 and 1000 mW, according to its power stability [Gauglitz and Vo-Dinh, 2006, p.58][Photonics Handbook, 2017].

The most common CW laser is an helium-neon (HeNe) laser, which is a very mature and reliable technology, reason for which the cost of this device is not very high. However, the main restrictions for this type of lasers is the limited achievable output power and the need to be air-cooled. Recently, the laser diode has become the most used laser type, which relies on creating charge carries in a p-n junction that combines and emits light. They are available at low cost, in small dimensions and they are able to deliver high output power, although their performance is highly temperature dependent. Furthermore, another option that is gaining more and more attention is the Diode-Pumped Solid State (DPSS) laser, in which the gain medium is neodymium-doped crystal (usually Nd:YAG or N:YV04), pumped by one or more laser diode. DPSS lasers can deliver high power, they allow both CW and pulsed operations and their size can be greatly reduced [McCreery, 2000, pp.127-148][Photonics Handbook, 2017; Slater et al., 2001].

Besides the wavelength, the other parameters of the laser important to consider were [Slater et al., 2001; Thomas, 2016]:

- Power, on which the power of the Raman scattering depends.
- Stability in power, important for the repeatable and long applications. Usually good Raman laser has a power stability of better than 1% peak-to-peak over 8 hours.
- Laser linewidth and stability in wavelength, respectively usually less than 1 cm^{-1} with less than 0.5% RMS of optical noise.
- Lifetime, which has to assure the instrument to work for all the operative time.

6.2.3. FILTER

Chapter 4 showed how important it is to reject the laser-line. In fact, the most of the scattered light is on the same frequency of the excitation laser, and this would mean for the weaker Raman scattering to be covered. Moreover, the laser-line would create too much fluorescence and background noise for the detector [Omega Optical, 2017; Slater et al., 2001]. Therefore, to fight these effects, it was fundamental to use and select the appropriate filter.

Optical filters are used to selectively transmit or reflect a wavelength or range of wavelengths. Figure 6.3 shows the four basic types of filters, based on the shape of the transmission curve: a long wave pass edge filter, a short wave pass edge filter, a notch filter and a laser-

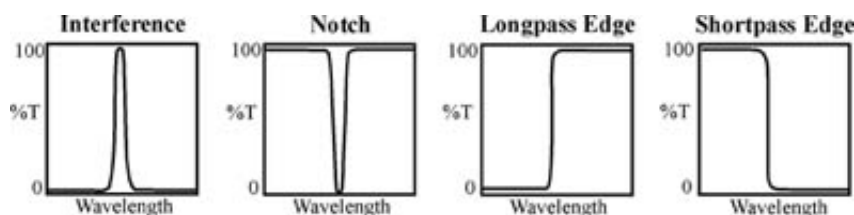


FIGURE 6.3: Filters options [Omega Optical, 2017]

line filter (in the Figure called *interference*). The edge filters transmit only the wavelengths respectively above or below a certain threshold, a notch filter blocks only the laser-line letting all the other ranges pass, while the laser-line filter allows only to the laser wavelength to be transmitted [RP Photonics Encyclopedia, 2017; Semrock, 2017c].

Obviously for this work the last type is not useful as it transmits only what it actually has to be rejected. Among the other types, the choice was driven by the payload requirements in Table 5.2: the experts asked for a spectral coverage between 561.89 and 675.81 nm. This means that the detection is linked only to a Stokes range, so only the wavelengths above the laser-line have to be measured. For this reason, the appropriate filter to be used is a long-pass edge filter. Parameters that have to be considered in the choice of the edge filter to use were the steepness, i.e. the parameter related to how fast the filter transitions is from blocking to transmission, and the OD, which is usually required to be higher than 5 for Raman spectroscopy [Omega Optical, 2017], because it is related to transmittance by [Edmund Optics, 2017f]:

$$T = 10^{-OD} \times 100 \quad (6.2)$$

where T is the transmittance.

6.2.4. FOCUSING AND COLLECTION OPTICS

The 180° configuration requires peculiar focus for what concerns the delivery of the excitation laser beam. Figure 6.1 shows that both the laser beam and the scattered light are on the same axis: therefore, it is important that the delivery of the excitation does not interfere with the collection of the scattering. This means that a mirror with peculiar characteristics must be used.

A mirror is an optical lens whose coating is selected so as to be highly reflective for a selective wavelength range. In this case, the mirror should reflect the laser beam of 532 nm towards the sample, with an incidence of usually 45°. However, the device that reflects the laser has to be able to transmit the Raman scattering to the spectrometer, as well. For this reason, in spite of a simple mirror, a beamsplitter can be used: the beamsplitters rely on coatings that partially reflect and partially transmit incident light according to the wavelength (that is the case of dichroic beamsplitters). For this work, the optical device should have a high reflectivity for the laser wavelength and a high transmittivity for the spectral range to be detected [Edmund Optics, 2013].

Besides the focusing optics, its counterpart is as well as important. The collection optics determines the amount of light reaching the spectrometer and the detector. Scattering light is diffusive light, therefore it is needed something that could collect it: the most promising optical element is a collimating lens. Collimating lenses make light parallel, so that it can enter the spectrometer set-up by creating a focus. They can be directly attached to the spectrometer or coupled to optical fibres. Normally, they are used to direct the excitation beam to the sample, but they can also be used as collecting optics for the reason explained above. There are two common types of collimators: refractive or reflective. The selection of the collimator depends on the entrance pupil diameter, wavelength range, and focal length of the optical system under test. For the measurements such the ones of this project, reflective collimators are recommended because they can work over larger wavelength ranges [Optikos, 2017].

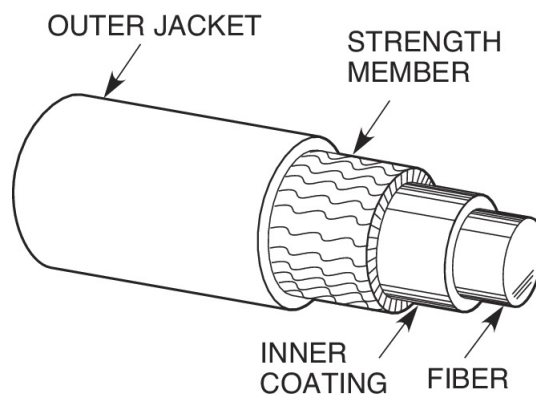


FIGURE 6.4: Single fibre cable structure [Newport, 2017]

Both the focusing optics and the collection optics can be substituted, at least in part, by optical fibre cables: the laser can be delivered by a single fibre to the sample and the Raman signal can be collected back by the fibre and transmitted to the spectrometer [Slater et al., 2001]. An optical fibre can be thought as a "light pipe", which means that the fibre guides light into an optical system via the phenomenon of total internal reflection, i.e. carrying information between two places using entirely optical technology. An optical cable is composed of really thin strands of glass or plastics. Figure 6.4 shows the structure of a single fibre cable. All fibres consist of a number of substructures including: a core, which carries most of the light; surrounded by a cladding (with a lower refraction index), which bends the light and confines it to the core forming the actual fibre; surrounded by an inner coating that does not carry light, but adds diameter and strength to the fibre; covered by a primary coating, the strength member, which provides the first layer of mechanical protection; and a secondary buffer coating, the outer jacket, which protects the relatively fragile primary coating and the underlying fibre [Optical Cable Corporation, 2017; Woodford, 2016].

The optical fibres can transmit signals via different modes, which are the paths that the light beams follow inside the cable. In the single-mode fibre, light travels straight down the middle without bouncing off the edges, while in the multi-mode fibre, the light beam travels into the fibre by following a variety of different paths. The former presents usually a smaller diameter and it is used in to cover large distances, while the latter sends information only over relatively short distances [Dowling, 1997; Optical Cable Corporation, 2017; Woodford, 2016]. Typical descriptive parameters for an optical fibre cable are the following [Dowling, 1997]:

- attenuation, which is the decrease in signal strength over distance
- bandwidth, the information capacity
- Numerical Aperture (NA)¹, the measurement of the light acceptance angle of a fibre
- cut-off wavelength (for single-mode fibre)
- mode field diameter
- chromatic dispersion.

¹The NA of an optical system characterises the range of angles over which the system can accept or emit light. It is conventionally defined as $NA = n \sin \theta$, where θ is the maximal half-angle of the cone of light that can enter or exit the lens.

Moreover, the physical size of the cable, its optical and mechanical performances and the jacket are to be considered in the selection of the appropriate optical fibre cable.

The use of optical fibres allows freedom and flexibility in the set-up of an optical instrument, because sample may be distant from the spectrometer, no special pointing is required and the losses within the fibres are very small. In this work, this was particularly promising in order to fit all the components in the restricted available volume. Moreover, they are ideal when samples have to be analysed from a large distance or present weird shapes [Anglia Instrumentation Ltd, 2017; BWTek, 2017; McCreery et al., 1983].

6.2.5. SPECTROMETER & DETECTOR

The spectrometer is the most important component at all for the Raman system; it is the one that diffracts the scattered light beam and transmits this diffracted beam to the detector to obtain the actual results. As explained in Chapter 4, the spectrometer includes an entrance slit, a collimated lens, a dispersion element and a second lens to focus the light onto the detector. In this case, a grating-based spectrometer is used.

Besides the already described Czerny-Turner configuration, reported here in the right part of Figure 6.5, which was identified as particularly promising for its compact design, a crossed Czerny-Turner set-up can be used, which is an elaboration of the first one. It consists of two concave mirrors and a diffraction grating, offering an even compacter and more flexible design that needs almost half the volume of the uncrossed version [BWTek, 2017; Rasmussen et al., 2015].

The slit is one of the most critical parameters of the spectrometer because it determines the amount of light that enters the optical bench, on which depends the spectral resolution. The slit cannot be too wide, or the spectral resolution would decrease, but neither too narrow, which can determine the loss of the flux and some information [BWTek, 2017]. Spectral resolution also depends on the focal length of the lenses and mirrors, the groove frequency and the detector pixel size. The diffraction grating determines the spectral wavelength range as well, which must be appropriate to the required Stokes range [Adar, 2013].

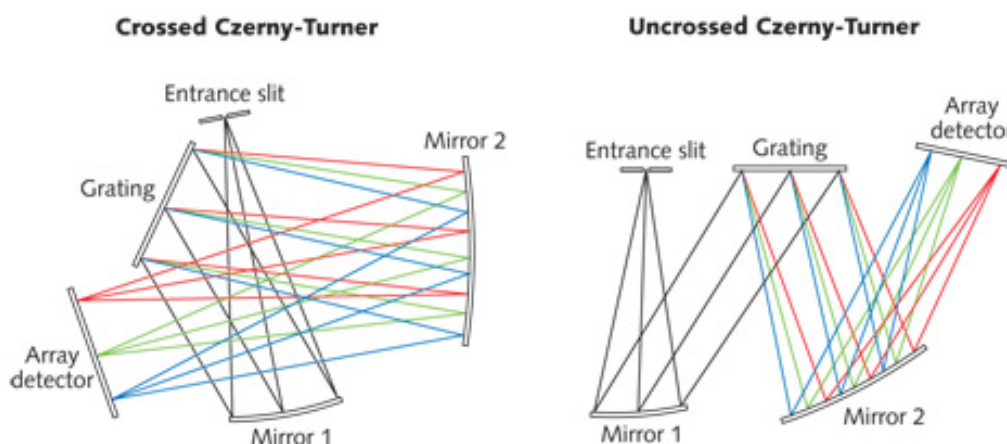


FIGURE 6.5: Crossed and uncrossed Czerny-Turner set-up [Rasmussen et al., 2015]

Considering the detector, a sensitive and low-noise detector is an imperative need. Photodetectors are characterised in different ways, according to their detector material: the detection capability depends on the absorbance characteristics of the used semi-conductor material, and it can vary extensively with the thickness of the detector [Gauglitz and Vo-Dinh, 2006; Rasmussen et al., 2015]. In the applications of IceMole, a multichannel detector is needed, in order to obtain the spectrum at once. Conventional CCDs can be constructed at low cost, which makes them an ideal choice for most miniature spectrometers. However, they presents two limitations: light can be scattered instead of absorbed and the thickness is maintained typically thick. A Back-Thinned Charged-Coupled Device (BT-CCD) is instead very sensitive, but more expensive. Another option would be to use Photodiode Array (PDA) detectors which, although they use larger pixels, they do not need a gate structure and they have a wider dynamic range and response [Chimenti and Thomas, 2013].

An important aspect that has to be considered for detectors is the need of using thermoelectric cooling devices, which allow to diminish the noise levels, by lowering the dark current, and increasing the sample integration time so as to obtain a lower detection limit [Chimenti and Thomas, 2013].

6.3. PRELIMINARY SYSTEM CONFIGURATION

With a view to derive a design that could satisfy the requirements, a preliminary design configuration for the Raman spectrometer was decided. This configuration derived from the presentation of the components and their characteristics in Section 6.2 and it is presented in Figure 6.6.

The interface between the IceMole probe and the ice is represented by a window, a layer of optical glass with the adequate characteristics to perform the measurements that is part of the wall of the probe. The window transmits the laser light beam to the sample, which is represented by the ice of the melted channel by IceMole. The laser provides the excitation beam via an optical fibre cable, which is connected directly to the window via a fibre support. The

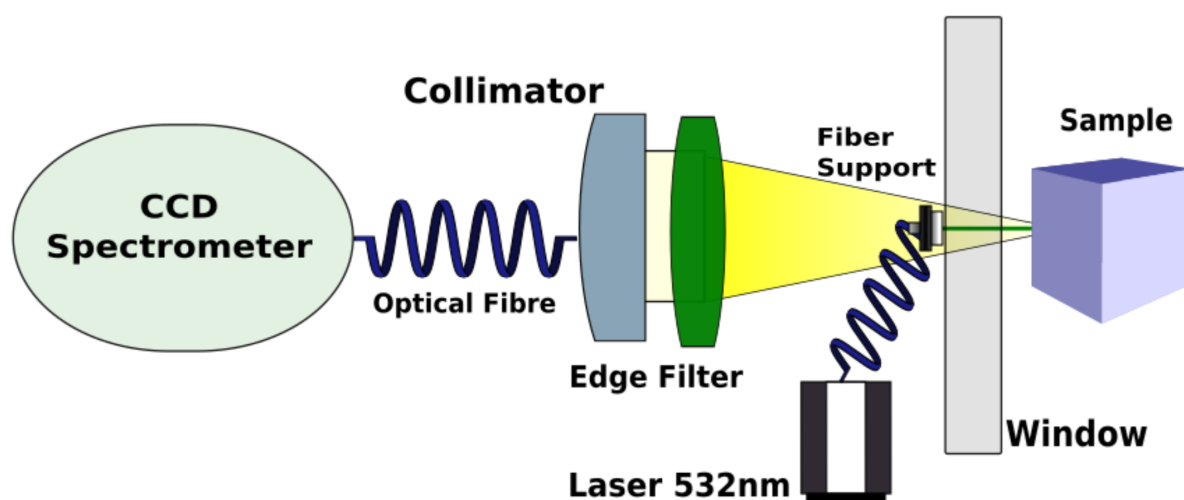


FIGURE 6.6: Preliminary system configuration

scattered light is transmitted through the window inside the probe and collected via an edge filter, which rejects the laser-line scattering, transmitting only the interesting Stokes range. A collimated lens is then directly connected via an optical fibre to a CCD spectrometer which performs the analysis of the scattered light to detect the potential biosignatures. The market offers several options for a spectrometer already integrated with a detector, so that time for designing these optical components can be saved. The choice of connecting both the laser and the spectrometer with optical fibres depends on the amazing advantages that derives from these technologies: above all the chance of arranging a flexible set-up, so as to exploit to the utmost the available volume.

The main choice in this phase was the one of using Components-Off-The-Shelf (COTS), for every part but the window, which has to be designed such as to be integrated with the wall of the probe itself. COTS allow to keep the entire cost of the system low and they give the opportunity of choosing among a huge variety of alternatives. Moreover, the use of COTS gives the chance of reducing the time schedule, because manufacturing and delivery of the components do not need too much time. The main aspects of this work were indeed the selection among the different available options on the market through careful trade-offs to satisfy the payload requirements (Table 5.2) and how to integrate them in order to meet with the technical specifications (Table 3.3). The first aspect is elaborated in next Chapter, while the last is elaborated in Chapter 8 with the modelling of the system with the help of a CAD software.

7

SELECTION OF COMPONENTS

The previous Chapter underlined the leading characteristics for each component of the Raman spectrometer and it presented a first primary system configuration with the aim of formulating a possible design for the instrument. The configuration determined some important high-level choices such as: the 180° configuration, the use of a window as interface between the instrument and the sample, the decision of relying on COTS of the market, the employment of the optical fibres and a CCD spectrometer.

This Chapter deals with the successive decisions to be taken in the design of the system, which strictly depend on the ones made before. Notice that the process of the design in engineering is an iterative process which requires a continuous verification of the previous choices and the flexibility to change those. First of all, the preliminary system configuration proposed in Section 6.3 is analysed at a deeper level, trying to understand if the introduced solution can be feasible for the instrument. This analysis is elaborated in Section 7.1 where the first iterations are presented. Successively, the selection of the components is performed through extensive trade-offs, that follow the rules of systems engineering, in Section 7.2. Each element is selected considering the parameters presented in Chapter 6 and presenting the several available options on the market. Eventually, Section 7.3 presents different options for the allocation of the components, by trying to fit them in the constrained volume. The options are elaborated in a CAD software, so as to visualise how much space it is needed to fit everything. The selection of the best option is fundamental to derive the final design in next Chapter.

7.1. ITERATION OF SYSTEM CONFIGURATION

The configuration presented in the previous Chapter seems to be the most feasible in the design of the Raman spectrometer for IceMole. The window facilitates the access to the sample and the optical fibres make the allocation of the single components easier and more flexible, as they can also be far from the sample because of the low losses in the cables. At the same time, the use of COTS allows to reduce the overall costs and assure the testing of the optical performance of each components.

However, the presence of a cable support in front of the window could create problems for the collection of the scattered light. In fact, the support blocks a part of the aperture of the window so as to stop some light to arrive to the detector.

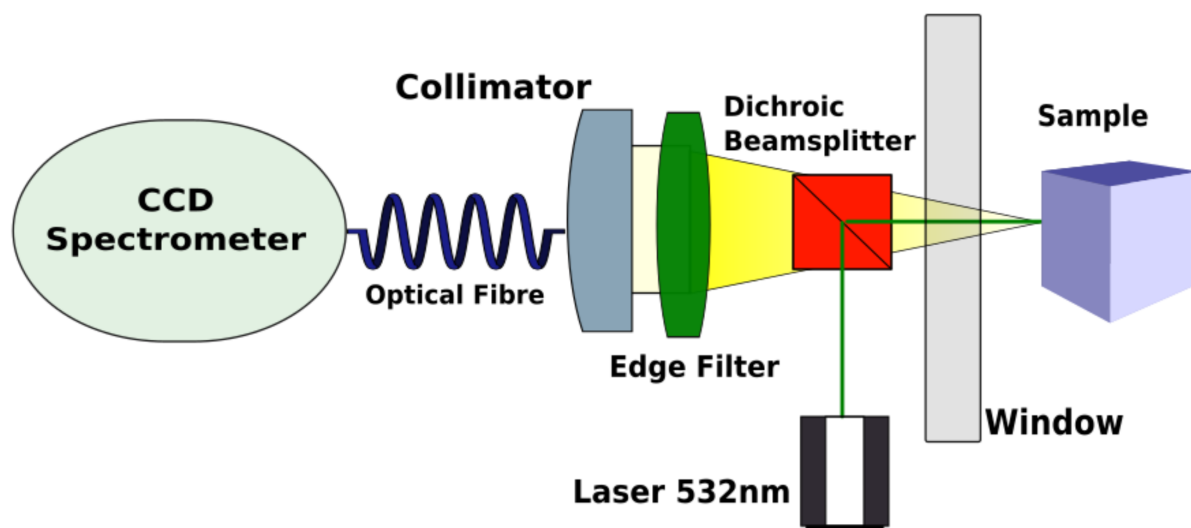
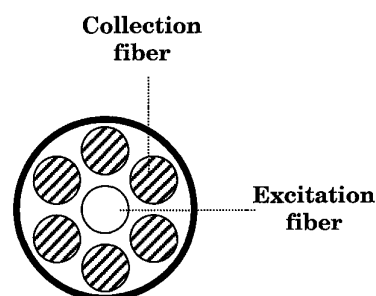


FIGURE 7.1: Iterated system configuration

A solution to this problem could be the use of optical fibres able to deliver the laser beam and to collect the scattering at the same time. Usually, their configuration is the one presented in Figure 7.2 with a *N-around-1* variant. That means that the central fibre delivers the excitation laser light, while the outer N fibres surrounding the central one collect the scattering. It can be achieved with a bifurcated optical fibre cable: one extremity is connected to the laser source, one is connected directly to the spectrometer and the last one is supported in front of the mirror [Slater et al., 2001]. Unfortunately, even this solution presents problems in the configuration of the spectrometer. In fact, the direct collection of the light from the same point where the excitation light comes from would suffer from the overlapping of the beams, but the main problem is actually the direct link to the spectrometer. In this way, the scattered light would not be filtered and the laser light would reach the detector. Currently, filtering for optical fibres is under research and development, but cannot be used yet.

FIGURE 7.2: *N-around-1* optical fibre (adapted from Slater et al. [2001])

Therefore, another solution to this problem is the use of a beamsplitter. As described before, a beamsplitter is an optical component that relies on coatings that partially reflect and partially transmit light according to the wavelength, and that usually accepts angles of incidence of $\sim 45^\circ$. In this project, the reflection of the laser at 532 nm is required and the transmission of the Stokes scattered range is necessary in order to comply with the requirements. According to this discussion, the iterated configuration is presented in Figure 7.1. The laser light is delivered indeed via free-space, through the beamsplitter. The optical device has to be positioned in such a way that the laser beam can be reflected to the window and the scattering can be transmitted to the spectrometer. The scattered light continues to be collected through the collimator connected to the spectrometer via an optical fiber.

7.2. TRADE-OFFS

In engineering, the design process requires to be able to make several and continuous choices. Usually, a series of concepts must be identified and then the selection among them is driven by a series of criteria that have to be generated according to the aim of the design and its requirements. Therefore, systems engineering introduces different trade-off methods in order to come up with a solution for each critical choice. A trade-off is defined as a situation in which one aspect is in contrast with another and losing one means gaining the other. These circumstances happen constantly in a design process and they have to be carefully elaborated. In order to succeed in this, several trade studies, i.e. decision-making processes that aim at identifying the most promising solution, were elaborated to support the choices.

Hence, each decision must follow a rigorous process which is described by Larson et al. [2009, pp.201-232]: (1) identify the request, the objectives and rank them, (2) recognise the context in which the decision has to be made, by assess and handle risk and uncertainties that can arise from decisions that require a trade-off between two elements, (3) select a method to evaluate the options (intuition, charts, heuristics, qualitative or quantitative analytical models, simulations or testing), (4) generate alternatives, (5) choose the best solution, (7) test and evaluate the choice. Therefore, once the criteria and the concepts are identified, the selection criteria have to be weighted among each other in order to compare all the options on the same basis. Then, to perform the trade-offs, there are three principal methods [Gill, 2015]:

- Classical, which includes numerical trade-off tables, where criteria are assigned to a weight and options are assigned to a value as well; and Pugh matrices (such the one presented in Table 3.1), where the options are assigned to 0, 1, -1 respectively if they fulfil, over-fulfil or under-fulfil a criteria. Then a weighted sum is made according to the weighting of the criteria, in order to select the best concept.
- Graphical, where the options are listed in the left column and the criteria are weighted accordingly to their assigned column width and a colour code is used to identify the performance of the options for the criteria.
- Analytical Hierarchical Process (AHP), which can determine the weight of the trade criteria by basing on the pair-wise comparison of the nodes in a hierarchical tree structure.

Therefore, this Section deals with the selection of all the components through the described trade-off methods, adding to them some reasoning behind each choice. For the following trade-offs, some major criteria were identified, that are related to the derived requirements. The main categories of criteria that were considered for each process are:

- **Size.** This is the drive parameter of the whole project, therefore all the components have to comply with the restricted available volume imposed by the design of the Ice-Mole probe. So, it is important that all of them could fit in the volume of 65 mm × 65 mm × 150 mm and this criterion was considered as the most important for all the trade-offs.
- **Performance.** Along with the size, it is fundamental that the components are able to achieve a high level of performance so that a valuable scientific return of the mission can be obtained. Naturally, the minimum performance parameters are different for each component and they are presented before each selection process.

- **Operating conditions.** They are related to the environmental conditions that the entire system has to withstand and they permit to understand if the components could work in such environments. Even in this case, the operating conditions are related to different parameters according to the component to select.

Eventually, the technical specifications of the selected components are presented in Appendix A.

7.2.1. WINDOW

The window is particularly important for the instrument because it has the primary role in the transmission of both the excitation beam and the scattered light from the sample. Therefore, as already underlined previously, the transmittance of the optical material plays a crucial role in the selection of the material. At the same time, it is important always to take in mind that the window has to interface with the harsh environmental conditions of IceMole testing sites and therefore the mechanical characteristics of the glass are key parameters as well. For this trade-off, size was not considered as a major criterion, while performance was evaluated in terms of transmittance at 532 nm, transmittance range and birefringence; while for the operating conditions, the Young modulus and the Mohs hardness were taken into account. The options to be considered were the ones presented in the previous Chapter: BK7 glass, UV grade fused silica, crystal quartz and sapphire.

The selection was performed through a graphical trade-off presented in Table 7.1, where the values related to a 10 mm-thick window are listed. As can be seen, the transmittance at the laser wavelength is good for all the four options, with a particularly high transmittance for UV fused silica and quartz. The same can be said for the transmittance range, for which all the options meet the requirement on the spectral range that needs to be measured. However, for the mechanical properties, the best performance is achieved by a sapphire window, because of the high values related to its Young's modulus and the Mohs hardness which are related to high performance in withstanding the harsh conditions of the ice. According to the last parameter, the birefringence of the material, BK7 and UV fused silica are not birefringent, while quartz and sapphire are, due to their crystalline nature.

Considering the colour code related to the graphical trade-off (green for excellent, blue for good, yellow for correctable deficiencies and red for unacceptable), the best choices were

TABLE 7.1: Graphical trade-off for the window material [IPS Optics, 2017; Newport, 2017]

	Transmittance @532 nm	Transmittance range	Young's modulus	Mohs hardness	Birefringence
BK7	0.97	0.38 – 2.1 μm	8.63×10^{10} Pa	5	No
UV Fused Silica	0.999	0.18 – 2.5 μm	7.36×10^{10} Pa	5.5 – 6.5	No
Quartz	0.98	0.15 – 3 μm	8.7×10^{10} Pa	7	Yes (+0.009)
Sapphire	0.97	0.17 – 5 μm	79×10^{10} Pa	9	Yes (–0.008)

■	Excellent, exceeds requirements	■	Correctable deficiencies
■	Good, meets requirements	■	Unacceptable

recognisable in the UV fused silica and in the sapphire window. Anyway, because of its better mechanical characteristics, the sapphire window was chosen as the most promising option, because, despite its birefringence, it allows to be sure of not fracturing or breaking during the descent of the probe. The drawback on birefringence can be almost ignored because of the huge heritage of the use of this material for Raman spectroscopy as presented in Hattrick-Simpers et al. [2011]; McCreery [2000]; Slater et al. [2001].

7.2.2. LASER

The laser has the job to deliver the excitation light at 532 nm. Because of the best achievements for Raman spectroscopy, Chapter 6 identified a CW laser as the best to be used in this application.

Therefore, four different COTS lasers were identified on the market from the producers Cobolt, RGLase, Laserglow Technologies and CrystaLaser® and they are presented in Table 7.2 in a graphical trade-off. For this process, the considered criteria were the size and the performance in terms of output power, power stability and RMS noise.

All the four components are CW diode pumped lasers, that allow different output power. For this parameter, it was chosen to select a 100 mW output power, as the best compromise between performance and power requirement, by allowing to excite at best the sample and to receive a strong scattered signal (keep in mind that the scattering power depends on the laser power as explained in Chapter 4). Therefore, all the four options satisfy this required value. For what concerns the RMS noise, the low-cost component of Laserglow Technologies and the diode pumped green 532 nm CrystaLaser® present both a terrible performance: the RMS noise reaches values of 20%, not acceptable in a precise application such as Raman

TABLE 7.2: Graphical trade-off for laser [Cobolt, 2016; CrystaLaser, 2017; Laserglow Technologies, 2017; RGLase, 2017]

	Producer	Output power	Power stability	RMS noise	Size
Cobolt 08-01 Series	Cobolt	25 ~ 200 mW	< 2% (over 8h)	< 0.2%	40 × 40 × 100 mm (with mounting support)
532 nm Raman Laser Module RM1	RGLase	20 ~ 300 mW	up to 3%	< 0.2%	66 × 46 × 140.8 mm (with mounting support)
LCS-0532 Low-Cost DPSS Laser System	Laserglow Technologies	15 ~ 100 mW	< 5% (over 4h)	< 20%	87 × 40 × 40 mm
Diode Pumped Green 532 nm	CrystaLaser®	5 ~ 500 mW	0.5% (over 24h)	~ 30%	30 × 30 × 120 mm (with mounting support)

■	Excellent, exceeds requirements	■	Correctable deficiencies
■	Good, meets requirements	■	Unacceptable

spectroscopy. That leaves to two options: the Cobolt laser and the RGLase component. The power stability is good for both of them, but it is their size that drove the choice: in fact, the RGLase module cannot comply with the requirement of size, because at least two of its dimensions are bigger than 65 mm.

For this reason, the Cobolt 08-01 Series laser was selected for this work. It is a diode pumped CW laser that operates at 532 nm and ensures a high level of reliability, with its ultra-robust compact sealed package. Moreover, it is equipped with a mechanism to prevent the reflection of the laser-line. By contacting the producer, a STEP file of the component was available for modelling its integration with the whole system in the successive steps of the project [Cobolt, 2016].

7.2.3. OPTICAL COMPONENTS

By the term optical components, all that optics that is used to deliver the excitation light and to collect the scattered light is intended. Considering the configuration in Figure 7.1, the choices to be made concerned the beamsplitter, the filter, the collimator and the optical fibre to use. Select the appropriate optics is extremely important for ensuring the information to reach the spectrometer and the detector so as to be analysed.

BEAMSPLITTER

The beamsplitter is used to direct the laser light towards the window, and therefore the sample, and to transmit the scattered light to the collection optics, i.e. filter and collimator. In fact, the beamsplitter is able to separate and reflect light as a function of wavelength. In this application, the kind of beamsplitter needed is a dichroic mirror, which is highly transmissive above a certain cut-on wavelength and highly reflective below it. Therefore it works as a long-pass filter, but it has the advantage of being used at non-normal angles of incidence (usually at $\sim 45^\circ$) [Edmund Optics, 2017a; Semrock, 2017a].

In order to select the beamsplitter, a comparison is presented in Table 7.3 among options found on the market. The considered producers were Edmund Optics and Semrock, which can be both consulted on the internet. In this case, the parameters on the line were size and performance in terms of reflectance, cut-on wavelength, transmittance, angle of incidence, and OD.

Three main categories of beamsplitters were investigated: all three work with an angle of incidence θ of $\sim 45^\circ$ and allow to reflect the laser beam at 532 nm with a good performance (at least 94%). The main difference between the three classes is in the cut-on wavelength which varies from 537.2 nm to 552 nm. However, all the beamsplitters still comply with the lower limit of the spectral range. The transmittance is optimal for the required spectral range as well, therefore one difference that can be underlined is in the OD. The Semrock Bright-Line® component has a higher OD, reason why it was chosen as the most promising element. Notice that for each category, at least two sizes are possible with mounting or not. In the case of the selected option, two designs are possible, rectangular or circular: which one is better has to be decided according to the CAD model.

FILTER

The filter is what distinguishes most the Raman spectrometer from the other types of spectrometers, because it allows to reject the Rayleigh scattering, by transmitting to the spec-

TABLE 7.3: Characteristics of beamsplitters [Edmund Optics, 2017a; Semrock, 2017a]

	Producer	R	Cut-on λ	T	θ	Size	OD
Dichroic Laser Beam Combiner	Edmund Optics	98% @514.5– 543.5 nm	552 nm	95% @561.4– 790 nm	45°	• \varnothing 12.5 × 3.5 mm (mounted) • \varnothing 25 × 3.5 mm (mounted)	3
532 nm RazorEdge Dichroic™ laser-flat beamsplitter	Semrock	>94% @532 nm	537.2 nm	>93% @538.9– 824.8 nm	45° ± 0.2%	• \varnothing 25 × 3.5 mm (mounted) • \varnothing 25 × 1.1 mm (unmounted)	3
532 nm BrightLine® single-edge super-resolution laser dichroic beamsplitter	Semrock	>94% @514 – 532 nm	538.4 nm	>93% @541.6– 1200 nm	45° ± 0.35%	•25 × 35.6 × 1.1 mm (unmounted) • \varnothing 25 × 1.1 mm (unmounted)	4

TABLE 7.4: Characteristics of long-pass edge filters [Edmund Optics, 2017d; Semrock, 2017b]

	Producer	Cut-on λ	T	θ	Size	OD
Raman Long-pass Edge Filters	Edmund Optics	537.3 nm	≥93% @538.9– 1200 nm	0° ± 2	• \varnothing 12.5 × 3.5 mm (mounted) • \varnothing 25 × 3.5 mm (mounted)	≥ 6
532 nm RazorEdge® ultrasteep long-pass edge filter	Semrock	533.3 nm	>93% @535.4– 1200 nm	0° ± 2	• \varnothing 25 × 3.5 mm (mounted) • \varnothing 25 × 2 mm (unmounted)	>6
532 nm EdgeBasic™ best-value long-pass edge filter	Semrock	542 nm	>93% @546.9– 900 nm	0° ± 2	• \varnothing 25 × 3.5 mm (mounted) • \varnothing 25 × 2 mm (unmounted)	>6

trometer only the spectral range required and related to the Stokes and/or anti-Stokes scattering.

Among the long-pass edge filters available on the market, even in this case the choice was among Edmund Optics and Semrock filters. A comparison of these products was carried out, considering their characteristics summarised in Table 7.4. The major parameters

for this comparison were similar to the ones used for the beamsplitter selection: size and performance in terms of transmittance, cut-on wavelength, angle of incidence and OD.

All three described categories transmit the appropriate spectral range, even if with many differences: the attention has to be focused on the cut-on wavelength, which determines the steepness of the filter and the transmission of the spectral range. The cut-on wavelength varies from 533.3 nm for the RazorEdge® component, which means that the steepness is very good, to 542 nm for the EdgeBasic™ filter, which however allows to meet the requirements. The transmittance range is wider for the Edmund Optics component and the RazorEdge® filter, while it is narrower for the last category, even if this is not a limitation in the design of the instrument. Moreover, the OD is very good for all three classes, respecting the standard requirement of being higher than 5 in Raman spectroscopy measurements. As well as for the beamsplitters, the products present at least two available sizes, with mounting or without. Because systems engineering always deals to design what is required and not looking for *something a bit better*¹, the Semrock EdgeBasic™ is sufficient to meet the required performance, that is why it was chosen as filter for the system. As well as for the beamsplitter, the size has to be selected according to what best fits in the CAD model.

COLLIMATOR

After passing through the filter, the scattered light has to be collected in some way and directed to the spectrometer. The system configuration shows that was decided to be achieved with the use of a collimator connected by an optical fibre to the spectrometer.

The options on the market are several, among which the most promising were identified in some components produced by Edmund Optics and Thorlabs. Hereafter, a brief description of each class of components is presented:

- **Adjustable aspheric FC collimators** by Thorlabs. Their goal is to collimate light via Anti-Reflective (AR) coated aspheric lenses. These collimators allow to choose among four different focal length options (2/4.6/7.5/11 mm), with three AR coating options (350 – 700 nm or 650 – 1050 nm or 1050 – 1620 nm). They are compatible with FC/PC optical fibre cables. Among this class of collimators, the most suitable product is the one with focal length f equal to 2 mm, AR coating of 350 – 700 nm, with dimensions $\varnothing 12.1 \times 17.2$ mm [Thorlabs, 2017a], NA equal to 0.5 and alignment wavelength at 635 nm (centre of the visible spectrum).
- **Air-spaced doublet collimators** by Thorlabs. They are large collimators that use a doublet aspherical lens which simplifies the link between free-space and optical fibres. However, they perform optimally only at the design alignment wavelength because of the risk of spherical aberrations. Versions compatible with SMA905 connectors or FC/PC connectors are available. The most promising component is the one with NA equal to 0.25, $f = 35.41$ mm, with AR coating of 350–700 nm and alignment wavelength 635 nm. Its dimensions are $\varnothing 24 \times 45.4$ mm [Thorlabs, 2017a].
- **Fixed focus collimation packages: FC/APC connectors** by Thorlabs. These collimators simplify fibre-coupled detection system and can be custom designed. They are

¹Akin's laws of Spacecraft Design #13: *Design is based on requirements. There's no justification for designing something one bit "better" than the requirements dictate.*, http://spacecraft.ssl.umd.edu/akins_laws.html

compatible with single mode optical fibre with FC/APC connectors and they are compact and easy to integrate in an existing set-up. The aspheric lens presents an AR coating on both size as to minimise the surface reflections. The component that could suit this application is the collimator aligned at 633 nm, AR coating of 350 – 700 nm, $f = 4.46$ mm and $NA = 0.56$. Its dimensions are $\varnothing 11 \times 13$ mm [Thorlabs, 2017a].

- **Fixed focus collimation packages: SMA905 connectors** by Thorlabs. These collimators present the same characteristics as the previous class, but they are compatible with SMA905 connectors. In this class, the optimal component for the project is the collimator aligned at 543 nm, the usual AR coating, with $f = 4.34$ mm and $NA = 0.57$. Its dimensions are $\varnothing 11 \times 15.8$ mm [Thorlabs, 2017a].
- **Fiber Optic Collimator and Focuser Assemblies** by Edmund Optics. These components are designed to collimate and/or focus light via diffracted limited lenses with AR coatings available in three ranges. There are models compatible with SMA or FC connectors. The suitable component in this class is the one with NA equal to 0.55, $f = 4.51$ mm, aligned at 543 nm, compatible with FC connectors and with AR coating of 350 – 600 nm. Its size is $\varnothing 11 \times 9.6$ mm [Edmund Optics, 2017b].

As can be observed, one of the most critical parameters was the optical fibre connector that has to be used, therefore it was important to know also the dimensions of such connectors to be able to perform an appropriate comparison and selection in terms of size. Optical fibre connectors are standard components that connect the fibre to the optical devices, so that light can pass. Good connectors have really small losses. Different types exist now on the market, but for this work, the collimators ask for FC/PC, FC/APC or SMA connectors, which are shown in Figure 7.3. In order to save space, the plastic sleeves can be removed and in this way the dimensions of the connectors are: FC/PC $\varnothing 9.8 \times 30$ mm, FC/APC $\varnothing 10 \times 25$ mm and SMA $\varnothing 9.2 \times 25$ mm.

By knowing these dimensions, it was possible to perform a comparison and a selection of the appropriate collimator adding a parameter that indicates the final length of the assembly of collimator and connector. This was calculated using the STEP files provided by

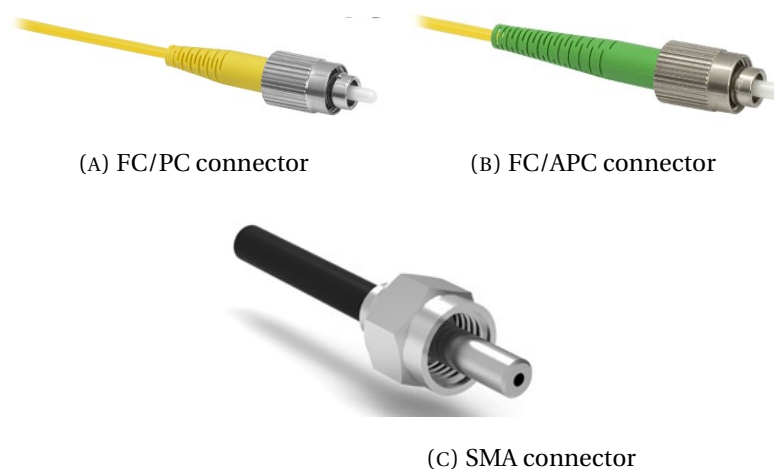


FIGURE 7.3: Fiber optic connector options [Industrial Fiber Optics, 2017; Thorlabs, 2017b]

the producers of the components and by measuring in a CAD model the dimensions. The results were the following (notice that they are not very accurate, but they give a good insight on how long the assembly is):

- **Adjustable aspheric FC collimators** by Thorlabs; ~ 33 mm.
- **Air-spaced doublet collimators** by Thorlabs; ~ 58 mm.
- **Fixed focus collimation packages: FC/APC connectors** by Thorlabs; ~ 38 mm.
- **Fixed focus collimation packages: SMA905 connectors** by Thorlabs; ~ 41 mm.
- **Fiber optic collimator and focuser assemblies** by Edmund Optics; ~ 23 mm.

Considering this as the driving parameter in the choice of the collimator, the last Edmund Optics device seems to be the better. However, it has a huge drawback: the AR coating does not cover the entire spectral range of the system. Therefore, this option had to be rejected. In a similar way, the air-spaced doublet collimator was discarded as well, because of the huge amount of space required by the assembly, which would represent almost 90% of one of the dimension of the system. Among the left options, the adjustable aspheric FC collimator has the shorter length. However, the adjustable focus is not needed inside the probe, because everything will be fixed before the deployment. Therefore, the most promising option fell in the class of Thorlabs fixed focus collimator. Always considering the length of the assembly as the driving criterion, the FC/APC connector allows to achieve the shorter length.

OPTICAL FIBRE

The choice of the optical fibre was strictly related to the choice of the collimator. Because the device complies with single optical fibres, this was the category selected for this application. Good optical fibres present high transmittance in the spectral response range of the spectrometer and the spectral range of light for measurements, a NA larger than the internal NA of the spectrometer, a core diameter larger than three times the slit width of the spectrometer (if the slit is larger than $70\ \mu\text{m}$) and a jacket with good light shielding [Anglia Instrumentation Ltd, 2017]. Table 7.5 shows the characteristics of a market single optical fibre produced by Thorlabs which is suitable for the application. Notice the small long-term bend radius that allows to better arrange the assembly of the system, but it is important to consider that an additional jacket has to be added. Usually, the final cable has a diameter of ~ 1 mm.

TABLE 7.5: Characteristics of Thorlabs single mode fiber [Thorlabs, 2017c]

Transmission	400 – 680 nm
Cladding	$\varnothing 125\ \mu\text{m}$
Coating	$\varnothing 245\ \mu\text{m}$
Jacket	UV Cured, Dual Acrylate
Short-Term Bend Radius	$\geq 6\ \text{mm}$
Long-Term Bend Radius	$\geq 13\ \text{mm}$
NA	0.12
Operating Temperature	$-60\ \text{to}\ 85\ ^\circ\text{C}$
Proof Test Level	$1.4\ \text{GN}/\text{m}^2$

7.2.4. SPECTROMETER & DETECTOR

Eventually, the last component, probably the most significant one, had to be selected. The Raman spectrometer receives from the optical fibre the scattered light collected by the collimator and all the previous optics. Its job is to diffract light through a grating and direct it onto the detector, so that the analysis can be performed.

In the selection of the most suitable COTS spectrometer, there are few parameters that played a fundamental role. In order of importance for this project:

- **Dimensions**, which has to comply with the technical requirements, and therefore each dimensions must be at maximum 65 mm;
- **Spectral resolution**, which should be ~ 0.3 nm, because of the conversion from cm^{-1} shown in the beginning of Chapter 6;
- **Spectral range**, which has to include the required $\sim 560 - 675$ nm;
- **Slit width**, which indicates the amount of light entering the spectrometer;
- **Number of pixels**, that are related to the performance of the detector;
- **Operating temperature**, which ensures the spectrometer to work under the environmental conditions dictated by glacial sites.

Notice that for the last three parameters, a threshold, or at least a value to comply with, was not set, because all three parameters can be easily corrected: the slit width conventionally can be costumed by the producer to achieve the required performance, the number of pixels can be changed (usually increased) by changing the detector and the temperature can be maintained with the use of heaters or cooling systems.

According to these criteria, a first selection of market components that could comply with them were identified, thanks to the communication with the technical support of the respective producers:

1. **Hamamatsu Mini-Spectrometer for Raman spectrophotometry**, high resolution type, TG series [Hamamatsu, 2017]
2. **Ibsen FREEDOM HR-VIS-NIR/mini Raman** [Ibsen Photonics, 2017]
3. **Ibsen FREEDOM HR-VIS** [Ibsen Photonics, 2017]
4. **Thorlabs Compact CCD Spectrometer** [Thorlabs, 2017d]
5. **Stellarnet Raman-SR** [StellarNet, 2017]

In order to select the best component, a graphical trade-off was elaborated and presented in Table 7.6. The five options are indicated with the numbers corresponding to the numbers in the list above. Notice that for some options, some information are not available (n.a.) for the required criteria. At first sight, it was possible to see that three of the five options cannot comply with the required dimensions because at least two of the three dimensions exceed 65 mm. This left to the choice between the two Ibsen components: in fact, both comply with the requirements for their dimensions. However, the HR-VIS-NIR/Mini Raman has a spectral resolution equal to 0.6 nm, which is unacceptable, because two times larger than the requirement.

TABLE 7.6: Graphical trade-off for spectrometers [Hamamatsu, 2017; Ibsen Photonics, 2017; StellarNet, 2017; Thorlabs, 2017d].

1 stands for Hamamatsu Mini-Spectrometer for Raman spectrophotometry, high resolution type; 2 stands for Ibsen FREEDOM HR-VIS-NIR/mini Raman; 3 stands for Ibsen FREEDOM HR-VIS; 4 stands for Thorlabs Compact CCD Spectrometer; 5 stands for Stellarnet Raman-SR.

	Dimensions	$\Delta\lambda$	Spectral range	Slit width	# pixels	Operating temperature
1	120 × 70 × 60 mm	0.3 nm	500 – 600 nm	10 μm	2048	+5 to +40 °C
2	61 × 65 × 19 mm	0.6 nm	475 – 1100 nm	5 μm	2048	–10 to +45 °C
3	61 × 65 × 19 mm	0.4 nm	360 – 830 nm	5 μm	2048	–10 to +45 °C
4	122 × 79 × 29.5 mm	0.5 nm	350 – 700 nm	20 μm	3648	n.a.
5	25 × 76 × 127 mm	0.4 nm	536 – 940 nm	n.a.	2048	n.a.

■	Excellent, exceeds requirements	■	Correctable deficiencies
■	Good, meets requirements	■	Unacceptable

Although the HR-VIS spectrometer has a resolution that does not comply with the criterion either, it is nearer the value of 0.3 nm and therefore it is quite acceptable. In fact, the slit width could still be reduced so as to increase the spectral resolution. This component works in a spectral range of 360 – 830 nm, which includes the range of the requirements. The number of pixels of its BT-CCD is 2048, which allow a good performance of the detector with high sensitivity and medium SNR. It complies with a SMA connector, with strict requirements for the dimensions, but that do not create any problems for the selected connector. The operating temperature almost complies with the requirements, but the lowest accepted temperature is still higher than –15 °C, which means that some precautions in ensuring the working of the instrument must be taken. A STEP file was provided by the producers, so to formulate the design in a CAD model.

7.3. PRELIMINARY CAD OPTIONS

Eventually, a first design of the system was elaborated via a CAD modelling tool, the CATIA™, a software developed by the French company *Dassault Systèmes*. The acronym stands for Computer-Aided Three-dimensional Interactive Application (CATIA) and it allows computer-aided design, manufacturing, engineering, product life management and 3-Dimensional (3D) modelling. This approach to the design was particularly helpful in visualise how the system can be once all the selected components are integrated. Above all, it gives an insight on if the system can comply with the requirements on volume and mass. Moreover, it would be possible also to simulate mechanical and thermal behaviour of the definitive Raman spectrometer, but this was not the part of this project at this point. The choice of trusting a CAD software is due to the fact that principal opto-mechanical producers, such the one chosen for the components, provide computer models of their products in the STEP format, which are easy to be downloaded and assembled together. Furthermore, by easily creating this assembly, documentation such as drawings and illustrations can be quickly produced. Same stands for the components that are not COTS and need to be designed and manufactured [Kiselev et al., 2016].

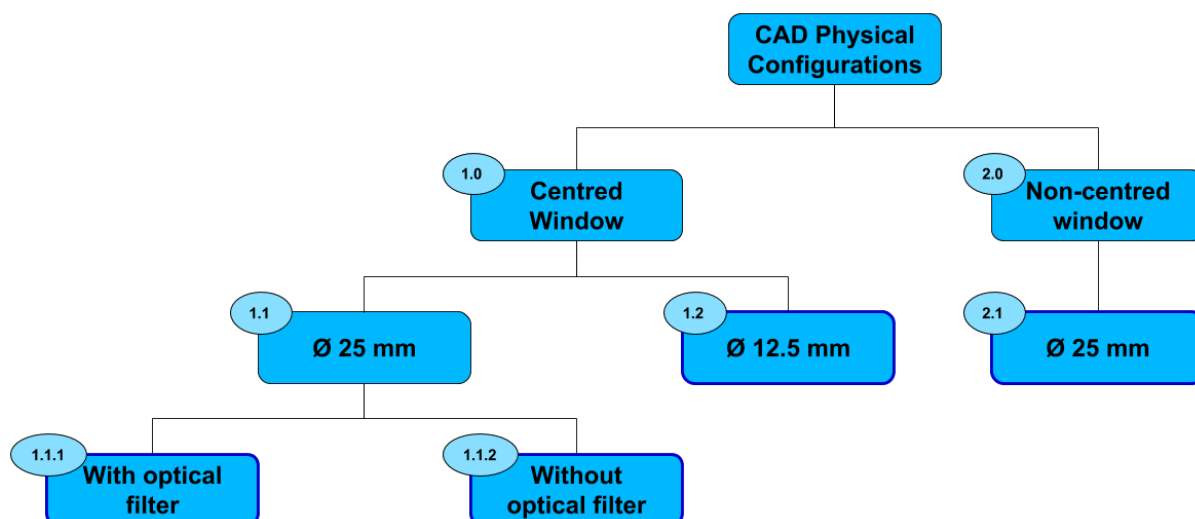


FIGURE 7.4: Design Option Tree (DOT) for CAD physical configurations

At this point of the project, with the **COTS** selected through the extensive decision processes presented above, it was important to understand how the real physical configuration can be, even to understand which sizes of the components are necessary. For that, a Design Option Tree (**DOT**) of the possible physical configurations elaborated on the software is shown in Figure 7.4. All the options are explained shortly hereafter, presenting the first elaboration of the project to see how to allocate all the components and explaining the reasons why or why not the options were cancelled from the list of possible concepts. Besides, it is explained the process behind how this **DOT** was created and why all the branches were considered. These preliminary physical configurations are shown in Figure 7.5

As can be observed from the **DOT**, the main decision concerned the allocation of the window with respect to the entire system. At the second level, the choice was instead about the **COTS** dimensions. Notice that all the concepts were modelled to fit in a designed case with the dimensions equal to $65\text{ mm} \times 65\text{ mm} \times 150\text{ mm}$ and for the optical components, rough mounting supports were modelled (which were then changed for the final design), that can allocate all the possible sizes for the beamsplitter and the filter indicated in Tables 7.3 and 7.4. Moreover, the laser and the spectrometer were not considered in these preliminary options, because they are allocated in the bottom of this case, therefore their dimensions do not interfere with the optical components allocation.

The considered options in the **DOT** are the following:

1.0 Centred window. The centred window seems to be the most common idea when one first think of an optical instrument. The entire system would be balanced in this way and it seems to be the option where most of the volume is used.

1.1 $\varnothing 25\text{ mm}$. At first, bigger optical components with a diameter of 25 mm were considered. In this way, the field of view of the instrument can be increased and most scattered light can be collected from the sample. However, it is important to remember that the final optical field of view is dictated by the collimator field of view and its **NA**. For this size of the components, the window was designed with a diameter of 20 mm, that increases up to 30 mm on the inside of the case,

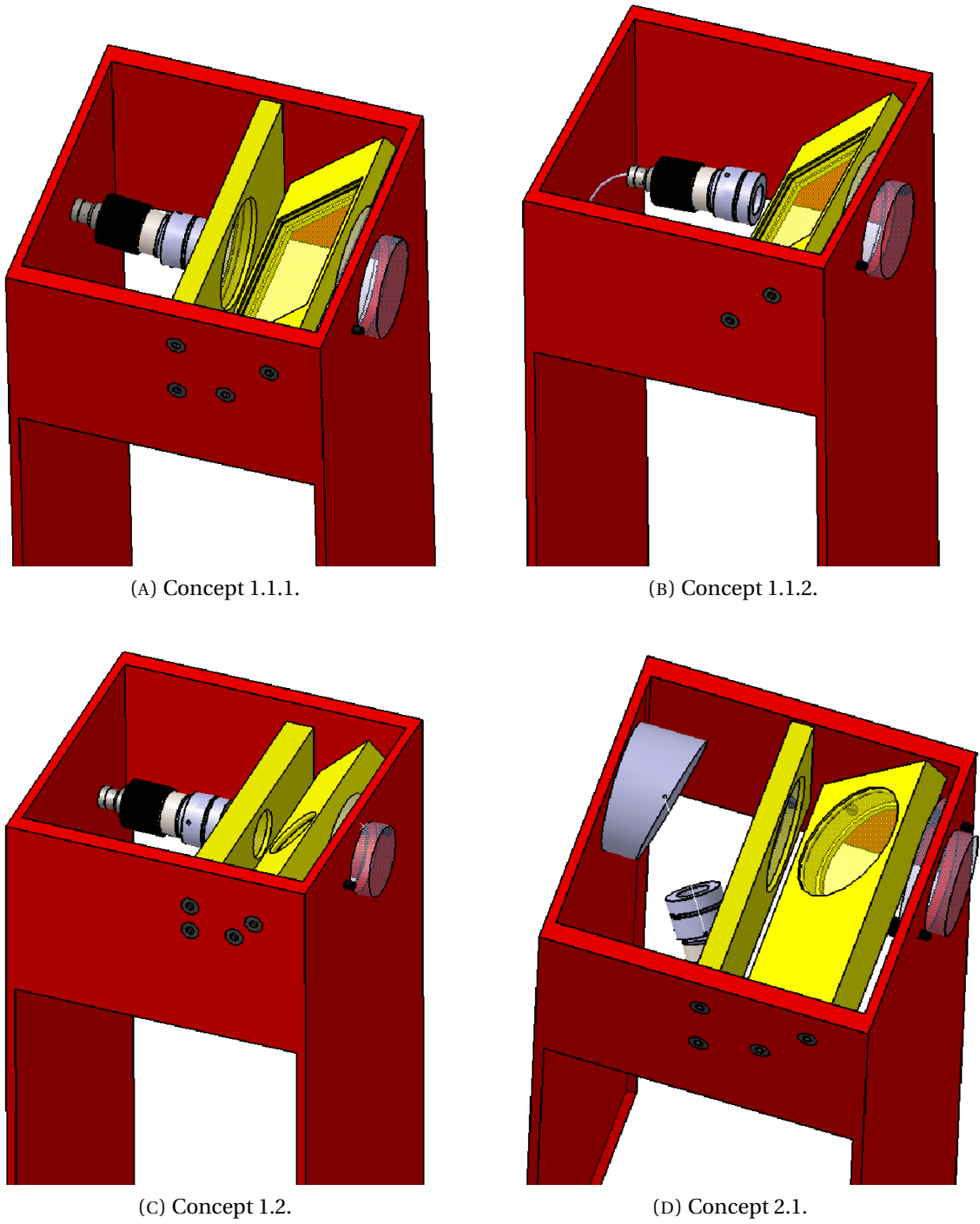


FIGURE 7.5: CAD physical configuration concepts

for mounting solutions (all the designed components are better described in next Chapter).

1.1.1 With optical filter. The very first concept, shown in Figure 7.5a, was created by following the system configuration decided in Figure 7.1. After the window, the scattered light is transmitted by the beamsplitter to the filter and then collected by the collimator. However, as can be observed, the assembly of collimator and FC/APC connector is too big and there is not enough space for the optical fibre to bend at the minimum long-term bend radius. Therefore, this option was not achievable.

1.1.2 Without optical filter. To overcome the problem encountered in the previous concept, an option without an optical filter was elaborated. That was possible because the beamsplitter works as a filter as well for what concerns the laser-line wavelength. However, it only has an OD equivalent to 4, which is high for a typical beamsplitter, but can be insufficient for the required performance of a Raman spectrometer. Anyway, this new configuration, shown in Figure 7.5b, provides enough space for the fibre to bend. Although this good achievement, investigation on optical benches breadboards are necessary to verify the performance without an optical filter with a higher OD.

1.2 $\varnothing 12.5$ mm. The second way to fight the lack of space for the optical fibre to bend in the centred window configuration was the use of smaller optical COTS. Therefore, the beamsplitter and the filter were chosen with the diameter of 12.5 mm, so that some space could be saved. For this size of the components, the window was designed with a diameter of 15 mm, that increases up to 25 mm on the inside of the case, for mounting solutions. Figure 7.5c shows the option with this configuration. The smaller lenses have a huge drawback, because they are available only with a larger thickness so that also the mounting supports require more volume. Therefore, even if some space it is still left, the optical fibre barely bends, by not allowing some contingency space before the wall.

Furthermore, it is particularly important to underline that reducing the size of the collection optics affects the signal of the Raman scattering. In fact, considering the explanations given in Chapter 4 and in particular Equation (4.15) and Figure 4.3, it is evident that the performance of the Raman spectrometer is directly proportional to the dimensions of the collection lenses. If they are reduced, also the signal diminishes because both A_D and Ω_D decrease. In the same way, also the resolution of the instrument worsens, because the light received at the detector is less [Guldimann and Kraft, 2011]. That is why this configuration needs major investigations on its performance before to ensure to satisfy the requirements.

2.0 Non-centred window. The allocation of the window can be also moved. In fact, the previous configurations showed that a lot of space on the sides is wasted. However, it was important to consider that this new concept requires a new optical component between the optical filter and the collimator that was not taken into account so far: a mirror. The introduction of this mirror allows the collimator to be moved in order to gain the room necessary to connect it to the optical fibre and the spectrometer. The whole discussion on the selection of the type and the size of the mirror is elaborated

in next Chapter. Be aware that the same component could not be introduced in the previous options with the centred window, because of problems of space to fit the collimator at the focus point of the mirror.

2.1 $\varnothing 25$ mm. With this new configuration, the choice of the size of the components was again the biggest. Same stand for the window. Adding the mirror, Figure 7.5d shows that the whole Raman spectrometer can comply with the requirement on the size of $65 \text{ mm} \times 65 \text{ mm} \times 150 \text{ mm}$, by making use of the system configuration elaborated before, only by adding a mirror. Notice that a second option on the size was not need for the non-centred configuration, because everything is shown to fit with the bigger size.

8

DEFINITIVE DESIGN

Last Chapter presented the concept that is most suitable in order to fit all the components in the available volume. Notice that this choice was derived by trial and error, trying to allocate the window in different positions and see which one allows to build the system and performs the measurements. Moreover, different diameters of the optical components were considered. Eventually, the most promising concept for the design resulted to be the non-centred window with the dimensions of the optical components equal to 25 mm, because of the promise of a higher scientific return.

In this Chapter, the final design is elaborated, adding to the optical components their mounting supports and presenting how they are integrated. This is part of Section 8.1. In addition, the definitive design of the Raman spectrometer does not only concern its assembly and the integration of its components but it is important to consider how the system has to be integrated into the IceMole probe too. Therefore, Section 8.2 deals with this aspect, by proposing a mounting procedure in order for the system to be operational within the probe. Then, a primary consideration of the mass, power and data budgets of the Raman spectrometer is presented in Section 8.3, so as to identify these characteristics for the successive iterations of the design, when the power supply and the transmission of the collected data will be elaborated. Eventually, a preliminary cost analysis of the system is presented in Section 8.4, considering the cost of the COTS and making some assumptions on the cost for manufacturing the designed supports.

8.1. FINAL CAD MODELLING

From Figure 7.5d, it was observed that the configuration with the non-centred window and with the use of a mirror allows the Raman spectrometer to fit in the volume of $65\text{ mm} \times 65\text{ mm} \times 150\text{ mm}$ imposed by the technical requirements of Table 3.3. At this point, the definitive design was elaborated, which means that all the selected components were assembled together in a final configuration, where the mounting supports and the mounting procedures were added as well. This Section aims at presenting which procedure was followed to derive and create the design and how all the components were assembled.

Case. The first component to be designed was a case that could contain all the components and that has the required size. Figure 8.1 shows a rendering of this modelled component. The

overall dimensions of the case point out the requirements and therefore were decided to be equal to the available volume (65 mm × 65 mm × 150 mm). As can be observed, the modelled case presents a rectangular crown in the higher part of the object, while it only presents two pads in the lower. This is because of mounting and size reasons: in the higher part, where the hole for the window is, the optical components must be mounted, while the bottom part hosts only the spectrometer and the laser, as they need direct access to the electronics and the power supply provided by IceMole. Therefore, two of the four walls can be eliminated saving some mass. The window hole is positioned non-centred, in accordance to the exit of the laser beam. The holes for the screws and the mounting mechanisms were added in a continuous process while designing and assembling the other components.

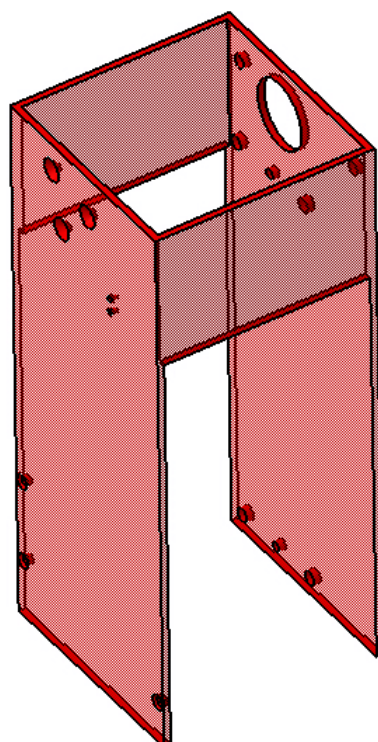


FIGURE 8.1: Rendering of modelled case

Mirror. As stated before, the main aspect of the non-centred configuration was the use of a mirror that could transmit the filtered scattered light to the collimator by allowing at the same time to have the components inside the case. The choice of the mirror was decided by trying to fit the component in the assembly and verifying that the assembly of collimator and connector at the right angle allows the fibre to bend and be connected to the spectrometer.

The first analysed option was a mirror that reflects the light at 90° . This means that with respect to the case the collimator is perpendicular to the other optical components. However, in this way the collimator would interfere with the position of the spectrometer. Instead, the 90° mirror can be turned about the vertical axis in order to reflect the light at the same height of the case with respect to the chief ray of the optical components. However, in order to get enough space for the collimator and the connector to fit in the design and not to interfere with the other optical lenses, the mirror has to be too inclined with respect to the direction of the light and the size needed to collect all the incoming light would be too big.

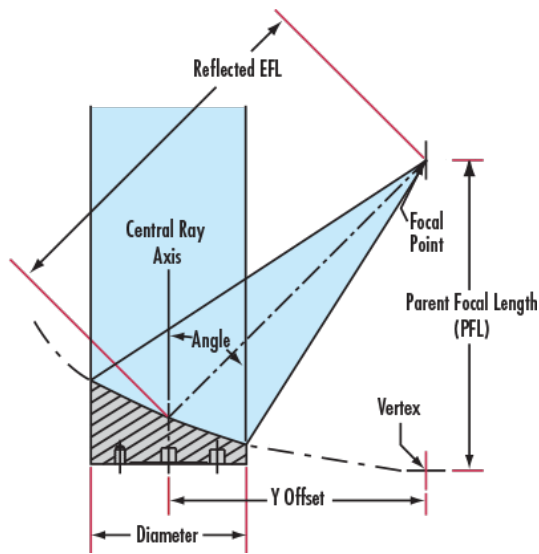


FIGURE 8.2: Working principle of an off-axis parabolic mirror [Edmund Optics, 2017e]

Therefore, the alternative was to consider an off-axis parabolic mirror, whose working principle is shown in Figure 8.2. With such a component, the light is reflected to a focal point which is identified by an angle and a y-axis offset. The effective focal length is measured on the axis that the chief ray follows at the angle of the mirror while a parental focal length is measured on the horizontal axis [Edmund Optics, 2017e].

First, it was taken into account a 45° off-axis parabolic mirror. However, for a mirror with a diameter of ~ 25 mm, the dimensions of the component were too large to fit in the amount of space available. Therefore, the choice was turned towards the use of a 30° mirror. By trying to fit this type of mirror in the assembly, it was successfully demon-

strated that the collimator and the connector can stay in the volume leaving enough space for the optical fibre to bend towards the spectrometer. The optical component was provided by Edmund Optics and it has a diameter of 25.4 mm, an effective focal length of 27.4 mm and a parental focal length of 25.4 mm. The last choice that had to be taken concerned the reflective coating, which has to perform in the same spectral range of the spectrometer. Therefore, it was decided to rely on protected aluminium, which reflects the wavelength range of 400 – 1200 nm [Edmund Optics, 2017e].

Optics Support. The optical components are very fragile and sensitive to temperature changes and mechanical stresses, which are very strong for the testing sites of the IceMole probe. Therefore, a support for the circular optical components was modelled to try to minimise these effects, by not mounting them directly. Notice that all the mounting supports were designed by referring to Yoder Jr [2005], as primary source of examples.

The support for the optics is thought as a tube attached to one wall of the case by some screws, in order to support all the lenses and minimise the stray light in the system, by guiding the path of the scattered light. The modelled component is shown in Figure 8.3. The external diameter is equal to 30 mm and the wall has a thickness of 1 mm. The bottom of the tube is maintained with 1 mm thickness in order to be able to mount the screws, whose position is dictated by the mirror alignment. Notice that in the tube two holes are created: one small in the right side, which allows the laser beam to arrive at the beamsplitter, while the other is big enough for the reflected light to be focused in the off-axis focal point. The latter has a more difficult construction on a plane at 30° and depends on the actual alignment of the mirror. Be careful that this hole was constructed according to a precise alignment of the mirror, if that would be moved then the hole has to be moved too. Even in this case, the holes for the screws and the mounting mechanisms were created in a continuous design process.

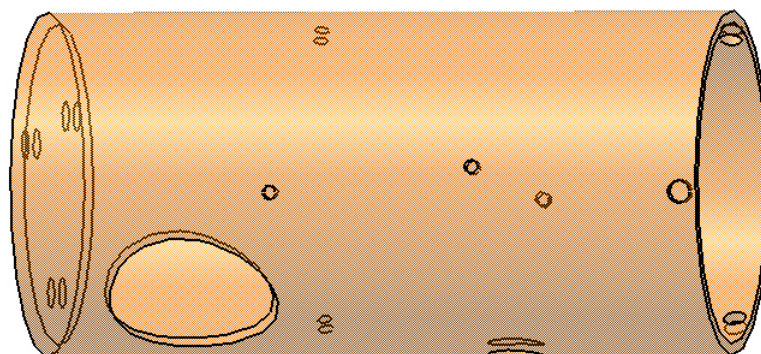


FIGURE 8.3: Rendering of modelled optics support

Window and Support. Considering that the selected optical lenses have a diameter of 25 mm, the window was designed with a diameter of 20 mm. This choice depends on the normal projection of the beamsplitter lens at 45° , which corresponds to a diameter of $25 \text{ mm} \cos(45^\circ) = 17,68 \text{ mm}$. As to simplify the manufacturing, this value was approximated to 20 mm, sufficient to analyse a large area of the ice sample. The window presents a thickness of 8 mm for mounting reasons. It indeed allows to maintain high optimal optical performance, as represented by the characteristics of sapphire presented in Table 7.1.

To mount the window to the optics support and the assembly, the same considerations about the thermal and mechanical stresses stand. Therefore, because of the sensitivity of the window, the support was created in a way that the window can be glued to some tabs constructed on a circular mounting support which in turn is assembled to the optics support with three screws. The window and its support are presented in Figure 8.4. The outer diameter of the support is equal to the inner diameter of the optics support (28 mm) and the inner equal to the diameter of the window. The tabs are 12 in a circular pattern of 15° with a thickness of 0.5 mm and a dimension of 1.5 mm.

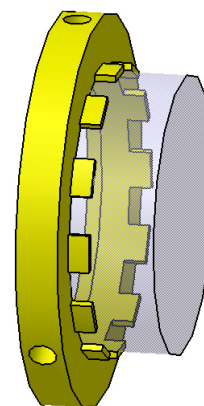


FIGURE 8.4: Rendering of modelled window support and window

Beamsplitter and Support. The 532 nm BrightLine© single-edge super-resolution laser dichroic beamsplitter of Semrock was not provided as a STEP file by the producer. Therefore it was designed as a pad of 1.1 mm and a diameter of 25 mm.

The mounting support of the beamsplitter was modelled with the same philosophy as the support of the window, to minimise thermal and mechanical stresses for such a fragile lens. However, the main aspect of this support is that it was built to be mounted at 45° . Therefore, the profile at this angle for the support is an ellipses with semi-minor axis equals to the inner diameter of the optics support, the semi-major axis as $28 \text{ mm} \cdot \sqrt{2} = \sim 36 \text{ mm}$ and

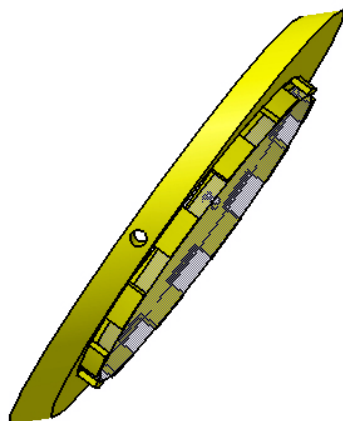


FIGURE 8.5: Rendering of modelled beamsplitter support and beamsplitter

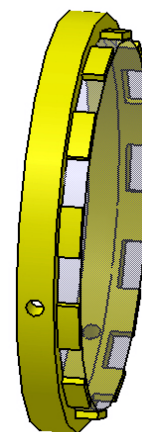


FIGURE 8.6: Rendering of modelled filter support and filter

a thickness of 3 mm. Then the lens is glued to the tabs, that have the same dimensions as the ones for the window support. The support is presented in Figure 8.5 and assembled to the optics support with two screws.

Filter and Support. Same as for the beamsplitter, the 532 nm EdgeBasic™ best-value long-pass edge filter of Semrock was not provided as a STEP file. Therefore it was designed as a pad of 2 mm and a diameter of 25 mm.

The mounting support of the filter can be considered the same as the one for the window. However, the inner diameter is equal to 25 mm and it has a thickness of 2.5 mm. The tabs for gluing the filter were modelled in the same way as for the other mounting supports. The assembly of filter and its support is presented in Figure 8.6 and assembled to the optics support with three screws.

Collimator and Support. The fixed focus collimator FC/APC was provided as a STEP file by Thorlabs and it was assembled with the appropriate connector given by Thorlabs, in order to select the appropriate component in the previous Chapter.

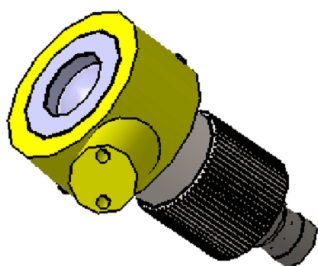


FIGURE 8.7: Rendering of modelled collimator support, collimator and FC/APC connector

the case by two additional screws.

The mounting support was modelled by considering the position that the collimator has to stand to receive the reflected light. Therefore it presents a particular configuration, shown in Figure 8.7 in the assembly with the FC/APC connector and the collimator. It was modelled with a surface at 60° that supports the collimator by screwing it and fixing it with two slotted set screws with cone point DIN EN 27434 M1.2 \times 6 mm. The support is assembled to

Laser and Spectrometer. The selected laser and spectrometer were provided as STEP files by respectively Cobolt and Ibsen producers. So they were directly assembled to the case on the long walls. Notice that the laser beam has to be centred with the beamsplitter.

With the modelling of all the single components and their supports, it was possible to assemble everything together and derive a final CAD model of the Raman spectrometer for the IceMole probe.

First, the optical lenses were assembled together in the optics support via the screws. All the optical components share the same axis, of course, and the position of each support is defined by the position of the holes for the screws. All the screws are slotted set screws with cone point, classified as DIN EN 27434. For the window they are three M2 × 4 mm, for the beamsplitter two M1.2 × 3 mm and for the filter three M1.2 × 2.5 mm. At the bottom of the optics support, the mirror is placed, and both the support and mirror are assembled together with the case by three 6-32 UNC screws (dictated by the design of the COTS mirror). Figure 8.8 shows the assembly of the optical components. The mounting procedure establishes the order with which the components are assembled: mirror, filter, beamsplitter and window.

Then, this assembly and the remaining components were assembled together inside the case. Figure 8.9 shows the final CAD model. As can be seen, the Ibsen spectrometer and the Cobolt laser are mounted in the bottom part of the case. Notice that the spectrometer occupies the entire long pad while the laser was positioned in such a way to centre the laser beam with the centre of the beamsplitter and the window. To the spectrometer, the SMA connector was added, as STEP file provided by Industrial Fiber Optics. The analysis system is mounted to the case by three countersink raised screws (common head style)-type H DIN EN ISO 7047 M3 × 6 mm, while the laser itself presents a mounting plate, that is connected to the case by two screws of the same type M3 × 4 mm. Notice that four other holes are created for screws with the diameter of M4.2 mm, but appropriate components to be added to the model were not found.

The optics support is aligned with the hole for the window and the holes for the screws in

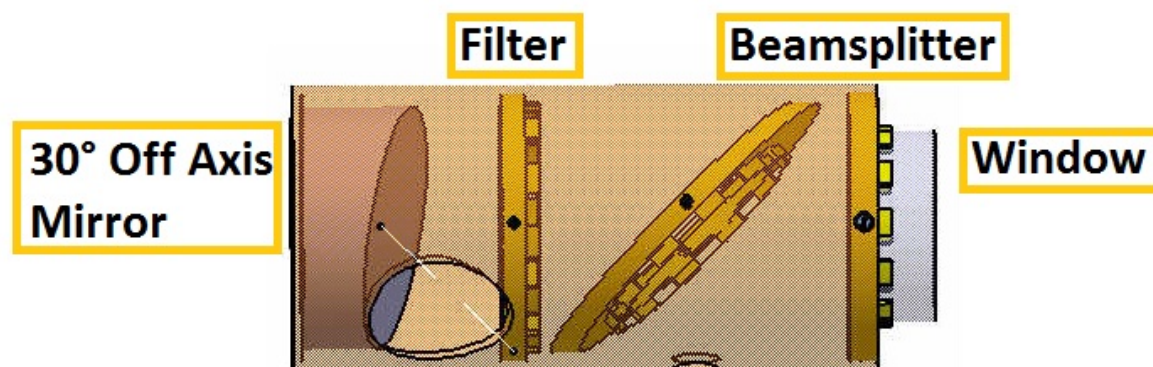


FIGURE 8.8: Rendering of the assembly of the optical components

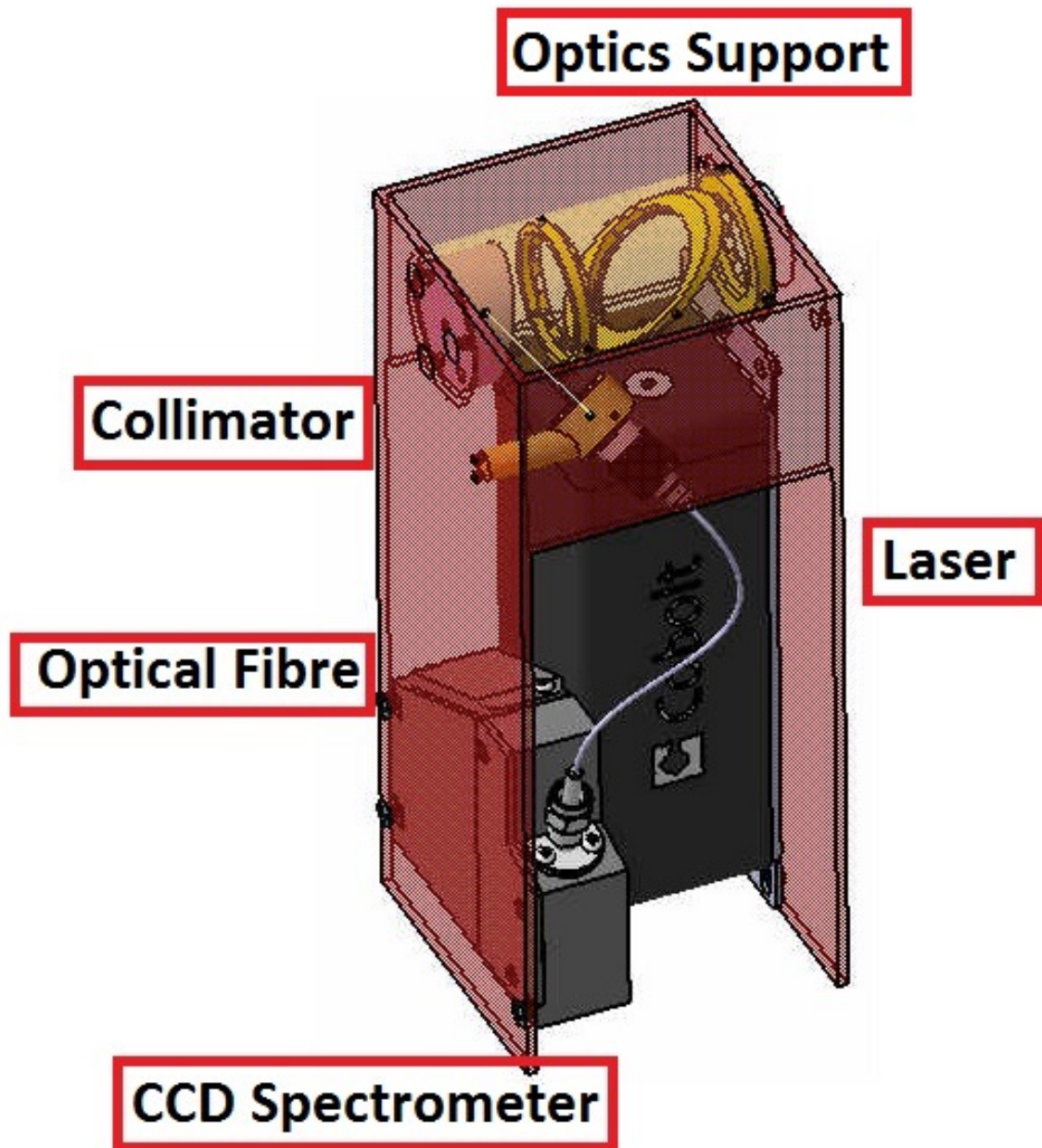


FIGURE 8.9: Rendering of the final assembly

the bottom of the tube. Notice that these holes were created exactly to achieve an appropriate angle for the focusing point of the mirror and cannot be changed without changing the alignment between mirror and collimator, and therefore also the position of the hole (however, such American screws are not included in the assembly, because appropriate components were not found). The support of the collimator is then positioned in such a way that the collimator axis is coincident with the axis on which the focus of the mirror lies. However it is not necessary for the collimating lens to be exactly in that point, because it has a large numerical aperture ($NA = 0.56$). The collimator support is mounted with the case by two slotted pan head screws with small head DIN 920 M1.2 \times 5 mm.

The final component that was created is the optical fibre: within the Wireframe and Surface Design ambient in CATIA™, the spline connecting the point on the FC/APC connector, tangent to it, and the one on the SMA connector, always tangent, and passing through a generic third point was created. Then, through the Rib function the profile of the fibre was created with a diameter of 1 mm. With the function Measure, it was possible to verify the length of the fibre needed, equal to ~ 76 mm and that the bending angle is never below 13 mm as required by the specifications of the Thorlabs single-mode optical fibre.

The final technical drawings of the modelled parts can be found in Appendix B, while for the COTS, the technical specifications and drawings are collected in Appendix A.

8.2. INTEGRATION INTO ICEMOLE

The Raman spectrometer was designed and assembled to fit in the miniaturised design of the current IceMole generation with cross sectional area equal to 80 mm \times 80 mm. Hence, the case of the system allows that it can be directly integrated into the probe.

Once the Raman spectrometer is assembled, it can be integrated into the IceMole probe. In order to do that, the design of the probe has to be changed from the current version: of course, the length of the probe has to be increased so that it could carry the instrument, and in one of the walls, the hole for the window has to be designed. Obviously, where the instrument is exactly allocated within the rear back of IceMole (as explained in Section 6.1), the walls do not have to present the conductive plates to perform the melting, not to damage the instrument. The hole in the probe wall has to guarantee that the window can be glued inside of it. This process is allowed by the fact that the internal cross sectional area of IceMole, considering the walls thickness of 4 mm, is equal to 77 mm \times 77 mm. In fact, the instrument case presents a smaller area, so that the mounting operations are possible. In order to ensure the preservation of the position and therefore of the alignment of the optical components, two additional holes for screws M4 were added in the modelled case, so as to allow to better support the system attached to one of the wall of the IceMole probe (see Figure 8.1).

8.3. MASS, POWER & DATA BUDGETS

Once the final design was defined, it was possible to consider the total mass. This is calculated in Table 8.1. The values of the masses were computed directly by the CATIA™ software with the function Measure Inertia: this function allows to input the density of the material and obtain the mass of the single component. The Table indicates the material for each component and its respective density, so as to determine the final mass. Notice that

TABLE 8.1: Mass budget (some material components or masses are assumed)

Component	Material	Density [g/cm ³]	Mass [kg]
Window	Sapphire	3.98	0.01
Support Window	Invar	8.1	0.007
Beamsplitter	Glass ¹	2.19	0.001
Support Beamsplitter	Invar	8.1	0.005
Filter	Glass ¹	2.19	0.002
Support Filter	Invar	8.1	0.003
Mirror	Aluminium ¹	2.7	0.012
Mounting Optics	Invar	8.1	0.05
Collimator	-	-	0.02 ²
Support Collimator	Invar	8.1	0.009
Laser	-	-	0.3 ³
Spectrometer	-	-	0.07 ⁴
Case	Invar	8.1	0.408
Optical Fiber Components	-	-	0.03 ⁵
		Total	0.927
		Contingency	0.2⁶
		Total mass	1.127

¹ Assumed material for COTS² [Thorlabs, 2017a]³ [Cobolt, 2016]⁴ [Ibsen Photonics, 2017]⁵ Assumed weight for the optical fiber, the connectors weigh 0.01 kg each [Industrial Fiber Optics, 2017; Thorlabs, 2017b]⁶ Considered for screws and for wrong assumptions, ~20% of the total

for some components, such the lenses, the material was assumed to be glass (or aluminium in the case of the mirror), while for the modelled supports the selected material was invar, a space-qualified alloy that allows to have high thermal and mechanical properties. On the other hand, the mass of the other remaining COTS were derived directly from the specification sheets (Appendix A).

As can be noticed, the total mass is equal to 0.927kg, which is well below the requirement for a mass lower than 2kg (SYS-03-IM-02). However, in the first sum, the screws and mounting systems are not considered, therefore an additional contingency of 200g needs to be taken into account, also in the case of wrong assumptions. Therefore, the computed total mass is 1.127kg, which makes sure that the system complies with the requirement.

For what concerns power requirement, the only components that need to be supplied with power are the spectrometer and the laser. For this reason, they are allocated in the bottom part of the case, in such a way that it is easier to access to the power bus of IceMole. The laser receives the power via a DC plug 2.5 mm/5.5 mm female, while for the spectrometer the electronics components for data and power management still have to be designed. The laser requires 5V DC and a maximum current of 5A, therefore the maximum required power can be computed from Ohm's law $P = Vi = 25W$. On the other hand, the spectrometer works with a maximum of 16V and an operational current of 150mA ($P = 2.4W$) [Cobolt, 2016; Ibsen Photonics, 2017]. Therefore, it can be expected a maximum of required power equals

TABLE 8.2: Cost budget

Component	Company	Cost
Beamsplitter	Semrock	545\$ 483.11€
Filter	Semrock	455\$ 403.33€
Mirror	Edmund Optics	260€
Collimator	Thorlabs	181€
Connector FC/APC	Thorlabs	7.75€
Connector SMA	Industrial Fiber Optics	5\$ 4.43€
Optical Fiber	Thorlabs	13€ ¹
Laser	Laser2000	7500€
Spectrometer	Ibsen	4295€
Total		13151.25€
Manufacturing Costs ²		50000€
Contingency		2500€ ³
Total cost		65651.25€

¹ Cost for 1 m² Assumed for manufacturing the mod-

elled components

³ ~ 20% of the total COTS cost

to ~ 27.4W and the integration with the probe should provide at least this amount for the system to operate.

The amount of data that the CCD spectrometer collects can be roughly estimated by considering the number of points that are identified in the spectrum divided by the spectral resolution of the instrument. The spectral range that arrives at the detector is 546.9 – 700 nm (combination of the optical properties of the components) and the resolution is equal to 0.4 nm:

$$\frac{700 - 546.9 \text{ nm}}{0.4 \text{ nm}} = \frac{153.1 \text{ nm}}{0.4 \text{ nm}} \approx 383 \quad (8.1)$$

Then, the Ibsen spectrometer converts the data in 16bit, therefore for each spectrum, $383 \cdot 16 \text{ bit} = 6128 \text{ bit} = 766 \text{ bytes}$ are obtained. Finally, to obtain the data rate, this last value has to be divided for the exposure time, which is supposed to be 10s. Therefore, the spectrometer transmits about 612.8 bit/s.

8.4. COST ANALYSIS

With a view of defining how much this system could cost, an official quotation was required to all the companies that provide the COTS. The costs are summed in Table 8.2. Notice that some of the costs need to be translated from Dollars to Euro with a factor of conversion equal to $1 \$ = 0.891384766 €$ ¹.

As can be seen, the total amount required to buy the COTS is ~ 13000€, but to this sum, the cost for the manufacturing of the modelled components, such all the lenses supports, the

¹Currency change rate on June 14th, 2017

optics support and the case, needs to be considered. An estimate for these is assumed to be 50000€. This huge amount of money allows to have enough contingency for the system to be built. Moreover, a contingency factor equals to ~ 20% of the total COTS cost can be taken into account, in order to be sure that the funding for designing, manufacturing and assembling the system would be sufficient. However, it is important to consider that at this point, the cost for the testing campaigns are not included, but they actually represent a huge part of the costs to build the system. They indeed guarantee the proper working of the system and they validate its capabilities. Part of the amount considered for the manufacturing processes can be considered to be used for testing, as its margin is very high, but however probably not sufficient.

PART III:
VERIFICATION

9

VERIFICATION, VALIDATION & CALIBRATION

The systems engineering approach relies on a continuous process that needs to perform verification and validation at each phase of the mission development. With the definition of the critical design, it is possible now to discuss about this aspect of engineering.

Figure 9.1 represents the V-model, which is one of the typical graphical representations of a system development life cycle. In this case, with respect to the NASA life cycle presented in Chapter 3, the V-model aims at highlighting the importance of decomposition and integration in the process, while underlining the continuous verification and validation investigations that tie the two branches of the scheme during the design [Gill, 2015]. It is particularly important to notice that the validation and verification have to be performed at different level of the process, starting from the high-level requirements, to the subsystem ones. However, although this model undoubtedly defines the development activities and their respective testing, these activities are quite simplified, by illustrating them as sequential steps rather than simultaneous and iterative.

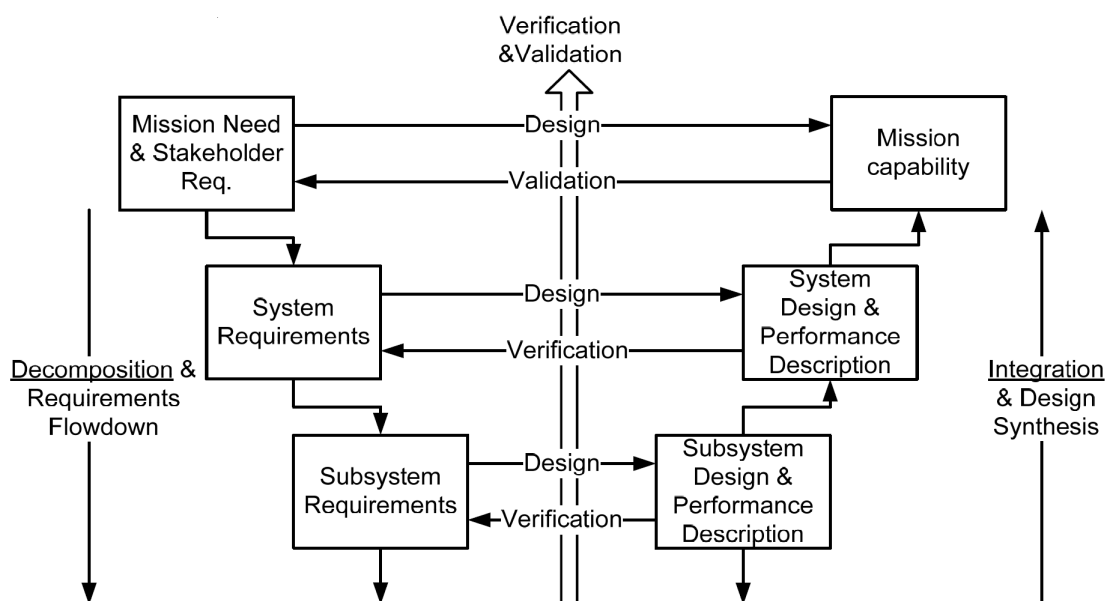


FIGURE 9.1: V-Model [Gill, 2015]

Verification is defined as the proof of compliance of the design solution specifications with the requirements, while validation is intended as the proof that the product accomplishes the intended purpose dictated by the stakeholders' expectations (from NPR 7120.5). These two terms are usually conflicting and improperly exchanged, but it is important to underline that one cannot substitute the other and that both the processes are needed to certify the correct and appropriate working of the developed system.

This Chapter aims indeed at developing the discussion concerning Verification & Validation (V&V) activities, in order to ensure the Raman system design to comply with the requirements and to be appropriate to satisfy the customers' need. Section 9.1 focuses on describing a V&V plan, by correlate the requirements to the right verification method and by proposing the testing that have to be effectuated. After that, Section 9.2 deals with the verification of the proposed design, by evaluating the requirements already verified and underlining which ones still need further investigation by means of a Verification Compliance Matrix (VCM). Then, an important aspect of such an instrument is considered. A Raman spectrometer, as well as all the spectrometers, has to be calibrated in order to obtain a high performance in collecting the spectra. So, Section 9.3 deals with the reduction of the detectable known data as well, in order to elaborate a spectrum that could give some additional information on what can be found in ice, by not repeating what is already known.

9.1. VERIFICATION & VALIDATION PLAN

Verification concerns the engineering part, by checking if the system is well-designed, error-free, etc., while validation wants to check if the system meets the customers' requests. Verification determines if the system is working, while validation determines if it is valid. The first process is a quite objective process, while validation is rather subjective, by relying on assessments. In fact, the main differences between the two actions concern the references used to check the correctness of an element, and the acceptability of the effective correctness. In verification, the expected result and the obtained result are evaluated in a binary mode (yes or no), while in validation, the result of the comparison may require a judgement of value regarding whether or not to accept the obtained result compared to a threshold or limit [SEBoK, 2013].

Typically, the words integration, verification, validation and testing are used in combination, so that within engineering the terminology of Assembly, Integration and Verification (AIV) or Assembly, Integration and Testing (AIT) are commonly adopted. V&V aim at guaranteeing the compliance of the system with the derived requirements and the stakeholders' expectations: first, the requirement validation is elaborated (are these the right requirements?); then the models must be validated (are those correct?); to arrive to the product verification (does the system meet the requirements?) and validation (is it the right system?); so as to obtain the flight certification (is the system ready to fly?) [Gill, 2015][Larson et al., 2009, pp.385-478].

For what concerns the validation of the requirements, it was already underlined how it is important to be sure of having translating right the customers' expectations. Hence, the requirements have to be VALID, which stands for Verifiable (verification must be objective and quantitative), Achievable (realistic), Logical (they need to present a logic derivation from the higher level to the lower), Integral (complete) and Definitive (each requirement addresses

only one aspect of the system design or performance) [Larson et al., 2009, p.392]. The requirements presented in Tables 3.2, 3.3 and 5.2 were indeed derived by considering these aspects. In fact, they all are VALID, as underlined by their rationales.

The models are instead employed in order to accomplish requirements analysis, system synthesis, design and development, verification and to simulate operations of the system. Among the several models, there can be distinguished the physical, graphical, mathematical and statistical models that are employed at different phases of the project [Larson et al., 2009, p.398]. So far, even in this work, different models were used to carry on the analysis of the system, such as the CAD model itself, the FFBDs and the representative drawings, for example. However, at this point, new models have to be elaborated to perform the product V&V.

Hence, a product V&V plan has to consider different aspects, such as: validate the performance and its functionality, establish V&V requirements, assess the system according to its mission scenario and the interaction among hardware, software, people and procedures [Gill, 2015]. The conventional V&V methods are the following [Firesmith, 2013][Larson et al., 2009, p.415][NASA, 2007, p.86]:

- Analysis, by using technical and/or mathematical models or simulations, scientific principles and procedures, which can be used when the accurate analysis is impossible, the testing is not cost-effective and inspection is not adequate.
- Demonstration, by the visual examination of the execution of a work product, it helps in visualising the correct working of the system.
- Inspection, by the visual examination of a non-executing work product, which is appropriate in the case of drawings, documents or data. Usually, it allows to verify physical design features or manufacturing identification.
- Testing, by the stimulation of an executable work product with known inputs and pre-conditions followed by the comparison of its actual with the required response. It is often the preferred method in V&V.

The verification methods for this project were already indicated in the requirements Tables before, in order to explain how each of them can be validated and verified. Table 9.1 summarises all the requirements with the respective V&V methods and the rationales for which that method was selected.

The Table shows that a new model has to be built in order to perform the verification on these aspects. Generally, for optical systems, a first model used for testing the performance and the compliance with the requirements is an optical breadboard. Then to this breadboard, structural, optical and thermal models can be applied, so as to verify the compliance with the customers' expectations. The testing have to be agreed within the research group working on the IceMole probe and the scientists in order to decide which are the best ways to evaluate the performance of the Raman spectrometer and its compliance with the requirements. For sure, a first demonstrator has to be built on which the optical components can be mounted to verify the optical properties, that the excitation laser wavelength is transmitted correctly and that the scattered light arrives at the spectrometer and can be analysed. These testing are to be performed in an optical laboratory. Other necessary testing concern the environmental conditions that the Raman spectrometer has to stand. These

TABLE 9.1: V&V of requirements
(A) V&V of top-level missions requirements (Table 3.2)

Req.ID	Topic	VM	Rationale
SYS-01	In situ measurements	D	The capability of the system to actually perform measurements in situ can only be verified by a demonstration: by the use of a prototype, the instrument can ensure its proper working directly in situ
SYS-02	Biosignatures identification	A,T	The capability of detecting biosignatures can be proved by analysis of the characteristics of the spectrometer, along with some optical testing performed on a model (probably a breadboard), that can verify the system to detect, at least, known biosignatures
SYS-03	Miniaturisation	A,I	The miniaturisation aspect is verified already by the CAD model, but during actual assembly can be verified by inspection
SYS-04	Terrestrial application of IceMole	T	To simulate the working of the system in the terrestrial application sites of the IceMole probe, environmental, thermal and pressure testing are necessary
SYS-05	Autonomy	D	With a demonstrator, the system can be verified to work without the need of human interface
SYS-06	Contamination	T	The contamination level can be examined by testing

(B) V&V of technical requirements (Table 3.3)

Req.ID	Topic	VM	Rationale
SYS-03-IM-01	Dimensions	A	The dimensions of the final model are evaluated by the CAD model, by means of analysis
SYS-03-IM-02	Mass	A	The mass of the final model is evaluated by the CAD model, by means of analysis
SYS-03-IM-03	Power bus	A	The power bus can be derived from the the electronics that has to be designed and the specifications of the components
SYS-03-IM-04	Power consumption	A	The power consumption as well can be derived from the electronics that has to be designed and the specifications of the components
SYS-04-IM-01	Pressure	T	Pressure standing is determined by environmental testing
SYS-04-IM-02	Temperature	T	Temperature standing is determined by environmental testing
SYS-05-IM-01	Communication protocol	A,D	Communication is verified by analysis of how the electronics to be designed transmit data and by the demonstration of how the signals are transmitted
SYS-06-IM-01	Sterilisation protocol	T	The sterilisation level can be examined by testing

(C) V&V of payload requirements (Table 5.2)

Req.ID	Topic	VM	Rationale
SYS-01- RS-01	Independent measure- ments	D,T	The verification that the system is able to perform the measurements without being conditioned by the previous ones can be achieved with testing and a demonstrator that has to show that each measurement is not contaminated by the preceding
SYS-01- RS-02	Integration time	A,T	The integration time is determined by the characteristics of the components and the successive testing to achieve the performance
SYS-01- RS-03	Calibration	T	Calibration is achieved during testing, better explanation can be found in next Section
SYS-02- RS-01	Stokes range	A,T	The Stokes range that the system is able to detect can be obtained by the analysis of the specification of the components and by the optical tests
SYS-02- RS-02	Spectral res- olution	A,T	The spectral resolution that the system is able to detect can be obtained by the analysis of the specifications of the components and by the optical tests
SYS-02- RS-03	Laser wave- length	A,T	The excitation laser wavelength that the system is able to detect can be obtained by the analysis of the specifications of the components and by the optical tests

include temperature changes, pressure changes, mechanical stresses, conditions of humidity and they are to be performed sequentially, one after the other, in order to verify that the performance of the spectrometer is maintained the same along all conditions. Those tests require controlled pressure and temperature testing chambers in which all the environments can be simulated. Then, of course, the testing should also include the probe and the testing has to be done on the assembly of the Raman spectrometer and IceMole. With the integration, the tests to be performed are the same as for the single instrument, but at this point the outcome should include the behaviour of the system within the assembly and at the end of these testing it has to be possible to have a working Raman spectrometer that could be used in the terrestrial deep ice applications of IceMole.

9.2. VERIFICATION OF THE PROPOSED DESIGN

The final design of the spectrometer presented in Chapter 8 was derived by following the requirements and by considering the compliance with them. Therefore, it can be said that the Raman spectrometer presents a size of 65 mm × 65 mm × 150 mm and an overall mass of ~ 1.125 kg; it excites the sample with a laser wavelength of 532 nm and it is able to measure the spectral range 546.9 – 700 nm with an accuracy of at least 0.4 nm, combination of the characteristics of the optical components (beamsplitter, filter, collimator, optical fibre and spectrometer). Those performances are supposed by analysing the characteristics of the components, but only testing can ensure them.

However, as was underlined, not all the requirements derived in the first part of this work were addressed during the project: above all, the data transmission and the power supply of the instrument were not considered during the proposal of the design of the Raman spectrometer, therefore those have to be part of a successive design phase in which these integration aspects are elaborated. Instead, with the final modelling of the system, the aspects that can be verified are the technical requirements concerning dimensions, mass and temperature and pressure standing, and the optical performances of the payload requirements.

In order to summarise the state of verification of the proposed design, a Verification Compliance Matrix (VCM) is elaborated in Table 9.2. In this matrix, each requirement is associated to the state of compliance: **C** if compliant, **C*** if compliant but need further investigations, **NC** if non-compliant and - if not applicable at this project level. As can be observed, the VCM reflects the VM explained in Table 9.1. In fact, the requirements whose compliance level is not applicable at this point of the project are those that require further testing or demonstration. Also for the payload requirements, even if the components were chosen to comply with them, further investigation is necessary to ensure the optical performances of the system.

TABLE 9.2: Verification Compliance Matrix (VCM)

C stands for compliant, **C*** for compliant but need further investigations, **NC** for non-compliant and - for not applicable at this project level

Req. ID	Topic	Level of Compliance
SYS-01	In situ measurements	-
SYS-02	Biosignatures identification	-
SYS-03	Miniaturisation	C
SYS-04	Terrestrial application of IceMole	-
SYS-05	Autonomy	-
SYS-06	Contamination	-
SYS-03- IM-01	Dimensions	C
SYS-03- IM-02	Mass	C
SYS-03- IM-03	Power bus	-
SYS-03- IM-04	Power consumption	-
SYS-04- IM-01	Pressure	-
SYS-04- IM-02	Temperature	-
SYS-05- IM-01	Communication protocol	-
SYS-06- IM-01	Sterilisation protocol	-
SYS-01- RS-01	Independent measurements	-
SYS-01- RS-02	Integration time	C*
SYS-01- RS-03	Calibration	-
SYS-02- RS-01	Stokes range	C*
SYS-02- RS-02	Spectral resolution	NC
SYS-02- RS-03	Laser wavelength	C

9.3. CALIBRATION & DATA REDUCTION

One of the payload requirements that was not addressed in the previous discussion is the following:

SYS-01-RS-03 *The system shall be calibrated before and after each measurement.*

Calibration is the process of comparing measured values with those of a standard of known accuracy. Therefore, calibration is that process that allows to eliminate, or at least minimise, those factors that can bring to inaccurate measurements [Advanced Instruments, 2017]. The formal definition of calibration is given by the Bureau International des Poids et Mésures - International Bureau of Weights and Measures (BIPM) in the international vocabulary of metrology which states that *it is the operation that, under specified conditions, in a first step, establishes a relation between quantity values with measurement uncertainties, and, in a second step, uses this information to establish a relation for obtaining a measurement result from an indication*¹.

Calibration is therefore an essential process which is required in several cases: for a new instrument, for a repaired or modified instrument, when during the measurements a critical event occurs (such as shocks, vibrations or physical conditions that have not been expected), or when the customers' expectations change [Wikipedia, 2017b]. The calibration is a process that has to be performed several times during the lifetime of the instrument because of the effects of time: the optical lenses degrade and misalignment can occur because the system can be subjected to mechanical and thermal stresses. This implies that the output of the measurements can change over time, which is the reason why calibration is fundamental. Furthermore, it is also a measure of the instrument accuracy, by analysing the error between the calibrated spectrum and the obtained one, so that the system can be classified.

A general procedure to calibrate an instrument does not exist, because it depends on the system itself and on its characteristics and requirements. However, it can be stated that typically, calibration involves the instrument to be used to detect test samples that are called *calibrators*. In this way, the instrument can register the data for each calibrator so as to correlate some specific points within the instrument spectral range, in order to teach the instrument to provide accurate results. Ideally, the more the calibrators used for the process, the higher the level of the performance; but the effort in register all the test samples would be huge, therefore a trade-off between the level of performance and this effort in testing has to be considered [Advanced Instruments, 2017; Wikipedia, 2017b].

For dispersive spectrometers, such the one under discussion, the calibration usually concerns the Raman shift scale by recording a well-known spectrum with narrow spectral bands. This is the most used direct calibration process, but it presents great drawbacks when it is important to quantify the detected substances. It is a method that involves different stages: first, the wavelength range of the spectrum is represented, then the approximate positions of prominent reference lines (like water in the case) are determined, so as to be able to compute the exact pixels positions and wavelengths of the entire set of reference lines; eventually, the entire abscissa of the spectrum is mapped. Another calibration method is by us-

¹International vocabulary of metrology — Basic and general concepts and associated terms (VIM), 2008, accessible at http://www.bipm.org/utils/common/documents/jcgm/JCGM_200_2008.pdf.

ing atomic emission spectra, which derive by the emission of an ordinary calibration lamp, whose lines are narrow, well-defined, intense and distributed over a large range in the visible spectrum [Gauglitz and Vo-Dinh, 2006; Mann and Vickers, 2001][McCreery, 2000, pp.251-292][Perret and Balber, 2011].

For an application such the one of this project, the calibration of the Raman spectrometer can be performed by registering the emission lines of a sample whose spectra is well-known and can be expected to be measured in the icy environments. Therefore, the most promising calibrators in this sense are ice, the material of the probe walls and some biosignatures that can be expected to be registered, the ones that lie in the spectral range of the payload requirements. In such a way, the systematic errors that can occur during the operations can be eliminated and the results can be more accurate, because the non-linear effects are reduced. For the reasons explained before, this process has to be repeated every time the probe is out of the ice, before each ice testing campaign, in order to assure the instrument to provide successful and trustworthy results.

If, during testing, it is observed that this type of calibration is not sufficient, another method of calibration can be proposed: the auto-calibration. This method relies on recording the data measured by the instrument and register the most prominent features. If needed, this process could be used during the operations of IceMole but it would require a large available amount of data to be recorded and enough processor capability to perform the calibration.

10

TECHNOLOGY ROADMAP TO SPACE MISSIONS

As underlined several times during this project, the proposed design deals with the terrestrial deep ice applications of the IceMole probe. In fact, the [EnEx](#) mission has not defined an aim and a schedule for space exploration missions yet, although the name of the initiative itself gives faith that this will be its future, even because of the studies conducted at [ISTA](#) in Munich (see Chapter 2 for better explanation). The applications on Earth are mainly due to the fact that the cost of the initiative can be maintained low and because that technologies to create space environments for testing are very challenging to achieve. The aim of this Chapter is to consider the whole discussion that brought to the definitive design of the Raman spectrometer and understand if and how much valid it is in the case the [EnEx](#) initiative will be moved towards a space objective.

In the context of the IceMole probe, a life detection instrument is now required because ice has been identified as a promising preserving means of ancient living forms. In fact, Price [2007] underlined how the characteristics of ice may have preserved some habitats for life. First, the ionic compounds are insoluble in the structure of ice and they can therefore be used by micro-organisms for their metabolism. Second, ice in contact with minerals creates a thin film of unfrozen water that the micro-organisms can use to extract energy from redox reactions. This theory is also supported by the theory of the Snowball Earth, which states that because of the reduced luminosity of the young Sun, the terrestrial planet may have been covered with ice during its early history, when life arose [Bada et al., 1994].

This discovery relates to where liquid water, one of the the primary elements related to life, was found, or is supposed to be, in space. Those are the reasons why astrobiology, i.e. the study of the origin, evolution ad distribution of life in the Solar system and beyond [Domagal-Goldman et al., 2016; Horneck et al., 2016] has turned its attention towards the icy moons Europa and Enceladus and the polar caps of Mars. In fact, the polar caps of Mars have always been known to be formed by water ice and the so-called dry ice, since observations with ordinary telescopes. In the same way, the spectrum of Europa has always pointed out the presence of a water ice crust. For the smaller moon Enceladus, it was the spacecraft *Cassini* to demonstrate the presence of a cryovolcanic active province at the South pole from which traces of ice elements were detected [Dachwald et al., 2013; Domagal-Goldman et al., 2016; Greenberg, 2009; Horneck et al., 2016; Procket and Pappalardo, 2007].

Section 10.1 hence presents these planetary bodies with their characteristics and explains why they are so interesting. Sections 10.2 and 10.3 evaluate respectively the derived requirements and the proposed design with respect to the space icy environments, in order to analyse what is still valid for space missions and what instead would have to be changed. Moreover, it is discussed at which point of the technology roadmap the proposed design is, what can be adapted to space and what needs further investigation.

10.1. ICY MOONS AND MARS' POLAR CAPS

For what concerns the Solar system, the most promising planetary bodies that have been identified for the chance of having preserved living micro-organisms are Mars and the so-called icy moons Europa and Enceladus. All three celestial bodies are presented in Figure 10.1 and their characteristics are summarised in the following.

Thanks to the technology of ordinary telescopes, Mars has always been known to possess two permanent ice polar caps similar to the terrestrial ones, since the observations of the astronomer Cassini in 1666. It was then thanks to the exploration missions towards the red planet and the landers employed on its soil that it was observed that those two caps are made primarily of water ice but they can also be covered by *dry* frozen carbon dioxide. These caps are subjected to seasonal changes, similar to the terrestrial ones, because of a similar obliquity to the orbit: according to if the pole finds itself in the darkness or not, the CO₂ respectively freezes or sublimates [Mellon et al., 2004]. However, so far no evidence of liquid water has been found on the surface, although some features allow to speculate an old existence of surface liquid water in the geological history of the planet [Dachwald et al., 2013].

Jupiter's sixth-closest-moon Europa was the topic of the extensive literature study that can be found in Russano [2016]. It is nowadays the most interesting celestial object in the Solar system, because thanks to the amazing achievements of the *Galileo* mission, it was proven to be the most promising environment in space to harbour life. In fact, the moon has demonstrated to possess all the elements that allow life to arise: liquid water, organic compounds and energy. Liquid water can be found in a form of a subglacial ocean at a ~ 150 km depth under the icy crust, which can shield potential living forms from the strong Jupiter

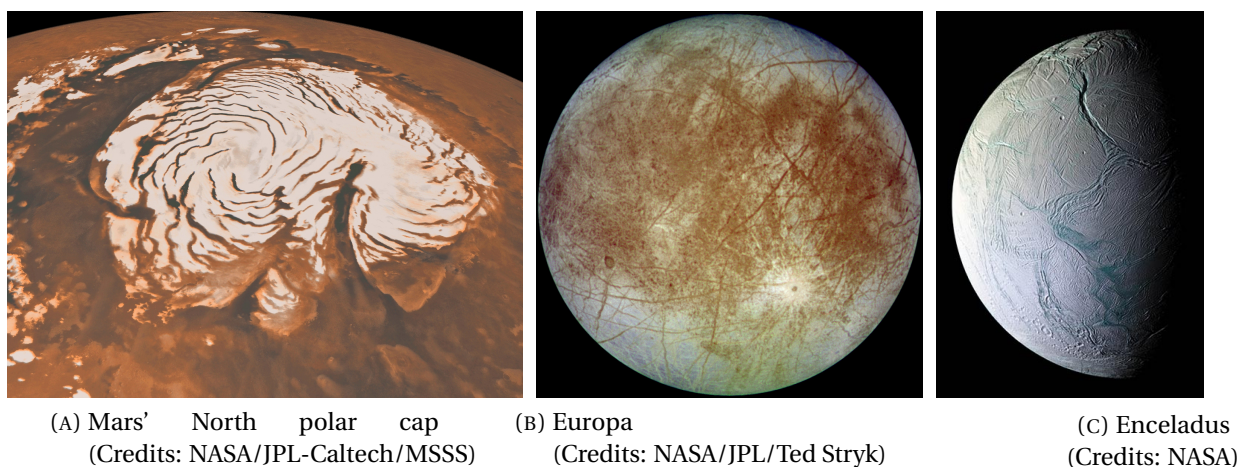


FIGURE 10.1: Icy environments in space

TABLE 10.1: Orbital and physical characteristics of icy environments in space [Lissauer and De Pater, 2013; Procket and Pappalardo, 2007]

	Europa	Enceladus	Mars
Mean Radius	1560.8 ± 0.5 km	252.1 ± 0.2 km	3389.9 km
Mean Orbital Radius ¹	671100 km	238037 km	1.524 AU ²
Mass	4.8017 × 10 ²² kg	1.0794 × 10 ²⁰ kg	0.64185 × 10 ²⁴ kg
Orbital Period	85 h (3.551 Earth days)	32.88 h (1.370 Earth days)	1.88 years
Inclination/Obliquity to orbit	0.47° ³	0.019° ⁴	25.19°
Geometrical Albedo	0.67 ± 0.03	1.375 ± 0.008	0.150
Surface Temperature	53 – 113 K	32.9 – 145 K 90 – 155 K ⁵	~ 150 K ⁶
Surface Pressure	10 ⁻¹² bar	n.a. ⁷	0.00636 bar
Surface Gravity	1.314 m/s ²	0.113 m/s ²	3.758 m/s ² ⁶

¹ Respectively from Jupiter, Saturn and Sun

² Where 1 AU = 1.496 · 10⁸ km [Lissauer and De Pater, 2013]

³ To Jupiter's equator

⁴ To Saturn's equator

⁵ At the tiger stripes

⁶ At polar caps

⁷ Probably ~ 10⁻⁷ – 10⁻⁴ bar

radiation. Organic and energy-rich compounds can be observed by the particular colour of the surface features. The energy is sustained by the tides created by the resonance with Ganymede and Callisto and due to the eccentricity of its orbit, phenomena that make Europa an active celestial body [Dachwald et al., 2013; Greenberg, 2009; Procket and Pappalardo, 2007].

On the other hand, the Saturn's moon Enceladus is quite smaller than Europa, but presents a similar composition. It is the primary future target of EnEx initiative, because, although Europa is probably the most interesting target, Enceladus could allow easier access to its subsurface source of material. It was deeply presented in the literature study in Russano [2017]. As already said, the South polar region of this moon presents a particular feature. It is characterised by the presence of an active region of cryovolcanism, i.e. a representation of low temperature volcanic activity, where organic compounds escape from four fractures in the ice, known as *tiger stripes*. The composition of these plumes was detected by the spacecraft *Cassini*, whose measurements allow to speculate on the presence of a sub-ocean below the moon icy crust. Moreover, this region presents no impact craters and the release of internal heat was observed, by highlighting the possibility of geological activities sustained by tidal forces created by orbital resonance with the moon Dione [Dachwald et al., 2013; Ingersoll and Pankine, 2010; Konstantinidis et al., 2015a; Porco et al., 2006].

10.2. EVALUATION OF THE REQUIREMENTS

Considering the three different scenarios that could be faced if the EnEx mission is moved towards these icy environments in space, in Table 10.1 the physical and orbital characteristics of the three celestial bodies identified as the most promising are summarised. By referring to this Table, it is possible to underline how the two icy moons and the red planet represent very harsh environments, which present very low temperature and pressure conditions,

making difficult the operations of the engineered landers, probes and instruments. Furthermore, even the surface gravity conditions for all the three scenarios are very low with respect to terrestrial gravity, which implies a more challenging environment to perform the ice penetration with the IceMole probe.

Therefore, there are three different scenarios, one for Europa, one for Enceladus and one for the polar caps of Mars, that have to be analysed in order to decide what needs to be changed if the designed Raman spectrometer has to be adapted to those conditions. First of all, the analysis concerns the evaluation of the requirements that were derived considering the terrestrial applications. Now that space harsh icy environments are taken into account, some of them have to change.

Talking about the top-level missions requirements of Table 3.2, most of them are still valid: the aim of the project is still to be able to perform measurements in situ, now more than ever, because there is no chance to bring the samples back to Earth; the instrument has to be able to detect biosignatures; and it still has to comply with the design of the IceMole probe. Of course, one of the requirements that has to be changed is the following:

SYS-04 *The system shall work in the terrestrial applications of IceMole*

Obviously, this requirement cannot be valid for space applications by definition. This sentence will have to be removed from the list of the requirements or will be changed in such a way to define which one of the three scenarios is considered. In fact, from this requirement, the majority of the technical requirements derives, which therefore will be changed accordingly. The requirement on autonomy

SYS-05 *The system shall operate autonomously*

will gain even more importance in space. In fact, the autonomy of operations is an essential condition when speaking about space missions. Either for Mars, that is the closest planet to Earth, either for Europa and Enceladus which are in the outer Solar system, it is fundamental to be aware that the communication link with the ground control centre on Earth is limited by several aspects, which determine the communication window and the delay in transmission. Hence, it is impossible to think that commands or data can be transmitted simultaneously. The contamination requirement

SYS-06 *The system shall comply with NRC Antarctica CoC recommendation 7*

it will be very important for planetary exploration. Obviously, the recommendation will not be the same, but it will concern the celestial bodies under discussion. For example, for Europa a planetary protection recommendation has been set by the NRC, in order to preserve its potential in harbouring life, which states that the maximum acceptable level of risk of contaminating the moon should be at maximum 0.1% [Greenberg, 2009, pp.323-354].

On the other hand, the technical requirements of Table 3.3 are the ones most affected by the change of the conditions of the scenarios. As already stated, the majority of the requirements derives from the compliance with the design of the IceMole probe and with the operational environments of the probe. Assuming that the design of IceMole will be maintained

the same as the one of the latest generation of the probe, the requirements that have to be discussed are the ones that derive from SYS-04, that was already discussed to be changed above. Therefore,

SYS-04-IM-01 *The system shall operate under atmospheric pressure*

is the requirement that mainly has to be carefully changed. Table 10.1 shows how the surface pressure conditions of Europa, Enceladus and Mars are extremely different with respect to the terrestrial ones. Going from the highest pressure to the lowest, the almost total absence of atmosphere of the planet makes the pressure of Mars already of a value $\sim 10^2 - 10^3$ times less than the one of Earth, while for Enceladus and Europa the situation is even worse, with values in the order of $10^{-12} - 10^{-7}$ bar. Therefore, the instrument will have to be validate for vacuum conditions, because even if it is inside of the probe, where some pressure will always be present, the conditions would not be as the terrestrial ones and considering a safety margin, it would be better to have the system designed for vacuum.

SYS-04-IM-02 *The system shall work in a temperature range between -15 and 15°C*

As well as the pressure conditions, the temperature conditions for the celestial bodies are very different from the terrestrial ones. In fact, the temperature at polar caps of Mars is $\sim 123.15^\circ\text{C}$, at the South polar region of Enceladus -183.15 to -118.15°C and at Europa -220.15 to -160°C , which represent extremely harsh environments. Even in this case, it can be considered that the Raman spectrometer is placed inside the probe, which can shield in part the system. However, the above requirement has to be changed in order to assure the working of the system, by lowering the lower threshold: probably a good requirement would be to ensure the correct functioning of the system until at least -50°C . About the environment standing requirements, for what concerns the space mission, it would be furthermore important to consider other conditions that do not concern on Earth, such as the magnetism of the celestial bodies and the radiation that can affect the instrument. This discussion is above all important when considering a mission towards Europa, which has a self-sustained magnetic field [Khurana et al., 1998] and receives a huge amount of radiation coming from Jupiter. The last technical requirement that still has to be discussed and changed is of course:

SYS-04-IM-03 *The system shall not be space-qualified yet*

It is evidently not possible to have such a requirement. The system will have to undergo all the procedures that will certify its space-qualification.

Last set of requirements are the payload requirements of Table 5.2. In this case, the performance of the payload is assumed to be maintained even in the space applications. It was indeed dictated by the scientific team and in the case of the change of the objective, it will be their job to communicate how the performance will have to be changed. Only one requirement among the derived ones needs to be discussed in the case of space missions. It is the following, concerning calibration:

SYS-01-RS-03 *The system shall be calibrated before and after each measurement*

As can be imagined, the calibration would not be possible in situ, therefore the instrument will have to be carefully calibrated on Earth before launch, but because of this complication,

it will probably rely on auto-calibration, as discussed in Section 9.3.

10.3. EVALUATION OF THE PROPOSED DESIGN

With the change of the requirements, it is evident that the design of the instrument will have to be changed as well, because the process followed during this work was indeed derived from the customers' needs and expectations and the requirements. In fact, the proposed design aims at complying with these and in case of modification, it is very likely that some of the design choices described in Chapters 6, 7 and 8 have to re-discussed and/or changed.

The first point to analyse is if the components that were selected for the design of the Raman spectrometer are space-qualified as well. Space-qualification is determined by a series of procedures and testing that would have to be performed on the components by the developing company or during integration and assembly. At this point, the space-qualification was not a requirement, therefore it is possible that some of the selected components cannot be used in space missions, but this is something to be determined. In the case some of them will be in this situation, the alternatives could be: one, it can be possible to look for new components that are already space-qualified; two, it can be considered to do space-qualification during the integration; or three, COTS can be dismissed and the components can be designed, modelled and space-qualified directly by the research group.

Traditionally, all the selected optical components can be used in space: the filter, the beamsplitter, the collimator and the optical fibre are components that have been already used in space for instruments such the one under discussion. For the modelled components, invar was selected as their material, so as to stand harsh conditions. It is an already space-qualified material that has been used in past missions. Sapphire can be used in space as well. However, it is important to consider the temperature and pressure conditions, that may imply some further changes in the design, because of stronger temperature gradients and stronger pressure gradients, that can create higher thermal stresses. Therefore, the design of the mounting supports could need some adaptations to the new requirements, but this could be evaluated only during testing. Therefore, the only components to be discussed are the spectrometer and the laser. Both the categories of the components are plenty of heritage of space applications, so, in case the respectively Ibsen and Cobolt components do not meet the space-qualification criteria, other solutions can be found on the market. For what concerns the spectrometer, it was already underlined that some precautions need to be taken for the terrestrial applications, therefore also for the space missions, similar analyses must be done, increasing the standing temperature range until the value of -50°C . The same can be said for the laser.

Considering these points, the proposed design cannot be used in space as it is, but it still needs to be improved. Future steps in the roadmap to space will be for sure the environmental testing and the measurement of the contamination risk. For what concerns the harsh condition standing, it will be particularly challenging to understand how the so-low pressure will be stand and how the environments will affect the optical performances of the instrument. The points listed are the critical steps to be investigated for the future of this project for the characterisation of the design for Mars, Europa and Enceladus missions.

PART IV:

**FINAL CONCLUSIONS AND
FUTURE STEPS**

11

CONCLUSIONS & NEXT STEPS

EnEx is a collaborative project among six German universities, funded by **DLR**. Its aim focuses on deep ice applications on Earth of a subsurface steerable probe with autonomous navigation. The navigation solution is integrated into the IceMole probe, developed at FH Aachen University of Applied Sciences since 2008. It is a manoeuvrable subsurface system for clean in situ analysis and sampling which combines melting with a hollow rotating ice screw. The most recent generation of the probe is a miniaturised version of the previous generation, with a cross sectional area of 80 mm × 80 mm, a length of 450 mm and a power consumption of ~ 5 kW.

The exploration of deep ice has become very important for biology, because ice has demonstrated to present the right characteristics to preserve living forms. Therefore, it is now important to develop a payload for the IceMole probe that is able to identifying potential living micro-organisms, by detecting their biosignatures. This **MSc** thesis focused indeed on designing a Raman spectrometer in order to achieve this goal.

This Chapters aims at summarising the results achieved during the project for the design of the instrument, by underlining the process followed. Furthermore, it gives some recommendations that need to be taken into account for the future development and applications of the Raman spectrometer.

11.1. CONCLUSIONS

The design process of the instrument followed a systems engineering approach by setting as first step the derivation of the requirements from the customers' needs and expectations. The key drivers were related to the miniaturised design of the system and the harsh conditions in which the Raman spectrometer will have to work, which mainly represent the technical system requirements. The payload requirements were particularly important for the development of this thesis as well, because they define the characteristics that the Raman spectrometer has to meet. They were derived with the help of a team of **DLR** experts of the Institute of Planetary Sciences and the Institute of Optical Sensor Systems, who expressed their needs in order to obtain valuable results during measurements.

The analyses of the Raman spectrometer will be performed during IceMole terrestrial deep ice applications and the instrument will observe the sample through a window in the

walls of the probe. This operational scenario obviates the problems related to design and sterilise a pumped system for collection and removal of the sample.

The proposed design arranges the system in a 180° configuration, which means that laser light and scattered light are respectively delivered and collected on the same axis. The design employs as many COTS as possible, in order to maintaining the cost low and to decrease the schedule time. The final model presents some main components that were selected through extensive reasoning. The sapphire window allows to stand critical pressure and it is very hard, by maintaining at the same time a high transmittance in the visible range. The laser excites the sample with a wavelength of 532 nm, which is the best compromise in terms of performance in detecting biosignatures, availability and cost of the components and danger of the laser itself. Then, the dichroic beamsplitter at 45° allows to reflect the laser light towards the sample and to transmit its scattered light. The long-pass edge filter transmits only the interesting Stokes range by rejecting the laser-line. The 30° off-axis parabolic mirror reflects the scattered light and focuses it in a precise point where the collimator collects the light. The light is then transmitted via the optical fibre to a COTS CCD spectrometer.

In conclusion, the final outcome of this thesis was a CAD model elaborated in the software CATIA™ of a miniaturised Raman spectrometer that could be used in the deep ice applications of the IceMole probe in the context of EnEx initiative. The instrument relies on the use of COTS, that were selected through extensive trade-offs. As the project followed a system engineering approach, the design complies with some of the technical and scientific constraints, without the need of further testing. The CAD model allowed to identify the best configuration for the components inside the instrument: the ultimate size of the Raman spectrometer is 65 mm × 65 mm × 150 mm and the overall mass is ~ 1.125 kg. The instrument excites the sample with a laser wavelength of 532 nm and it is able to measure the spectral range 546.9 – 700 nm with an accuracy of at least 0.4 nm, combination of the characteristics of the optical components (beamsplitter, filter, collimator, optical fibre and spectrometer).

This result allows to positively answer to the main research question of the project which aimed at investigating the possibility of designing a Raman spectrometer that could comply with the constraints dictated by IceMole. The proposed design was successful in answering this: the instrument complies with the strict requirements on size, mass and environmental conditions and it ensures the required payload performances. In fact, although this project dealt with the main topic of miniaturisation, it was possible to satisfy the requirements by the only means of COTS, without losing any performance (except for the spectral resolution, which is anyway very close to the required one).

11.2. RECOMMENDATIONS AND NEXT STEPS

The design of the Raman spectrometer was elaborated with the aim of being integrated into the new generation of the IceMole probe. The outcome of this MSc thesis demonstrates that this can be successfully achieved. To this end, some future steps are presented hereafter.

In order to be able to check the compliance of the system with all the derived requirements, the proposed design will be fully verified and validated, by following the preliminary proposed V&V plan. In fact, V&V is fundamental in systems engineering in order to have a result that works properly, that complies with the requirements and that allows to satisfy the customers' needs and expectations. The proposed V&V plan identified an optical bread-

board as a promising model to evaluate the optical performances. Its development will be the first step in the future of the project.

The other main step for the system will be the integration into the IceMole probe. To this end, a new generation of IceMole will be designed, so that it could host the payload. The length of the probe will be increased and the window in the walls will be modelled, in order to guarantee to the spectrometer to perform its measurements. Further investigations on the integration into IceMole will concern the electronics and the power supply. On one hand, for the electronics, the management of the data acquired from the measurements will be mainly influenced by the characteristics of IceMole on-board processor. According to those, the spectra will be transmitted directly to surface or if necessary they will be elaborated with a second processor and only the final result, which means a signal that says if there are biosignatures or not, will be transmitted. On the other hand, how the required power will be supplied to the instrument will have to be investigated by the design team of the probe, in order to complete the integration of the system.

In the long-term future, the proposed Raman spectrometer will be then improved for a subsurface probe for space exploration and life detection missions. These missions will have as targets those celestial bodies that are promising for harbouring potential living micro-organisms: the polar caps of Mars, Jupiter's moon Europa, and Saturn's moon Enceladus. By moving the aim of the [EnEx](#) initiative towards space, the future steps will concern making the instrument suitable for it. Because of the harsh conditions of space targets, the requirements will be validated for them or changed accordingly, as well as the design choices will be re-discussed in order to achieve the best performance.

REFERENCES

- AcqNotes. System Requirements Review (SRR). <http://www.acqnotes.com/acqnote/acquisitions/system-requirements-review-srr>, 2017. Visited on April 1st, 2017.
- Adar, F. Evolution and Revolution of Raman Instrumentation - Application of Available Technologies to Spectroscopy and Microscopy. In *Handbook of Raman Spectroscopy: from the research laboratory to the process line*. CRC Press, 2001.
- Adar, F. Considerations of Grating Selection in Optimizing a Raman Spectrograph. *Spectroscopy*, 28(10), 2013.
- Advanced Instruments. What is calibration? <https://www.aicompanies.com/education/calibration/what-is-calibration/>, 2017. Visited on June 10th, 2017.
- Anglia Instrumentation Ltd. Fiber optics. <http://www.angliainst.co.uk/fibre-optics.asp>, 2017. Visited on April 30th, 2017.
- AzO Optics. Optical Transmittance. <http://www.azooptics.com/Article.aspx?ArticleID=823>, 2014. Visited on April 30th, 2017.
- Bada, J. L., Bigham, C., and Miller, S. L. Impact melting of frozen oceans on the early Earth: implications for the origin of life. *Proceedings of the National Academy of Sciences*, 91(4): 1248–1250, 1994.
- Bisson, P. J. and Whitten, J. E. A compact Raman converter for UV-VIS spectrometers. *Review of Scientific Instruments*, 86(5):055107, 2015.
- Blacksberg, J., Alerstam, E., Maruyama, Y., Cochrane, C. J., and Rossman, G. R. Miniaturized time-resolved Raman spectrometer for planetary science based on a fast single photon avalanche diode detector array. *Applied optics*, 55(4):739–748, 2016.
- Brewer, P. G., Malby, G., Pasteris, J. D., White, S. N., Peltzer, E. T., Wopenka, B., Freeman, J., and Brown, M. O. Development of a laser Raman spectrometer for deep-ocean science. *Deep Sea Research Part I: Oceanographic Research Papers*, 51(5):739–753, 2004.
- BWTek. Spectrometer Knowledge. <http://bwtek.com/spectrometer-part-5-spectral-resolution/>, 2017. Visited on April 1st, 2017.
- Chimenti, R. V. and Thomas, R. J. SPECTROMETERS: Miniature spectrometer designs open new applications potential. <http://www.laserfocusworld.com/articles/print/volume-49/issue-05/features/spectrometers--miniature-spectrometer-designs-open-new-applicati.html>, 2013. Visited on April 30th, 2017.
- Cobolt. Cobolt 08-01 Series. http://www.coboltlasers.com/wp-content/uploads/2016/07/D0141-C_ManualCobolt08-01Series_June_2016.compressed.pdf, 2016. Visited on May 10th, 2017.

- Courreges-Lacoste, G. B., Ahlers, B., and Pérez, F. R. Combined Raman spectrometer/Laser-Induced Breakdown Spectrometer for the next ESA mission to Mars. *Spectrochimica Acta Part A: Molecular and Biomolecular Spectroscopy*, 68(4):1023–1028, 2007.
- Crocombe, R. A. Handheld spectrometers: the state of the art. In *SPIE Defense, Security, and Sensing*, pages 87260R–87260R. International Society for Optics and Photonics, 2013.
- Crystalaser. Diode Pumped Green 532nm. <http://www.crystalaser.com/CL532.pdf>, 2017. Visited on May 10th, 2017.
- Dachwald, B., Ulamec, S., and Biele, J. Clean in situ subsurface exploration of icy environments in the Solar system. In *Habitability of Other Planets and Satellites*, pages 367–397. Springer, 2013.
- Dachwald, B., Mikucki, J., Tulaczyk, S., Digel, I., Espe, C., Feldmann, M., Francke, G., Kowalski, J., and Xu, C. IceMole: A maneuverable probe for clean in situ analysis and sampling of subsurface ice and subglacial aquatic ecosystems. *Annals of Glaciology*, 55(65):14–22, 2014.
- Das, R. S. and Agrawal, Y. Raman spectroscopy: recent advancements, techniques and applications. *Vibrational Spectroscopy*, 57(2):163–176, 2011.
- DLR. Searching for life in the depths of Enceladus. http://www.dlr.de/dlr/en/desktopdefault.aspx/tabid-10081/151_read-2751/year-all/#/gallery/4874, 2012. Visited on March 27th, 2017.
- Domagal-Goldman, S. D., Wright, K. E., Adamala, K., Arina de la Rubia, L., Bond, J., Dartnell, L. R., Goldman, A. D., Lynch, K., Naud, M.-E., Paulino-Lima, I. G., et al. The Astrobiology Primer v2.0. *Astrobiology*, 16(8):561–653, 2016.
- Dowling, P. From glass to optical fiber. <http://www.cablinginstall.com/articles/print/volume-5/issue-10/contents/design/from-glass-to-optical-fiber.html>, 1997. Visited on April 30th, 2017.
- Edmund Optics. Optical Coatings. <https://www.edmundoptics.eu/resources/application-notes/optics/an-introduction-to-optical-coatings/>, 2013. Visited on April 30th, 2017.
- Edmund Optics. Dichroic Laser Beam Combiners. <https://www.edmundoptics.com/optics/optical-filters/longpass-edge-filters/dichroic-laser-beam-combiners-8f67c2b5/>, 2017a. Visited on May 9th, 2017.
- Edmund Optics. Fiber Optic Collimator and Focuser Assemblies. <https://www.edmundoptics.com/optics/optical-lenses/aspheric-lenses/Fiber-Optic-Collimator-and-Focuser-Assemblies/>, 2017b. Visited on May 9th, 2017.
- Edmund Optics. Optical Glass. <https://www.edmundoptics.com/resources/application-notes/optics/optical-glass/>, 2017c. Visited on April 30th, 2017.
- Edmund Optics. Raman Longpass Edge Filters. <https://www.edmundoptics.com/optics/optical-filters/longpass-edge-filters/raman-longpass-edge-filters/>, 2017d. Visited on May 9th, 2017.

- Edmund Optics. Off-Axis Parabolic Metal Mirrors. <https://www.edmundoptics.com/optics/optical-mirrors/off-axis-parabolic-mirrors/off-axis-parabolic-metal-mirrors/>, 2017e. Visited on May 20th, 2017.
- Edmund Optics. Optical Filters. <https://www.edmundoptics.com/resources/application-notes/optics/optical-filters/>, 2017f. Visited on April 30th, 2017.
- Edwards, H. G., Hutchinson, I., and Ingley, R. The ExoMars Raman spectrometer and the identification of biogeological spectroscopic signatures using a flight-like prototype. *Analytical and bioanalytical chemistry*, 404(6-7):1723–1731, 2012.
- Efremov, E. V., Ariese, F., and Gooijer, C. Achievements in resonance Raman spectroscopy: Review of a technique with a distinct analytical chemistry potential. *Analytica Chimica Acta*, 606(2):119–134, 2008.
- Firesmith, D. Using V Models for Testing. https://insights.sei.cmu.edu/sei_blog/2013/11/using-v-models-for-testing.html, 2013. Visited on June 10th, 2017.
- Fischer, R. E., Tadic-Galeb, B., and Yoder, P. R. *Optical system design*. Mc Graw Hill, 2008.
- Gauglitz, G. and Vo-Dinh, T. *Handbook of Spectroscopy*. John Wiley & Sons, 2006.
- Gill, E. AE4-S12-03 Space Systems Engineering – Lecture Notes. TU Delft, 2015.
- Gnyba, M., Smulko, J., Kwiatkowski, A., and Wierzba, P. Portable Raman spectrometer-design rules and applications. *Bulletin of the Polish Academy of Sciences: Technical Sciences*, 59(3):325–329, 2011.
- Greenberg, R. *Europa—the Ocean Moon: Search for an Alien Biosphere*. Springer Science & Business Media, 2009.
- Guldimann, B. and Kraft, S. Focal Plane Array Spectrometer: miniaturization effort for space optical instruments. In *SPIE MOEMS-MEMS*, pages 79300O–79300O. International Society for Optics and Photonics, 2011.
- Hamamatsu. Mini-spectrometer TG series C11713CA. <http://www.hamamatsu.com/us/en/product/application/1505/4517/4387/C11713CA/index.html>, 2017. Visited on May 10th, 2017.
- Hattrick-Simpers, J. R., Hurst, W. S., Srinivasan, S. S., and Maslar, J. E. Optical cell for combinatorial in situ Raman spectroscopic measurements of hydrogen storage materials at high pressures and temperatures. *Review of Scientific Instruments*, 82(3):033103, 2011.
- Horiba Scientific. Raman Academy. <http://www.horiba.com/scientific/products/raman-spectroscopy/raman-academy/>, 2017. Visited on April 1st, 2017.
- Horneck, G., Walter, N., Westall, F., Grenfell, J. L., Martin, W. F., Gomez, F., Leuko, S., Lee, N., Onofri, S., Tsiganis, K., et al. AstRoMap European Astrobiology Roadmap. *Astrobiology*, 16(3):201–243, 2016.
- Ibsen Photonics. OEM Spectrometers. <http://ibsen.com/products/oem-spectrometers/>, 2017. Visited on May 10th, 2017.

- Industrial Fiber Optics. Connector, SMA 905 Style. <http://i-fiberoptics.com/connector-detail.php?id=40&cat=&subcat=>, 2017. Visited on May 9th, 2017.
- Ingersoll, A. P. and Pankine, A. A. Subsurface heat transfer on Enceladus: Conditions under which melting occurs. *Icarus*, 206(2):594–607, 2010.
- IPS Optics. Introduction to optical materials and optical design data. <http://www.ispoptics.com/>, 2017. Visited on April 30th, 2017.
- Janis. Systems for Raman Spectroscopy. http://www.janis.com/Raman_Applications_KeySupplier.aspx, 2017. Visited on April 30th, 2017.
- Khurana, K. K., Kivelson, M. G., Stevenson, D. J., Schubert, G., Russell, C. T., Walker, R. J., and Polansky, C. Induced Magnetic Fields as Evidence for Subsurface Oceans in Europa and Callisto. *Nature*, 395:777–780, 1998.
- Kiselev, R., Schie, I. W., Aškračić, S., Krafft, C., and Popp, J. Design and first applications of a flexible Raman micro-spectroscopic system for biological imaging. *Biomedical Spectroscopy and Imaging*, 5(2):115–127, 2016.
- Konstantinidis, K., Kowalski, J., Flores Martines, C., Dachwald, B., Ewerhart, D., and Förstner, R. Some necessary technologies for in-situ astrobiology on Enceladus. In *66th Astronautical Congress*, 2015a.
- Konstantinidis, K., Martinez, C. L. F., Dachwald, B., Ohndorf, A., Dykta, P., Bowitz, P., Rudolph, M., Digel, I., Kowalski, J., Voigt, K., et al. A lander mission to probe subglacial water on Saturn’s moon Enceladus for life. *Acta Astronautica*, 106:63–89, 2015b.
- Kowalski, J., Linder, P., Zierke, S., von Wulfen, B., Clemens, J., Konstantinidis, K., Ameres, G., Hoffmann, R., Mikucki, J., Tulaczyk, S., et al. Navigation technology for exploration of glacier ice with maneuverable melting probes. *Cold Regions Science and Technology*, 123: 53–70, 2016.
- Kratzke, R. The Dreaded System Requirements Rrulleview. <http://community.vitechcorp.com/index.php/The-Dreaded-System-Requirements-Review.aspx>, 2015. Visited on April 1st, 2017.
- Kudelski, A. Analytical applications of Raman spectroscopy. *Talanta*, 76(1):1–8, 2008.
- Larkin, P. *Infrared and Raman spectroscopy; principles and spectral interpretation*. Elsevier, 2011.
- Larson, W. J., Kirkpatrick, D., Sellers, J. J., Thomas, L. D., and Verma, D. *Applied Space Systems Engineering*. McGraw-Hill Learning Solutions, 2009.
- Laserglow Technologies. Lcs-0532 Low-Cost DPSS Laser System. <https://www.laserglow.com/specsheets/C531005DX.php>, 2017. Visited on May 10th, 2017.
- Leimena, W., Artmann, G., Dachwald, B., Artmann, A., Goßmann, M., and Digel, I. Feasibility of an in-situ microbial decontamination of an ice-melting probe. *Eurasian Chemico-Technological Journal*, 12(2):145–150, 2010.

- Lewis, E. N., Treado, P. J., and Levin, I. W. A miniaturized, no-moving-parts Raman spectrometer. *Applied Spectroscopy*, 47(5):539–543, 1993.
- Lissauer, J. J. and De Pater, I. *Fundamental Planetary Science: Physics, Chemistry and Habitability*. Cambridge University Press, 2013.
- Mann, C. K. and Vickers, T. J. The Quest for Accuracy in Raman Spectra. In *Handbook of Raman Spectroscopy: from the research laboratory to the process line*. CRC Press, 2001.
- McCreery, R. L. *Raman Spectroscopy for Chemical Analysis*. John Wiley & Sons, 2000.
- McCreery, R. L., Fleischmann, M., and Hendra, P. Fiber optic probe for remote Raman spectrometry. *Analytical Chemistry*, 55(1):146–148, 1983.
- Mellon, M. T., Feldman, W. C., and Prettyman, T. H. The presence and stability of ground ice in the southern hemisphere of Mars. *Icarus*, 169(2):324–340, 2004.
- NASA. *Systems Engineering Handbook*. NASA press, 2007.
- Newport. Optical Materials. <https://www.newport.com/n/optical-materials>, 2017. Visited on April 30th, 2017.
- NIST. Fundamental Physical Constants. <http://physics.nist.gov/cuu/Constants/>, 2017. Visited on February 28th, 2017.
- Ocean Optics. Raman. <https://oceanoptics.com/measurementtechnique/raman/>, 2017. Visited on April 30th, 2017.
- Omega Optical. Raman Spectroscopy. <http://www.omegafilters.com/applications/raman-spectroscopy/>, 2017. Visited on April 30th, 2017.
- Optical Cable Corporation. Multimode and Single-Mode Optical Fibers for LAN Systems. <http://www.occfiber.com/main/index.php?p=27>, 2017. Visited on April 30th, 2017.
- Optikos. Collimators for Optical Testing. <http://www.optikos.com/products/collimators-optical-testing/>, 2017. Visited on April 30th, 2017.
- Perret, E. and Balber, T. A High-Precision Calibration Method for Spectrometers. <http://www.americanlaboratory.com/914-Application-Notes/1596-A-High-Precision-Calibration-Method-for-Spectrometers/>, 2011. Visited on June 10th, 2017.
- Photon etc. Raman Shift Calculator. <http://photonetc.com/raman-shift-calculator>, 2017. Visited on April 30th, 2017.
- Photonics Handbook. Lasers. https://cohrcdn.azureedge.net/assets/pdf/Lasers_--Photonics_Handbook.pdf?page=8, 2017. Visited on April 30th, 2017.
- Porco, C., Helfenstein, P., Thomas, P., Ingersoll, A., Wisdom, J., West, R., Neukum, G., Denk, T., Wagner, R., Roatsch, T., et al. Cassini observes the active South pole of Enceladus. *science*, 311(5766):1393–1401, 2006.

- Price, P. B. Microbial life in glacial ice and implications for a cold origin of life. *FEMS Microbiology Ecology*, 59(2):217–231, 2007.
- Princeton Instruments. Raman Spectroscopy Basics. http://content.piacton.com/Uploads/Princeton/Documents/Library/UpdatedLibrary/Raman_Spectroscopy_Basics.pdf, 2017. Visited on February 20th, 2017.
- Procket, L. M. and Pappalardo, R. T. Europa. In *Encyclopedia of the Solar System*, pages 431–448. Academic Press, 2007.
- Raman, C. V. and Krishnan, K. A change of wave-length in light scattering. *Nature*, 121(3051): 619, 1928.
- Rasmussen, T., Rasmussen, M., Hansen, P., Jespersen, O., Rasmussen, N., and Rose, B. How to design a miniature Raman spectrometer. <http://www.spectroscopyonline.com/how-design-miniature-raman-spectrometer>, 2015. Visited on April 30th, 2017.
- RGBLase. 532nm Raman Laser Module. <http://www.rgblase.com/Down%20load/Raman532.pdf>, 2017. Visited on May 10th, 2017.
- RP Photonics Encyclopedia. Optical Filters. https://www.rp-photonics.com/optical_filters.html, 2017. Visited on April 30th, 2017.
- Rull, F., Sansano, A., Diaz, E., Canora, C., Moral, A., Tato, C., Colombo, M., Belenguer, T., Fernandez, M., Manfredi, J., et al. ExoMars Raman Laser Spectrometer overview. In *Proceedings of SPIE*, volume 7819, pages 781915–781911, 2010.
- Rull, F., Sansano, A., Díaz, E., Colombo, M., Belenguer, T., Fernández, M., Guembe, V., Canchal, R., Dávila, B., Sánchez, A., et al. A new spectrometer concept for Mars exploration. In *SPIE Optical Engineering+ Applications*, pages 81520K–81520K. International Society for Optics and Photonics, 2011.
- Russano, C. Exploration of the European Sub-Ocean. TU Delft University of Technology, 2016. In AE2010 Literature Study.
- Russano, C. Life Detection Instruments for EnEx Initiative. TU Delft University of Technology, 2017. In AE5050 Internship Report.
- RWTH Aachen. Enceladus Explorer. <http://www.institut3b.physik.rwth-aachen.de/cms/ParticlePhysics3B/Forschung/~gbvk/Enceladus-Explorer/>, 2016. Visited on March 27th, 2017.
- Schott. Transmittance of Optical Glass. <http://www.schott.com/uk/english/index.html>, 2005. Visited on April 30th, 2017.
- SEBoK. System Verification. http://sebokwiki.org/wiki/System_Verification, 2013. Visited on June 10th, 2017.
- Semrock. Dichroic Beamsplitters/Longpass. <https://www.semrock.com/filtersRefined.aspx?id=497,52&page=1&so=0&reccs=10>, 2017a. Visited on May 9th, 2017.

- Semrock. Edge/Long-pass Filters. <https://www.semrock.com/filtersRefined.aspx?id=21,52&page=1&so=0&recs=10>, 2017b. Visited on May 9th, 2017.
- Semrock. Filter Types for Raman Spectroscopy Applications. <https://www.semrock.com/filter-types-for-raman-spectroscopy-applications.aspx>, 2017c. Visited on April 30th, 2017.
- Serdyuk, I. N., Zaccai, N. R., and Zaccai, J. *Methods in Molecular Biophysics: Structure, Dynamics, Function*. Cambridge University Press, 2007.
- Siegman, A. E. *Lasers*. University Science Books, 1986.
- Slater, J. B., Tedesco, J. M., Fairchild, R. C., and Lewis, I. R. Raman Spectrometry and Its Adaptation to the Industrial Environment. In *Handbook of Raman Spectroscopy: from the research laboratory to the process line*. CRC Press, 2001.
- Smith, E. and Dent, G. *Modern Raman Spectroscopy: A practical approach*. John Wiley & Sons, 2013.
- Smith, W. Practical understanding and use of Surface Enhanced Raman Scattering/Surface Enhanced Resonance Raman Scattering in chemical and biological analysis. *Chemical Society Reviews*, 37(5):955–964, 2008.
- StellarNet. StellarNet Spectrometers Models. <http://www.stellarnet.us/spectrometers/?gclid=CPW11f2z5dMCFRMTGwodL3IKPQ>, 2017. Visited on May 10th, 2017.
- Tarcea, N., z, M., Rösch, P., Frosch, T., Schmitt, M., Thiele, H., Hochleitner, R., and Popp, J. UV Raman spectroscopy—A technique for biological and mineralogical in situ planetary studies. *Spectrochimica Acta Part A: Molecular and Biomolecular Spectroscopy*, 68(4):1029–1035, 2007.
- Tarcea, N., Frosch, T., Rösch, P., Hilchenbach, M., Stuffer, T., Hofer, S., Thiele, H., Hochleitner, R., and Popp, J. Raman spectroscopy—A powerful tool for in situ planetary science. In *Strategies of Life Detection*, pages 281–292. Springer, 2008.
- Thomas, F. How to choose a laser for Raman Spectroscopy. <http://mylaserspectrum.com/2016/04/laser-raman-spectroscopy/>, 2016. Visited on April 30th, 2017.
- Thorlabs. Collimation/Coupling. https://www.thorlabs.com/navigation.cfm?guide_id=27, 2017a. Visited on May 9th, 2017.
- Thorlabs. Single Mode Fiber Optic Connectors. https://www.thorlabs.com/navigation.cfm?guide_id=2322, 2017b. Visited on May 9th, 2017.
- Thorlabs. Single Mode Fiber. https://www.thorlabs.com/newgrouppage9.cfm?objectgroup_id=949, 2017c. Visited on May 9th, 2017.
- Thorlabs. Compact CCD Spectrometers. https://www.thorlabs.com/newgrouppage9.cfm?objectgroup_id=3482&gclid=CKC6hNa709MCFUEz0wodTGIOTg, 2017d. Visited on May 10th, 2017.

- US Air Force. MIL-STD-499A, Engineering Management. <http://www.product-lifecycle-management.com/download/MIL-STD-499A.pdf>, 1974. Visited on January 30th, 2017.
- Vandenabeele, P. *Practical Raman Spectroscopy: an Introduction*. John Wiley & Sons, 2013.
- Wang, A., Haskin, L. A., Lane, A. L., Wdowiak, T. J., Squyres, S. W., Wilson, R. J., Hovland, L. E., Manatt, K. S., Raouf, N., and Smith, C. D. Development of the Mars microbeam Raman spectrometer (MMRS). *Journal of Geophysical Research: Planets*, 108(E1), 2003.
- Wikipedia. Young's modulus. https://en.wikipedia.org/wiki/Young%27s_modulus, 2017a. Visited on April 30th, 2017.
- Wikipedia. Calibration. <https://en.wikipedia.org/wiki/Calibration>, 2017b. Visited on June 10th, 2017.
- Wikipedia. Hardness. <https://en.wikipedia.org/wiki/Hardness>, 2017c. Visited on April 30th, 2017.
- Wolffenbuttel, R. F. MEMS-based optical mini-and microspectrometers for the visible and infrared spectral range. *Journal of Micromechanics and Microengineering*, 15(7):S145, 2005.
- Woodford, C. Fiber optics. <http://www.explainthatstuff.com/fiberoptics.html>, 2016. Visited on April 30th, 2017.
- Yoder Jr, P. R. *Opto-Mechanical Systems Design*. CRC press, 2005.
- Zimmerman, W., Bonitz, R., and Feldman, J. Cryobot: an Ice Penetrating Robotic Vehicle for Mars and Europa. In *Aerospace Conference, 2001, IEEE Proceedings*, volume 1, pages 311–323. IEEE, 2001.

APPENDICES

A

COMPONENTS' TECHNICAL DATA SHEETS

This Appendix collects the technical data sheets of the selected components for the proposed design of the Raman spectrometer.

SAPPHIRE

Sapphire (Aluminium Oxide)	
Density	3.98 g/cm ³
Young's Module	79 × 10 ¹⁰ Pa
Mohs Scale	9
Melting Temperature	2030 °C
Thermal Expansion Coefficient	5.0 – 6.6 × 10 ⁻⁶ K ⁻¹
Specific Heat Capacity	0.761 × 10 ⁻³ J/(kg °C)
Transmission range	0.17 – 5 μm
Birefringence	-0.008

INVAR

Invar (Nickel-Iron Alloy)	
Density	8.1 g/cm ³
Young's Module	137 – 145 × 10 ¹⁰ Pa
Poisson ratio	0.29
Hardness	1200 – 2400 × 10 ⁶ Pa
Melting Temperature	1427 °C
Thermal Expansion Coefficient	1.7 – 2.0 × 10 ⁻⁶ K ⁻¹
Specific Heat Capacity	0.515 J/(g °C)
Curie Temperature	279 °C

SEMROCK 532 nm BRIGHTLINE® SINGLE-EDGE SUPER-RESOLUTION LASER DICHOIC BEAMSPLITTER

Optical Specifications

Specification	Value
Reflection Band 1	R _{abs} > 94% 514 – 532 nm
Reflection Band 1 (p-pol)	R _{abs} > 90% 514 – 532 nm
Reflection Band 1 (s-pol)	R _{abs} > 98% 514 – 532 nm
Reflection Band 2	R _{avg} > 90% 350 – 514 nm
Edge Wavelength 1	538.4 nm
Transmission Band 1	T _{avg} > 93% 541.6 – 1200 nm
Laser Wavelengths 1	514.5 nm, 532 nm

General Filter Specifications

Specification	Value
Angle of Incidence	45 degrees with a shift of 0.35%/degree (40 – 50 degrees)
Cone Half-angle	0.5 degrees
Optical Damage Rating	1 J/cm ² @ 532 nm (10 ns pulse width)
Flatness (1 mm thickness)	1λ P-V RWE @ 632.8 nm
Flatness (3 mm thickness)	λ/5 P-V RWE @ 632.8 nm
Steepness	Steep
Effective Index	2.14

Physical Filter Specifications (applies to standard sized parts; contact us regarding other sizes)

Specification	Value
Transverse Dimensions (L x W)	25.2 mm x 35.6 mm
Transverse Tolerance	± 0.1 mm
Filter Thickness (1 mm, unmounted)	1.05 mm
Filter Thickness Tolerance (1 mm, unmounted)	± 0.05 mm
Filter Thickness (3 mm, unmounted)	3.0 mm
Filter Thickness Tolerance (3 mm, unmounted)	± 0.1 mm
Clear Aperture	≥ 80% (elliptical)
Scratch-Dig	60-40
Substrate Type	Fused Silica
Substrate Thickness (1 mm, unmounted)	1.05 mm
Substrate Thickness Tolerance (1 mm, unmounted)	± 0.05 mm
Substrate Thickness (3 mm, unmounted)	3.0 mm
Substrate Thickness Tolerance (3 mm, unmounted)	± 0.1 mm
Orientation	Reflective surface marked with laser dot - Orient in direction of incoming light

SEMROCK 532 nm EDGEBASIC™ BEST-VALUE LONG-PASS EDGE FILTER

Optical Specifications

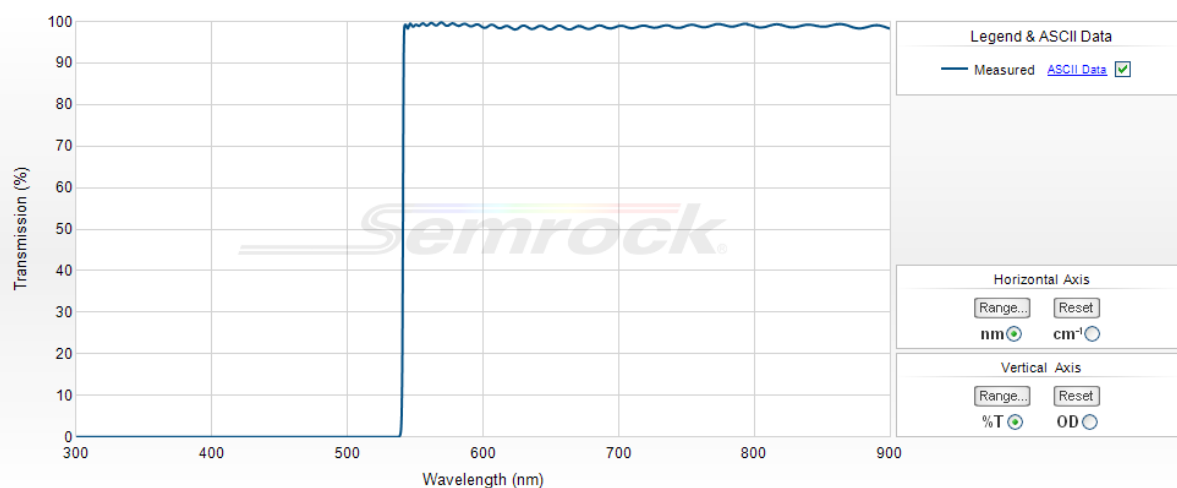
Specification	Value
Transmission Band 1	$T_{avg} > 93\%$ 546.9 – 900 nm
Edge Wavelength 1	542 nm
Blocking Band 1	$OD_{avg} > 5$ 270 – 425.6 nm
Blocking Band 2	$OD_{abs} > 6$ 425.6 – 532 nm
Transition Width (nm)	13.3 nm
Transition Width (cm ⁻¹)	458 cm ⁻¹

General Filter Specifications

Specification	Value
Laser Wavelength 1	532 nm
Laser Wavelength 1 (low)	532 nm
Laser Wavelength 1 (high)	532 nm
Angle of Incidence	0 ± 2 degrees
Cone Half-angle	5 degrees
Optical Damage Rating	Not tested
Effective Index	1.82

Physical Filter Specifications (applies to standard sized parts; contact us regarding other sizes)

Specification	Value
Transverse Dimensions (Diameter)	25 mm
Transverse Tolerance (mounted)	+ 0.0 / - 0.1 mm
Filter Thickness (Mounted)	3.5 mm
Filter Thickness Tolerance (Mounted)	± 0.1 mm
Clear Aperture	≥ 22 mm
Scratch-Dig	60-40
Substrate Thickness (unmounted)	2.0 mm
Substrate Thickness Tolerance (unmounted)	± 0.1 mm
Orientation	Arrow on ring indicates preferred direction of propagation of light



EDMUND OPTICS 25.4 × 25.4 mm PFL 30° OFF-AXIS PARABOLIC ALUMINIUM MIRROR

Common Specifications for Product Family

Surface Roughness (Angstroms):	<175 RMS	Substrate:	Aluminum 6061-T6
--------------------------------	----------	------------	------------------

Specifications

Type:	Off-Axis Parabolic Mirror	Coating:	Protected Aluminum
Effective Focal Length EFL (mm):	27.22	Focal Length Tolerance (%):	±1
Diameter (mm):	25.4	Diameter Tolerance (mm):	+0.00/-0.38
Off-Set Angle (°):	30°	Parent Focal Length PFL (mm):	25.4
Wavelength Range (nm):	400 - 12,000	Coating Specification:	R _{avg} >85% @ 400 - 700nm R _{avg} >70% @ 700 - 2000nm R _{avg} >97% @ 2 - 12µm
Coating Type:	Metal	Y Offset (mm):	13.61
Reflected Wavefront, RMS:	λ/4	RoHS:	Compliant

NOTES:

- SUBSTRATE MATERIAL:
ALUMINUM
- FINISH (EXCEPT SURFACE S1):
BLACK ANODIZED
- COATING (APPLY ACROSS CLEAR APERTURE)
S1: PROTECTED ALUMINUM
R(AVG) >85% @ 400 - 700nm
R(AVG) >97% @ 2 - 12MM

SURFACE ROUGHNESS : <175 RMS

- EFL TOLERANCE: ±1%
- ROHS COMPLIANT

**FOR INFORMATION ONLY:
DO NOT MANUFACTURE
PARTS TO THIS DRAWING**

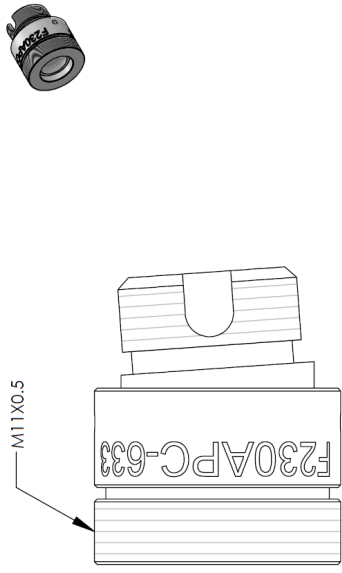
SPECIFICATIONS SUBJECT TO CHANGE WITHOUT NOTICE
DIMENSIONS ARE FOR REFERENCE ONLY

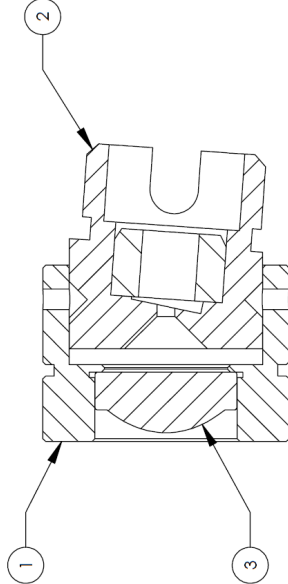
REV. A	S1	Edmund Optics®	
SHAPE	PARABOLIC		
REFLECTIVE WAVEFRONT DISTORTION AT (RMS) TYP.	λ/2	THIRD ANGLE PROJECTION	TITLE
SURFACE FIGURE AT (RMS)	λ/4	ALL DIMS IN mm DWG NO 63180	Ø25.4 X 25.4mm EFL 30° OFF-AXIS PARABOLIC ALUMINUM MIRROR
CLEAR APERTURE	90%		SHEET 1 OF 1
BEVEL	PROTECTIVE AS NEEDED		

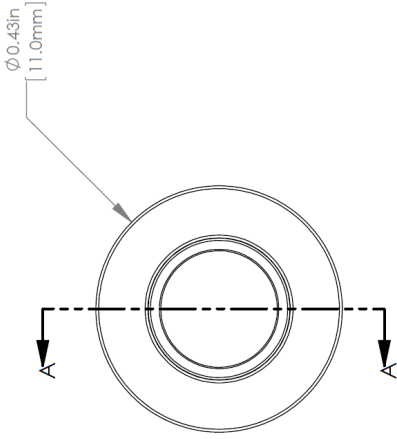
THORLABS FIXED FOCUS COLLIMATION PACKAGES: FC/APC CONNECTORS

ITEM	MATERIAL
① HOUSING	303 STAINLESS STEEL
② FC/APC PLUG ADAPTER	303 STAINLESS STEEL
③ ϕ 6.3mm, f=4.46mm LENS	MOLDED ASPHERE

SPECIFICATIONS	
DESIGN WAVELENGTH	633nm
DESIGN MFD	4.3 μ m
OUTPUT $1/e^2$ BEAM DIAMETER	0.84 mm
FULL ANGLE BEAM DIVERGENCE	0.055° $^{+0.01}_{-0.08}$
AR COATING	Ravg<0.5% FROM 350-700nm







THORLABS FIBER COLLIMATION PACKAGES ARE DESIGNED TO COLLIMATE A LASER BEAM PROPAGATING OUT THE END OF AN OPTICAL FIBER. EACH COLLIMATION PACKAGE IS FACTORY ALIGNED SO THAT THE BEST POSSIBLE DIVERGENCE IS ACHIEVED.

**FOR INFORMATION ONLY
NOT FOR MANUFACTURING PURPOSES**

DRAWING PROJECTION		THORLABS www.thorlabs.com	
NAME	DATE	λ =633nm FC/APC COLLIMATION PACKAGE, NA=0.56 f=4.46mm	REV
DRAWN ST	18/MAY/15	MATERIAL	A
APPROVAL BW	20/MAY/15	SEE TABLE	APPROX WEIGHT
COPYRIGHT © 2015 BY THORLABS		ITEM #	F230APC-633
VALUES IN PARENTHESIS ARE CALCULATED AND MAY CONTAIN ROUND-OFF ERRORS			9.0 g

COBOLT 08-01 SERIES LASER



Cobolt 08-01 Series

DATA SHEET | D0142-D | OCTOBER 2016



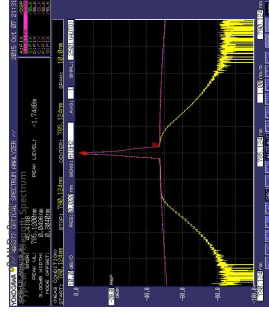
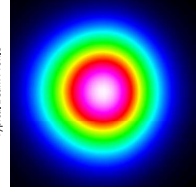
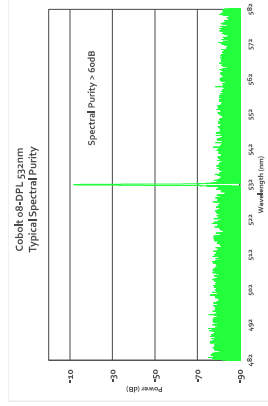
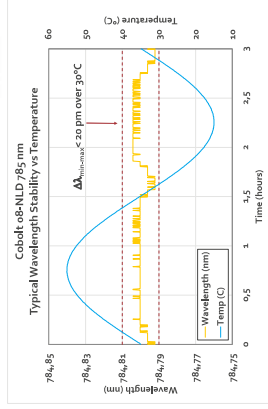
Compact narrow linewidth lasers

- Single frequency diode pumped lasers (DPLs) and narrow linewidth diode (NLD) lasers
- Up to 500 mW continuous-wave power
- Integrated spectral filter
- Integrated isolator option, immune to optical feedback
- Ultra-robust hermetically sealed package and proven field reliability
- 532 nm, 561 nm and 785 nm

The Cobolt 08-01 Series is a family of narrow linewidth continuous-wave lasers, including diode pumped lasers as well as frequency stabilized diode lasers operating at fixed wavelengths between 532 nm and 785 nm with output power up to 500 mW. The lasers are designed and manufactured to ensure the highest level of reliability.

Cobolt lasers are built using proprietary HTCure™ manufacturing technology for ultra-robustness into a compact hermetically sealed package. The lasers emit a high quality laser beam with very stable characteristics and dependable performance, tailored to meet the expectations from manufacturers of high-end Raman spectroscopy instrumentation.

The Cobolt 08-01 Series is intended for stand-alone use in laboratory environments or for integration as an OEM component in instruments, including not only Raman spectroscopy, but also other applications, where a stable and narrow linewidth is crucial.



Cobolt AB | Solna, Sweden | PHONE +46 8 545 912 30 | FAX +46 8 545 912 31 | E-MAIL info@cobolt.se | www.cobolt.se

Cobolt o8-01 Series

	532	561	532	785
	o8-DPL		o8-NLD	
Center-Wavelength (nm)	532.1 ± 0.3	561.2 ± 0.3	532.1 ± 0.3	784.8 ± 0.5
Power (mW)	25	25	25	500
	50	50	50	
	100	100	100	
	200	100	160	
Integrated Optical Isolator	no	no	Yes	Yes
Optical Isolation	n/a	n/a	> 20 dB @25 °C	
Beam divergence (full angle, mrad)	< 1.2		horizontal: < 20	vertical: < 2.5
Spectral bandwidth (FWHM)	< 1 MHz		40 pm*	
Spatial mode	(TEM ₀₀), M ² < 1.1		Multimode	
Beam symmetry	> 0.95:1		n/a	
Beam diameter at aperture	700 ± 70 µm		horizontal: 1.4 ± 0.2 mm vertical: 1.7 ± 0.2 mm	
Noise, 250 Hz - 2 MHz (rms)	< 0.25%, (typical < 0.15%)		typical < 0.5%	
Power stability over 8 hrs	< 2%		< 1%	
Polarization Extinction Ratio (PER)	> 100:1			
Maximum base plate temperature	50 °C		55 °C	
Total system power consumption	< 20 W		< 15 W	
Laser head dimensions	100 x 40 x 40 mm		128 x 40 x 40 mm	
Key box dimensions	43.5 x 30 x 24 mm			
Communication	USB			
Power Supply Requirements	wavel-08-01-pwr-100 (CDRH/CE: Key Control Box included)		wavel-08-11-pwr-100 (CDRH/CE: Key Control Box included)	
Model number structure	wavel-08-01-pwr-200 (OEM: Auto-start mode)		wavel-08-11-pwr-200 (OEM: Auto-start mode)	
Warranty	12 months, unlimited hours of operation		12 mo. or 5000 hrs.	

*Typical Value

Options & Accessories

- Mount for external fiber coupling
- Laser head heatsink
- Keybox for CDRH operation



Mount for external fiber coupling

This device is sensitive to Electrostatic Discharge (ESD). Always handle diode lasers with extreme care to prevent electrostatic discharge, the primary cause of unexpected diode failure.



WARNING LASER RADIATION
Avoid Exposure to beam
Class 3B Laser Product
Classified per IEC 60825-1:2014

Wvl (nm)	Max:Pwr (mW)
532	300
561	300

WARNING INVISIBLE LASER RADIATION
Avoid eye or skin exposure to direct or scattered radiation
Class 4 Laser Product
Classified per IEC 60825-1:2014

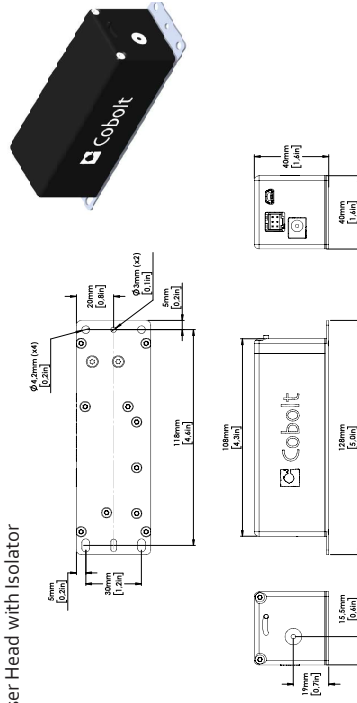
Wvl (nm)	Max:Pwr (mW)
785	2000



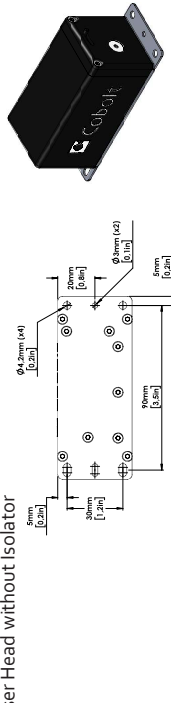
Cobolt o8-01 Series

Mechanical Specifications

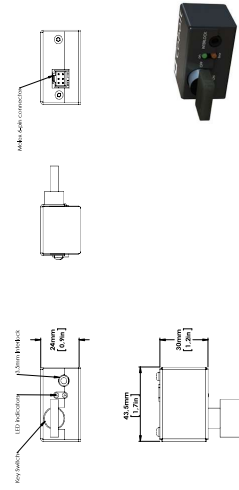
Laser Head with Isolator



Laser Head without Isolator



Key Box



Electrical Interface

Interface	Location	Connector
Input power	Laser Head	DC plug 2,5 mm / 5,5 mm female
Remote interlock connector	Laser Head	OEM : Molex pin 1 & 2
Data port	Laser Head	USB-type mini B
Key control Box connector	Laser Head	Molex 6-pin male
Laser Head connector	Key box	Molex 6-pin male
Remote Interlock connector	Key box	CDRH : 3-5 mm audio female

Cobolt Head Office

Cobolt AB
Vretenvägen 13
SE-171 54 Solna, Sweden
Phone: +46 8 545 912 30
Fax: +46 8 545 912 31
E-mail: info@cobolt.se

German Sales Office (incl. Austria and Switzerland)

HÜBNER GmbH & Co. KG
Heinrich-Hertz Strasse 2,
34123 Kassel, Germany
Phone: +49 6251 770 6686
Fax: +49 6251 860 9917
E-mail: photronics@hubner-germany.com

USA Sales Office

Cobolt Inc.
2635 North First Street, Suite 228
San Jose, California, 95134, USA
Phone: 1 (408) 708 4351
Fax: 1 (408) 490 2774
E-mail: info@coboltinc.com

Find local sales representatives at www.cobolt.se/contact-us

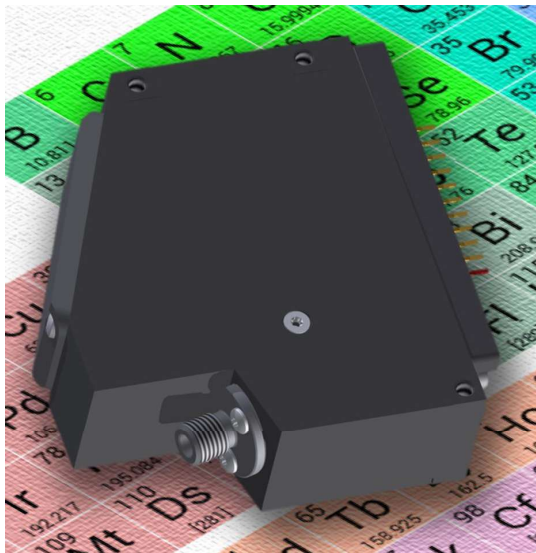
Australia, Benelux, Brazil, China, Estonia, Latvia, Lithuania, France, India, Israel, Italy, Japan, Poland, Russia, Belarus, Singapore, Malaysia, Thailand, South Korea, Spain and Portugal, Taiwan, UK and Ireland

IBSEN FREEDOM HR-VIS SPECTROMETER



FREEDOM HR-VIS

Product Specification



Ibsen Photonics A/S, Ryttermarken 15-21, DK-3520 Farum, Denmark / Tel.: (+45) 44 34 70 00

Validation date: 25-March-2015

Version: 2.0

Page 1 of 15

1 Introduction

The FREEDOM HR-VIS is a robust, athermal, industrial grade diode array based spectrometer for OEM integration. The key benefits of the product are:

- Compact size of only 61 x 65 x 19 mm
- High resolution – down to 0.4 nm
- Cost efficient
- Low stray light < 0.03%
- OEM integration friendly design that allows easy adaptation to your own electronics and detector
- Robust and athermal design

See also Table 2 for more details on the specifications of the FREEDOM HR-VIS spectrometer.

This document is a detailed product specification describing the FREEDOM HR-VIS principle of operation (see Chap. 2) and technical specifications (Chap. 3).

The FREEDOM spectrometer is intended for integration with your own electronics and therefore the electrical interface of FREEDOM is a direct access to the pins of the line detector array. For more information about the detector array interfaces supported by FREEDOM HR-VIS please see the respective data sheets from the suppliers listed in Chap. 2.2.

FREEDOM can also be supplied with the VersaPic USB/RS-232 controller and VersaSpec software. Please see chapter 4 for a description of this electronics and software option.

2 Principle of operation

2.1 Spectroscopy

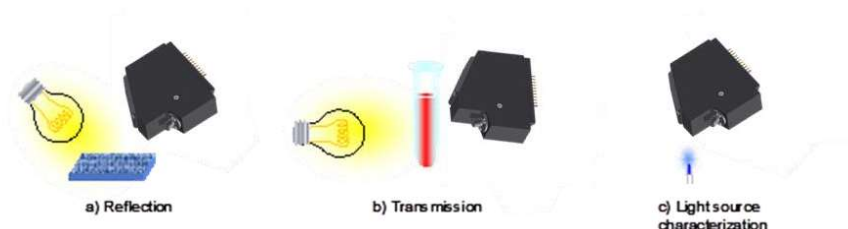


Figure 1: Using the FREEDOM HR-VIS in typical spectroscopic applications.

Figure 1 illustrates how the FREEDOM HR-VIS can be used in various spectroscopic applications.

In most applications either a transmission or reflection geometry is used. A broadband light source like a lamp is used to illuminate the sample under test and the spectrometer is then used to collect the transmitted/reflected light. The spectrometer will measure a spectrum that in turn can be used to determine certain characteristics of the sample.

As indicated on Figure 1 c) the FREEDOM HR-VIS spectrometer can also be used for determining the spectral content of a light source or a fluorescent substance.

2.2 FREEDOM HR-VIS

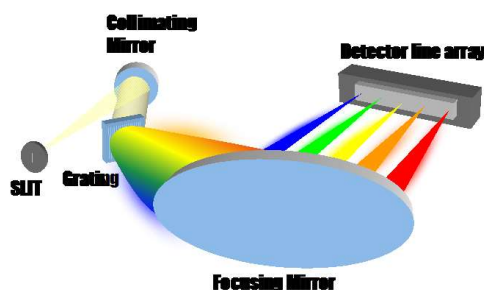


Figure 2: Optics schematic diagram.

The schematic diagram for the optics of the FREEDOM HR-VIS spectrometer is illustrated in Figure 2. The FREEDOM HR-VIS is based on Ibsen Photonics' MGM platform utilizing a collimating mirror, a transmission grating and a focusing mirror. The FREEDOM HR-VIS uses a very high diffraction efficiency fused silica transmission grating produced by Ibsen Photonics internally as shown in Figure 3.

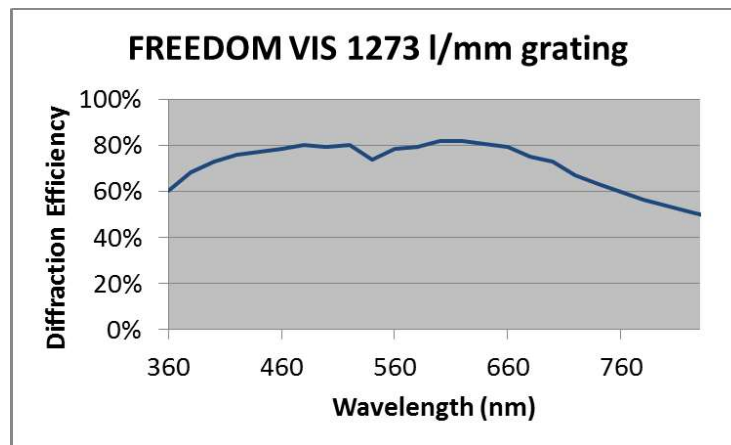


Figure 3: Typical diffraction efficiency of Ibsen transmission grating.

The numerical aperture of the spectrometer is 0.11 (equivalent to an F-number of 4.5).

The FREEDOM HR-VIS spectrometers can be configured by Ibsen with a range of input slits providing the optical FWHM resolution that best suits your requirements. Since a slit will limit the amount of available light on the detector we always recommend that you work with the largest possible optical resolution that is acceptable in your application. In Figure 4 you can find the relation between slit width and resolution.

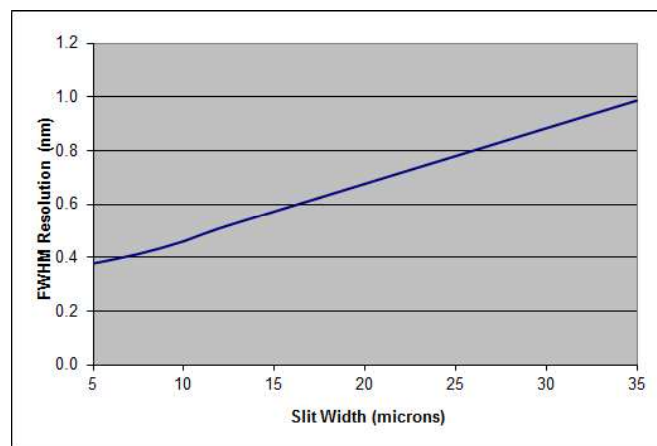


Figure 4: FWHM resolution of FREEDOM HR-VIS as a function of input slit width.

FREEDOM HR-VIS supports as standard two different line array detectors with various benefits as outlined in Table 1. However, Ibsen Photonics can in most cases customize a

FREEDOM spectrometer to accept almost any other line array detector. Please, contact Ibsen Photonics directly to discuss adaptation to a non-standard detector array.

For specifications of the electrical interface to the line array detectors please see the data sheets for the individual detectors.

Table 1: Line array detectors supported by FREEDOM HR-VIS.

Detector	SONY ILX511B	Hamamatsu S10420-1106
FREEDOM Part #	FHV-300	FHV-315
Number of pixels	2048	2048
Pixel width	14 μm	14 μm
Pixel height	200 μm	896 μm
Technology	CCD	BT-CCD
Benefits	High sensitivity Low cost	High sensitivity Medium S/N
Drawbacks	Low S/N and Dyn. Range	High cost
Documentation	[1]	[2]

3 Specifications

3.1 Specifications

Table 2: FREEDOM HR-VIS specifications (typical values)

Parameter	FHV-300	FHV-315	Comment
Wavelength range	360 – 830 nm	360 – 830 nm	
Numerical aperture	0.11	0.11	
Minimum Optical resolution	0.4	0.4	FWHM with 10 micron slit
Stray light	< 0.03 %	< 0.03 %	At +/- 40 nm from peak
Detector	SONY ILX511B 2048 CCD	Hamamatsu S10420-1106 BT-CCD	
Dimensions	61 mm x 65 mm x 19 mm	61 mm x 65 mm x 19 mm	
Dynamic range	700:1	4800:1	
S/N	185:1	542:1	
Operating temperature interval	-10 to + 45 °C	-10 to + 45 °C	Non condensing
Storage temperature interval	-30 to + 80 °C	-30 to + 80 °C	
Temperature shift	< 0.02 nm / °C	< 0.02 nm / °C	

Specifications are subject to change without prior notice.

3.2 Parameter definitions:

3.2.1 Wavelength range

The wavelength range is defined as the range of wavelengths that is captured by the detector.

3.2.2 Numerical aperture (NA)

The numerical aperture of the spectrometer defines the range of angles by which the spectrometer can accept light.

3.2.3 Minimum optical resolution

The resolution is defined as the FWHM peak width as measured by the spectrometer when the input is a single wavelength (i.e. a monochromatic light source). The minimum resolution is the smallest resolution that can be obtained with the spectrometer.

3.2.4 Grating efficiency

The grating efficiency is the absolute diffraction efficiency for the transmission grating including AR-coating.

3.2.5 Stray light

Stray light is measured as the light at wavelengths of +/- 40 nm on each side of the peak recorded, when the input is a monochromatic light source.

3.2.6 Wavelength shift

The wavelength shift is defined as a wavelength shift per degree C and is a deterministic, nearly linear function of temperature.

3.3 Package dimensions

The package dimensions are shown in Figure 5 for FREEDOM HR-VIS. Note that all dimensions are given in mm.

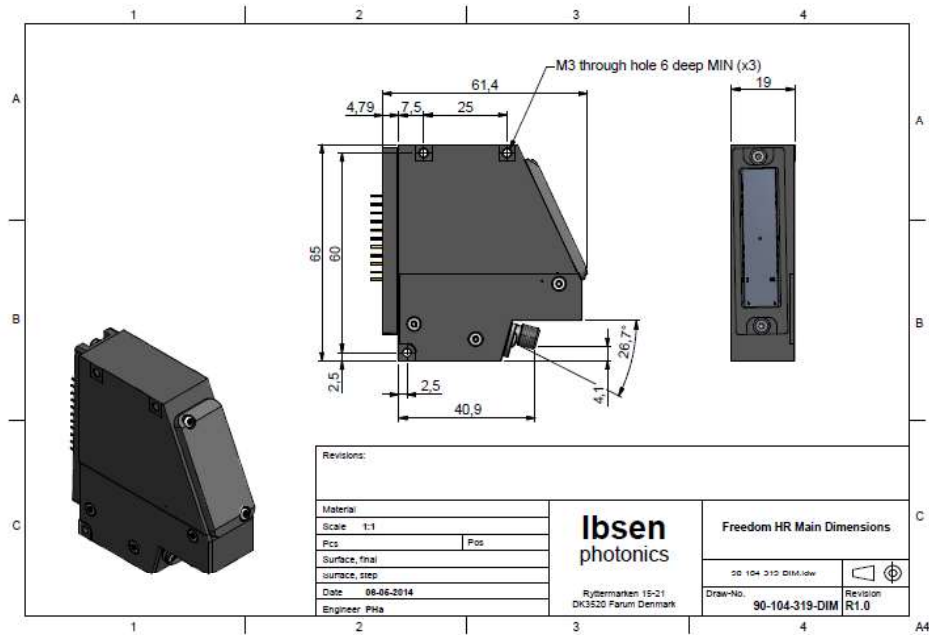


Figure 5: Package dimensions of FREEDOM HR-VIS.

3.4 Spectrometer mounting

FREEDOM HR-VIS has three M3 through holes (6 mm deep) for mounting the spectrometer housing to a chassis and base.

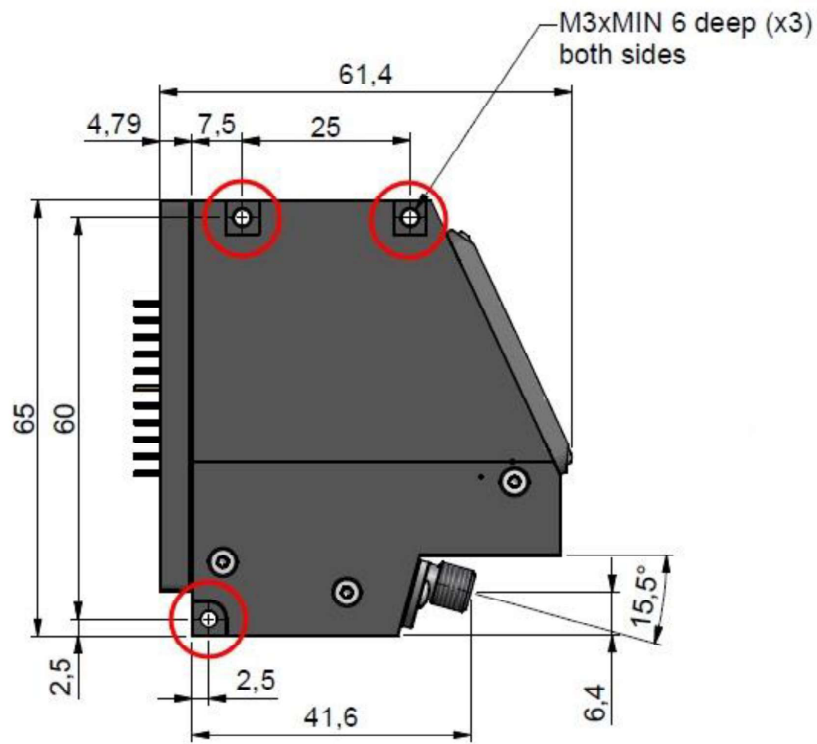


Figure 6: Spectrometer mounting

3.5 SMA adapter

The input adaptor accepts any SMA connector unless they exceed the dimensions shown below.

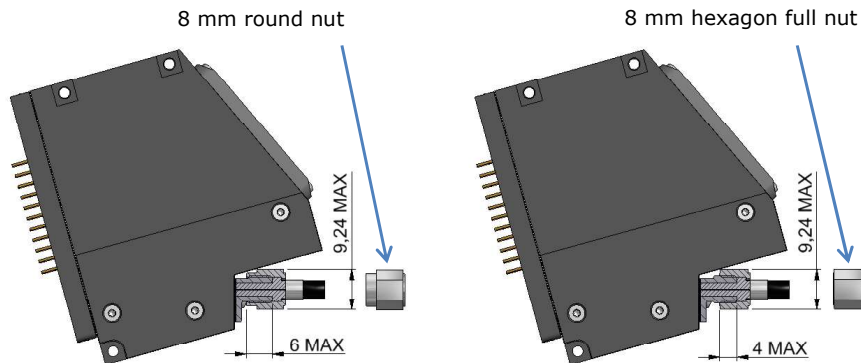


Figure 7: Maximum screw in depth for SMA hexagon nut types.

Ideally a round hexagon is used, but there is also space for a hex nut provided the max outer diameter of the nut is 9.24 mm max and the screw in depth of 4 mm max. Smaller outer diameter allows screw in depths up to 6 mm as illustrated in Figure 7.

On the rear side of the sensor frame two M2 threaded holes enables the mounting of a printed circuit board (PCB) to be fixed along with the sensor. The threaded holes are machined after surface treatment and hence conductive. The thickness of the sensor frame is 4.5 mm thus **it is very important that the screw in depth do not exceed 4 mm as this would permanently damage the spectrometer!** Note the frame is tilted in relation to the housing.

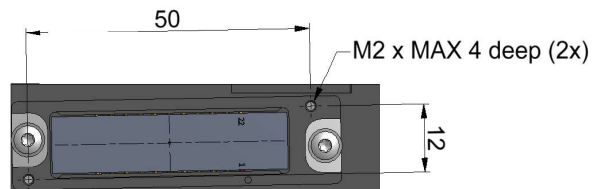


Figure 8: Mounting holes for sensor PCB.

4 Operation with VersaPic USB/RS-232 Controller and software

FREEDOM can optionally be supplied with the VersaPic USB/RS-232 controller, drivers, and software. You can use this option to be able to quickly evaluate FREEDOM for your application before you make your own electronics and/or software. The VersaPic USB/RS-232 controller can also be used as the electronics in your final instrument and you can use the VersaSpec software development kit (SDK) for writing your application.

4.1 OEM Spectrometer Software

Ibsen offers a common software platform across all spectrometers. On Figure 9 you can see a summary of the various software levels.

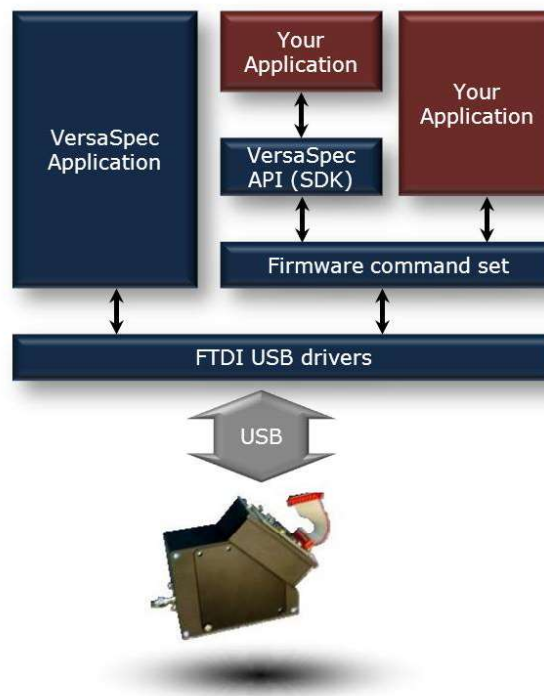


Figure 9: Overview of software interfaces

4.1.1 Drivers

In order to get communication to work with the spectrometer you need to install a USB driver and a virtual COM port driver. These come with the download package from our

website (<http://www.ibsenphotonics.com/about/customers/customer-download/versaspec-v3-1-6>) or can be downloaded from the FTDI home page.

4.1.2 Firmware (RS-232/USB) commands

The lowest level that you can communication with the spectrometer is by Firmware commands. These will provide you with most flexibility but also requires most work since you have to perform the communication command by command. The Firmware command set is independent of operating system so you are not tied to using Windows for instance. A Firmware Command Reference Manual can be provided on request.

4.1.3 Software Development Kit (SDK)

The SDK operates at a layer above the Firmware commands using a set of Windows DLL's. These DLL's group several firmware commands into more convenient function calls to make it easier to program using C, LabVIEW or similar higher level programming languages. The Software Development Kit has its own User's Manuals included in the package as well as some programming examples.

4.1.4 VersaSpec

The VersaSpec software is application software that runs under Windows mostly intended for quick evaluation of our spectrometers. You can set basic parameters like integration time, number of averages but most of the Firmware parameters cannot be set by the VersaSpec.

4.2 VersaPic Electronics specifications

The VersaPic electronics consists of two PCB's connected via a ribbon cable as shown on Figure 10. One PCB is mounted on the spectrometer and holds the detector in a socket. The other PCB is the USB controller performing the A/D conversion and read out circuitry for USB.

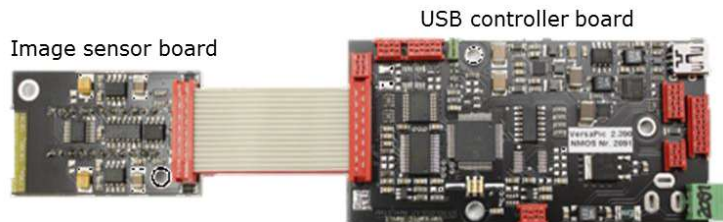


Figure 10: Set of electronics

Electrical Parameters	
Power supply	USB-Hub powered or + 6 ... 16 V DC
Operation current	<150 mA (on USB)
Quiescent current (power down)	< 5 mA (interface dependent)

Ibsen Photonics A/S, Ryttermarken 15-21, DK-3520 Farum, Denmark / Tel.: (+45) 44 34 70 00

Validation date: 25-March-2015

Version: 2.0

Page 13 of 15

Analog to Digital Conversion Unit	
Resolution	16 bit, 2 bit RMS (without oversampling), 4 bit INL, no missing code
Sampling speed	10 MS/sec.
Sampling mode	Sample and Hold: 1, 4 - fold prog. oversampling or Correlated Double Sampling
Inputs	2 (odd and even), programmable for positive or negative video signals
Input full scale range	2 V or 4 V, programmable
Gain	1...5 programmable in 64 steps
Offset	External compensation or programmable up to +/- 300 mV
Interfaces	
USB 2.0	Full speed (12 Mbit/sec) (virtual COM Port)
RS232	8, N, 1, RxD, TxD, no flow control up to 115200 bit/sec.
TTL-UART	up to 921600 bit/sec
SPI	up to 5 Mbit/sec.
Process control	
Trigger input	TTL, slope programmable
Shutter output	TTL, programmable state and delay
Flash lamp control	programmable flash length, programmable burst

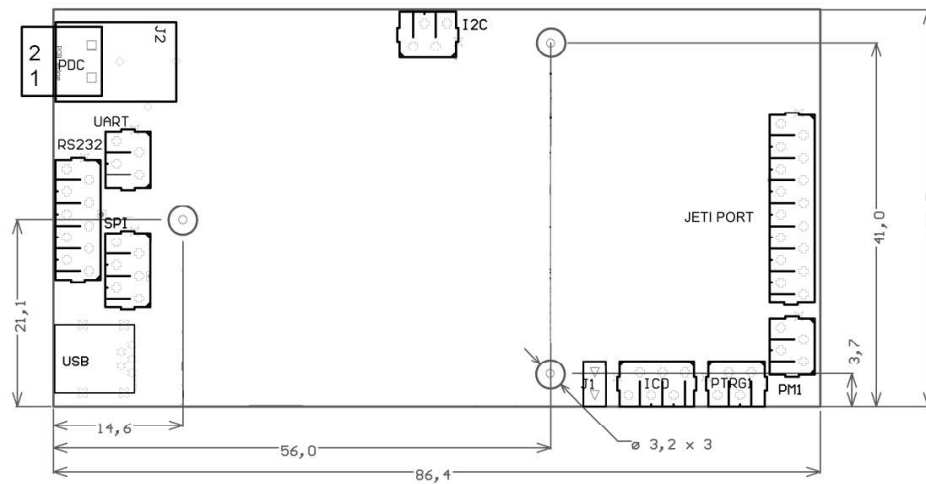


Figure 11: Dimension of VersaPic Controller.

4.3 Wavelength calibration

The FREEDOM HR-VIS is wavelength calibrated at a fixed temperature of 25 deg C according to a polynomial of 4th degree:

$$\text{Eq. 1} \quad \lambda[\text{nm}] = A + B_1 \text{pix} + B_2 \text{pix}^2 + B_3 \text{pix}^3 + B_4 \text{pix}^4, \quad \text{pix} = 0..N_{\text{max}} - 1$$

This equation describes the relation between the beam spot position (pix) on the detector array and the optical wavelength (λ). N_{max} is the number of pixels in the detector array.

The coefficients A , B_1 , B_2 , B_3 , and B_4 are measured for each FREEDOM HR-VIS unit and are supplied with the Certificate of Conformance. In case the Ibsen Photonics VersaPic controller electronics is used, the coefficients are stored in flash memory on the VersaPic board during manufacturing. The coefficients are used by the VersaSpec Windows software to display the measured power versus wavelength directly. If you need to write your own software it is possible to read the coefficients by using the firmware commands as described in the respective manuals.

5 Related documents

ID	Document
[1]	SONY ILX511B Data Sheet
[2]	Hamamatsu S10420 Data Sheet
[3]	VersaPic and software VersaSpec V3.x, Operating Instructions
[4]	Firmware Commands VERSA PIC, Operating Instructions

6 Revision history

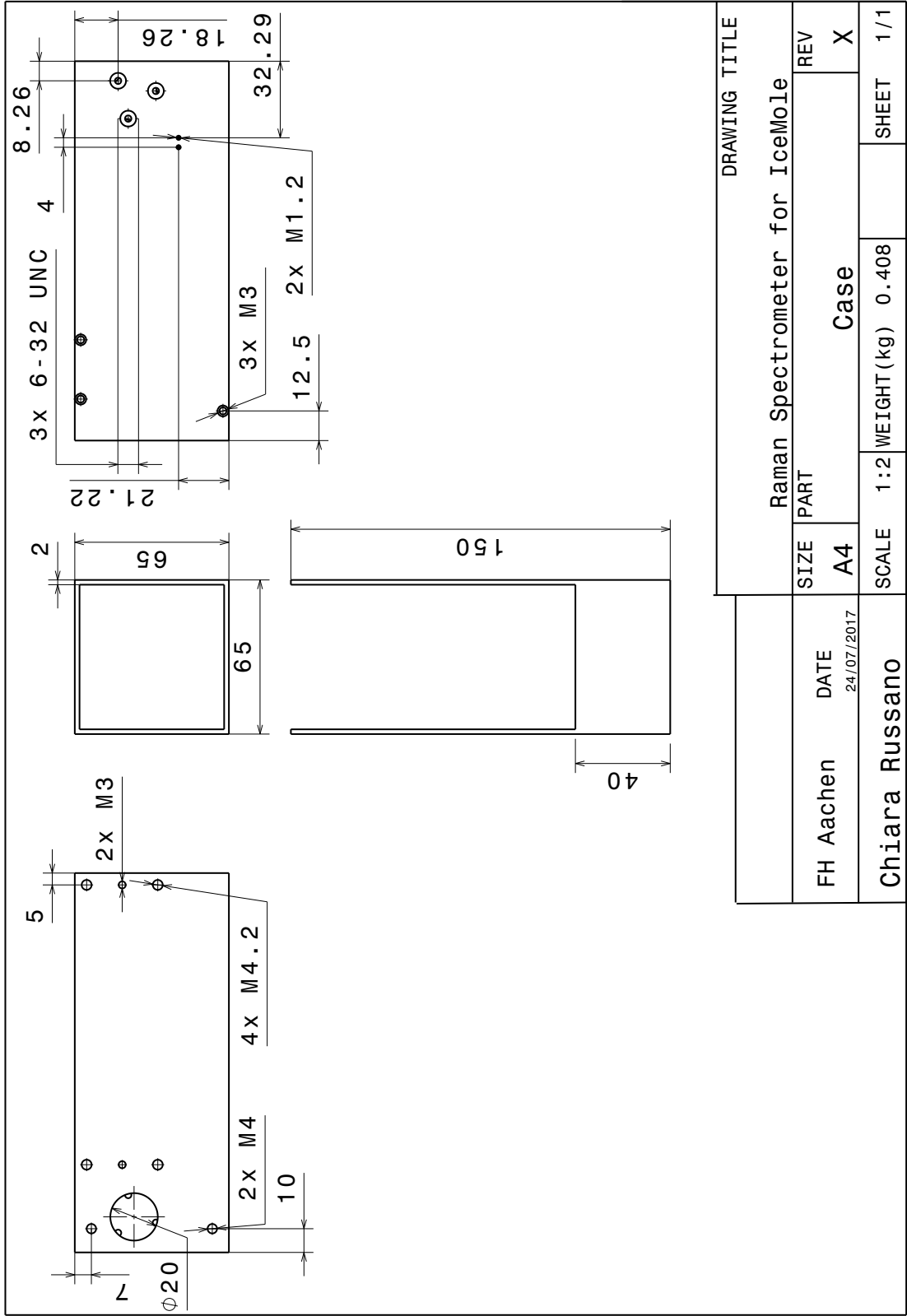
Revision no.	Revision
1.0	Final version
2.0	Updated slit size in Table 2, software on website, VersaPic picture, Eq. 1 corrected

B

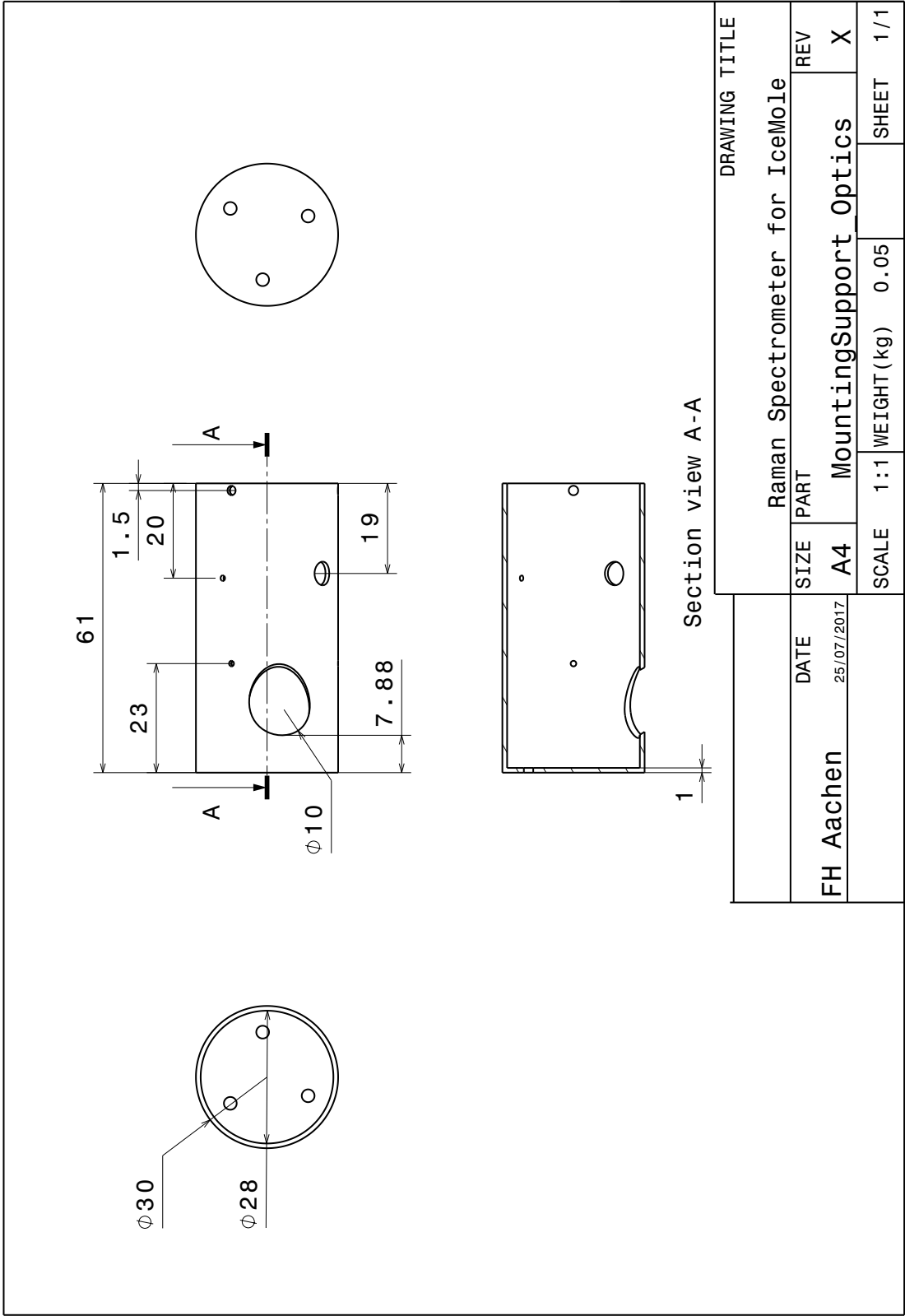
CAD DRAWINGS

This Appendix presents the technical drawings of the components that were modelled through the CAD software CATIA™: the case, the optics mounting support, the window mounting support, the beamsplitter mounting support, the filter mounting support and the collimator mounting support.

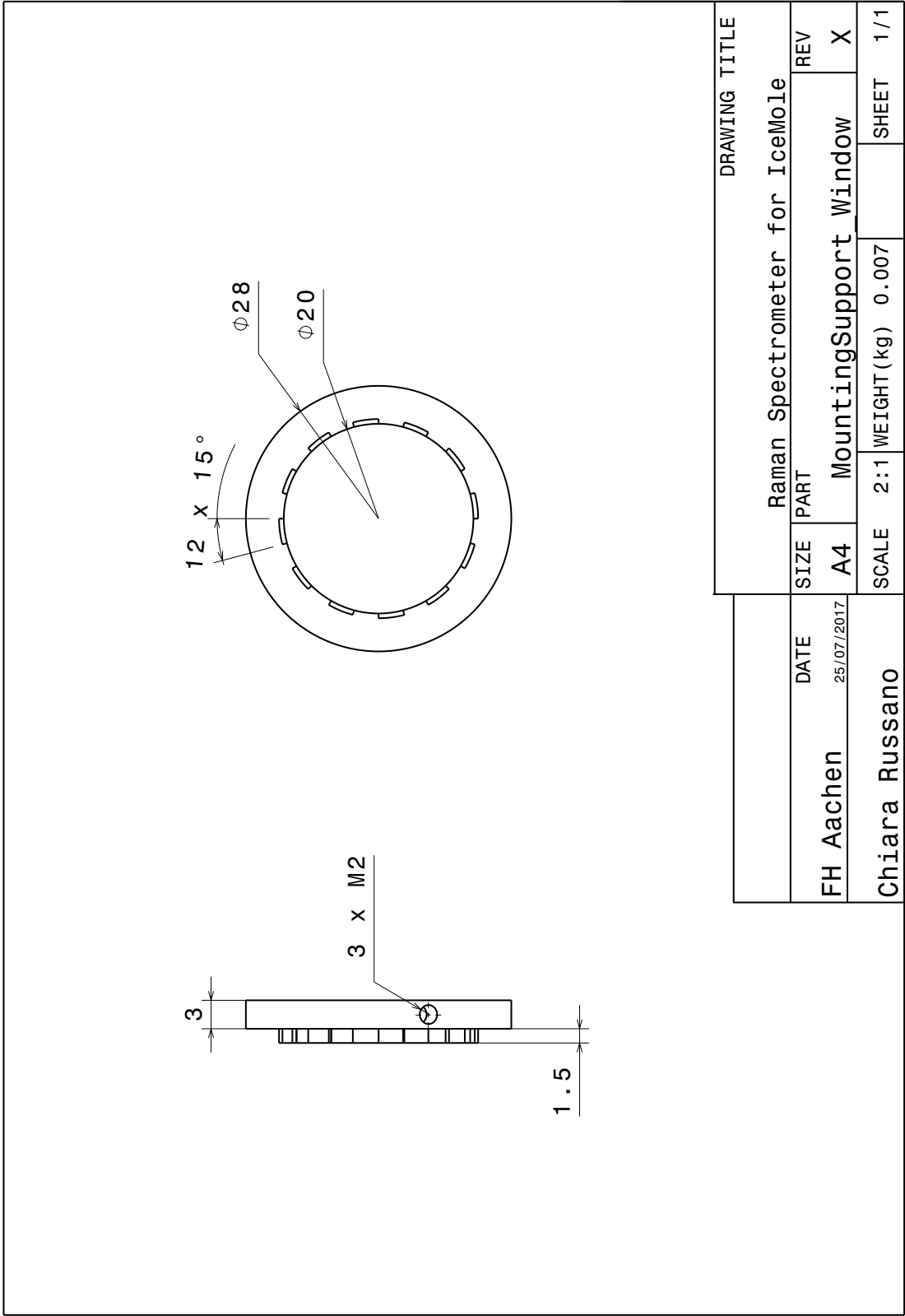
CASE



OPTICS

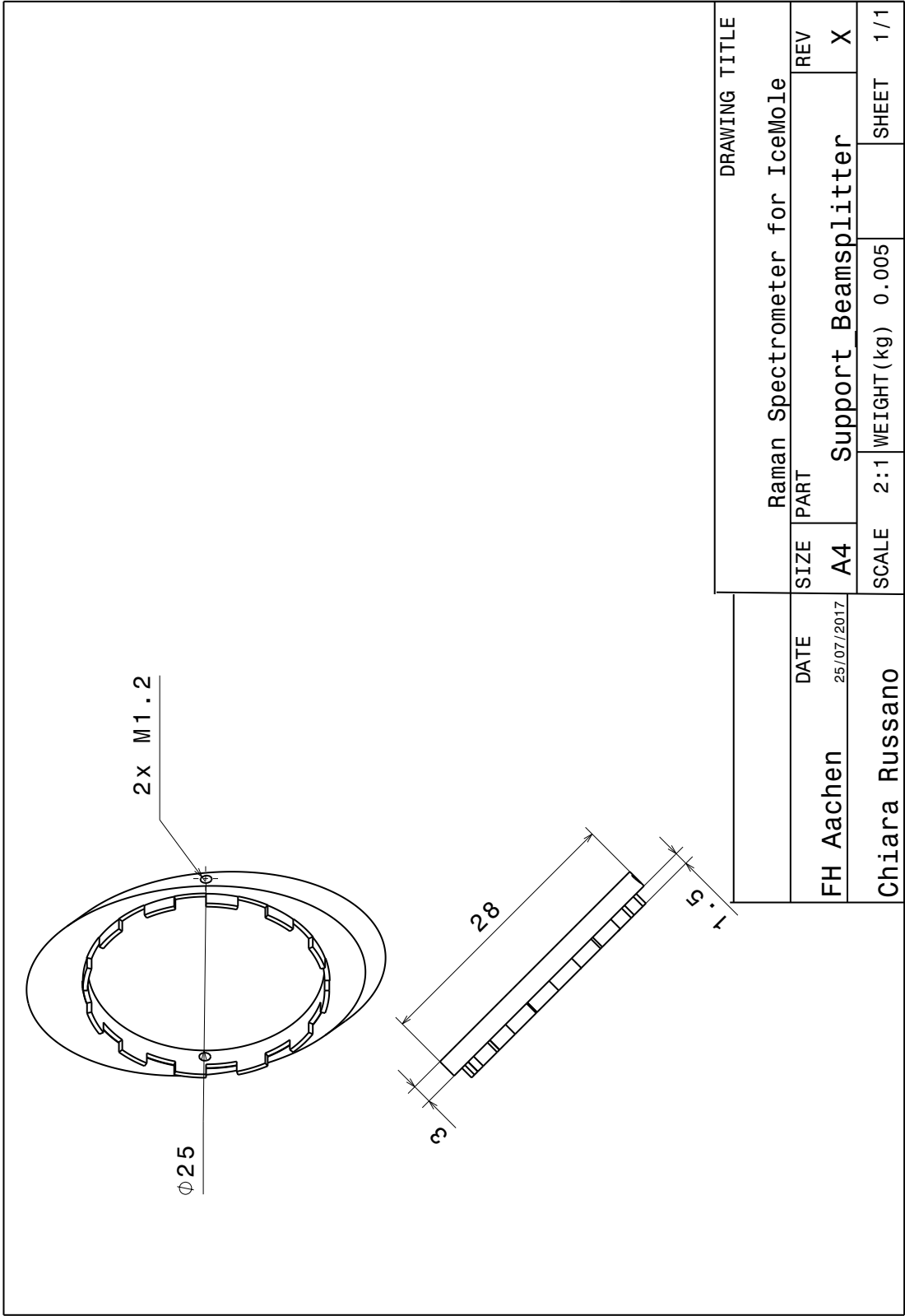


WINDOW



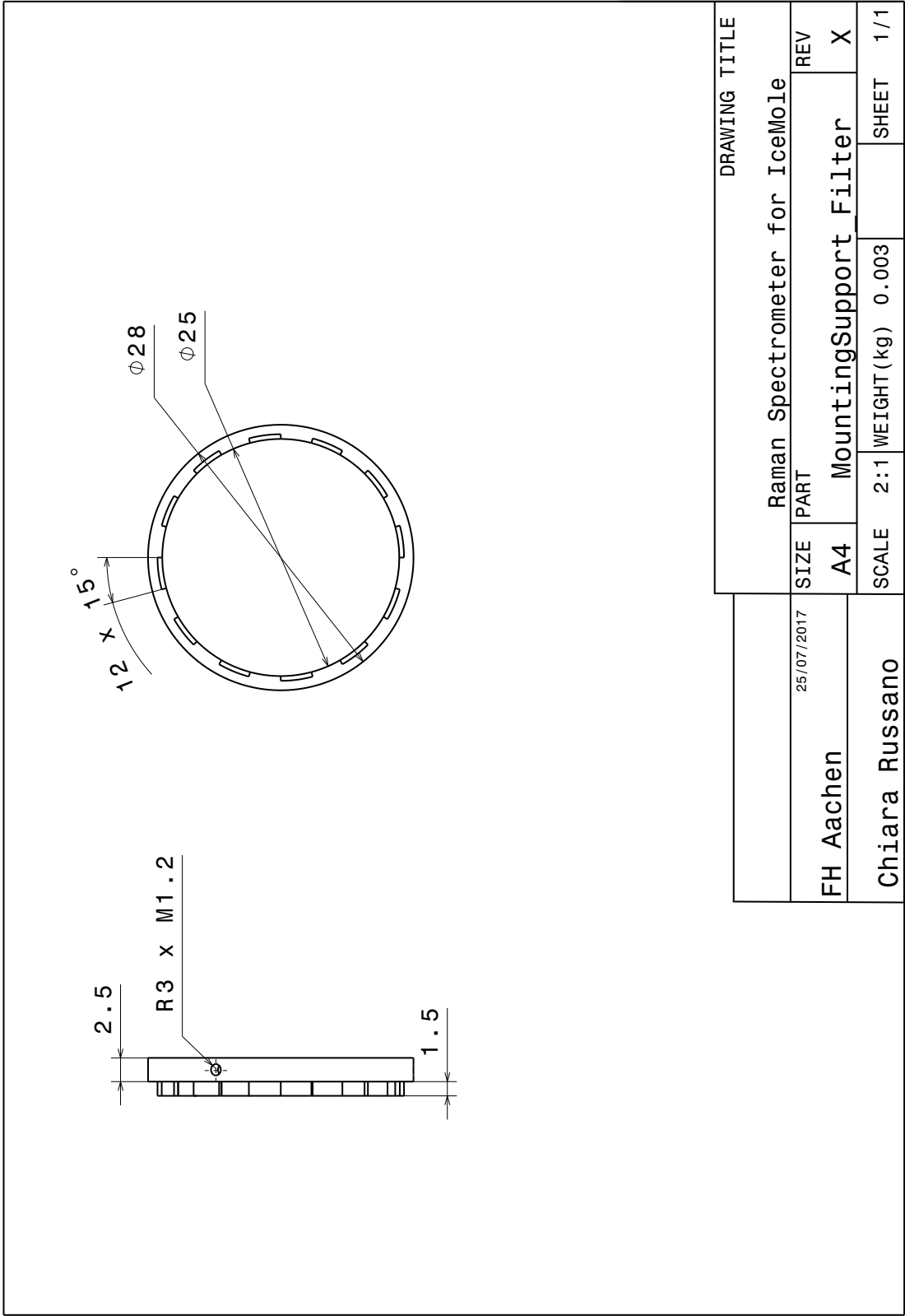
DRAWING TITLE	
Raman Spectrometer for IceMole	
DATE	REV
FH Aachen	X
25/07/2017	
SIZE	PART
A4	MountingSupport Window
SCALE	WEIGHT (kg)
2:1	0.007
SHEET	
1/1	

BEAMSPLITTER



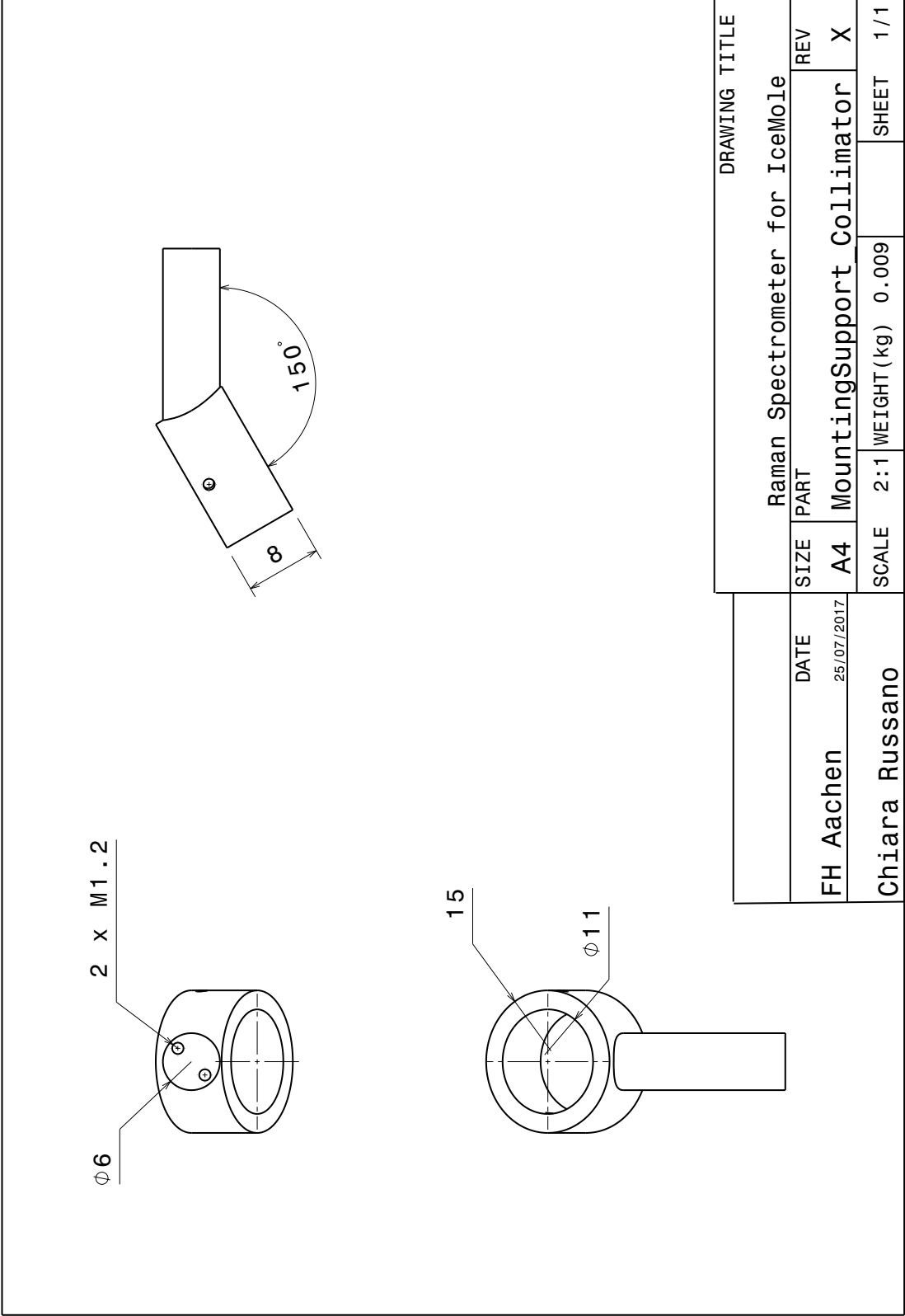
DRAWING TITLE		Raman Spectrometer for IceMole	
DATE	SIZE	PART	REV
FH Aachen 25/07/2017	A4	Support Beamsplitter	X
Chiara Russano	SCALE	2:1	WEIGHT (kg) 0.005
			SHEET 1/1

FILTER



DRAWING TITLE		Raman Spectrometer for IceMole	
DATE	SIZE	PART	REV
25/07/2017	A4	MountingSupport Filter	X
DESIGNER	SCALE	WEIGHT (kg)	SHEET
Chiara Russano	2:1	0.003	1/1

COLLIMATOR



DRAWING TITLE	
Raman Spectrometer for IceMole	REV
FH Aachen	25/07/2017
Chiara Russano	
DATE	
SIZE	PART
A4	MountingSupport Collimator
SCALE	2:1
WEIGHT (kg)	0.009
SHEET	1/1